E-ISSN 2228-8082
Volume 74, Number 7, July 2022

SMJ

Siriraj Medical Journal

The world-leading biomedical science of Thailand

MONTHLY

SICPH Siriraj International Conference In Medicine and Public Health 2022

ORIGINAL ARTICLE
REVIEW ARTICLE

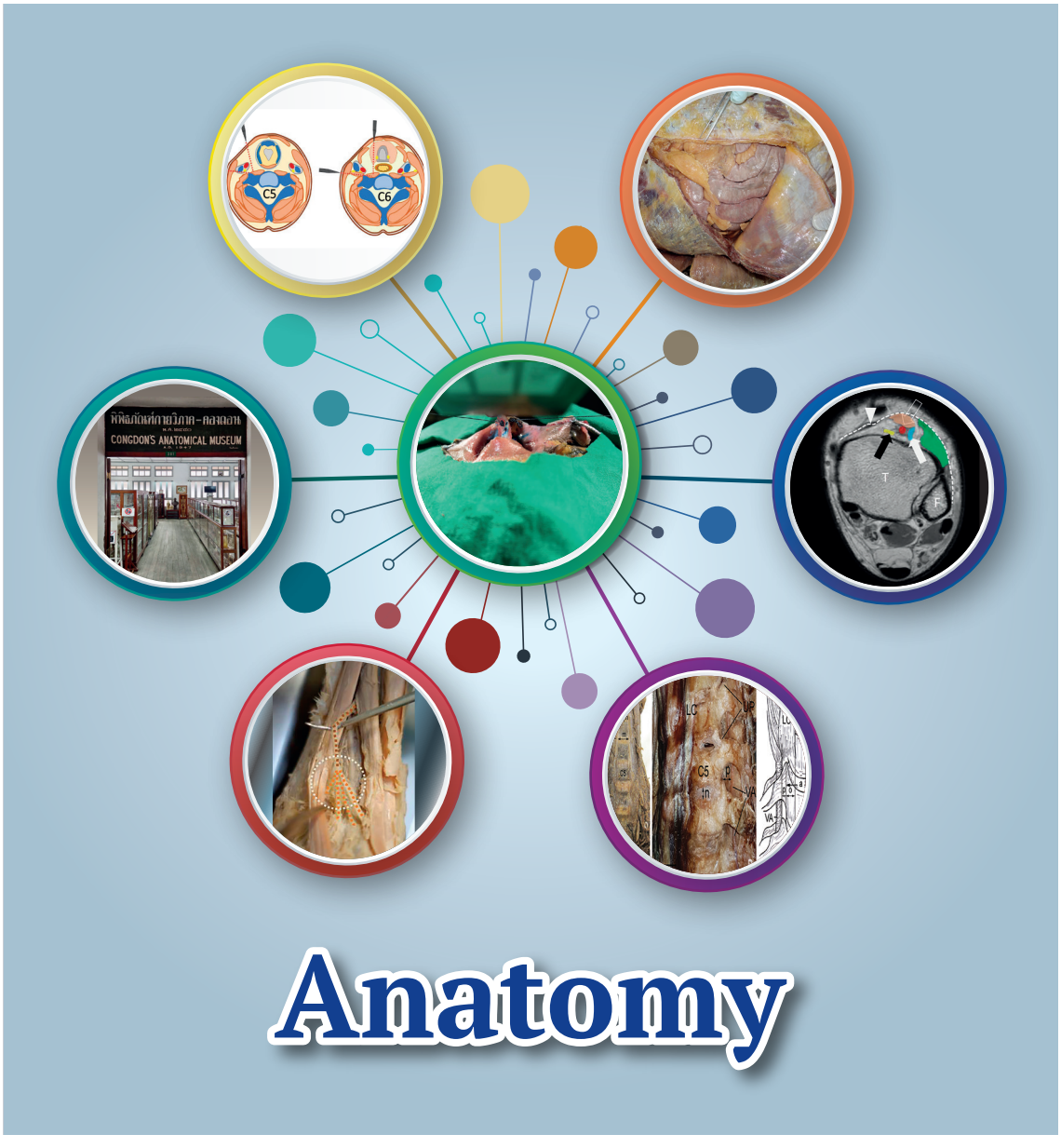

Indexed by Scopus®

THAILAND SECTION 1954

https://he02.tci-thaijo.org/index.php/sirirajmedj/index
E-mail: sijournal92@gmail.com

Siriraj Medical Journal SMJ

Volume 74, Number 7, July 2022

ORIGINAL ARTICLE

REVIEW ARTICLE

SIRIRAJ MEDICAL JOURNAL

www.smj.si.mahidol.ac.th

SIRIRAJ MEDICAL JOURNAL is published bimonthly, 6 issues a year (Jan-Feb, Mar-Apr, May-Jun, Jul-Aug, Sep-Oct and Nov-Dec) and distributed by the end of the last month of that issue.
SIRIRAJ MEDICAL JOURNAL is listed as a journal following the Uniform Requirements for Manuscripts Submitted to Biomedical Journals (URM) by the International Committee of Medical Journal Editors (ICMJE) since 9 July 2010 [http://www.icmje.org/journals.html].

Proposed Potential Anatomical Landmarks for Percutaneous Botulinum Toxin Injection in Anterocollis-typed Cervical Dystonic Patient: A Pilot Study Utilizing Thiel-embalmed Human Cadavers

Sanan Cheewadhanaraks, M.D.*, Witsanu Kumthornthip, M.D., Napakorn Sangchay, M.D., Ph.D.***

**Department of Anatomy, **Department of Rehabilitation Medicine, Faculty of Medicine Siriraj Hospital, Mahidol University, Bangkok 10700, Thailand.*

ABSTRACT

Objective: Botulinum toxin (BoTX) injection to the longus colli (LCo) muscle has been demonstrated to have a role in treating cervical dystonic (CD) patients. It can, however, cause critical complications and awareness of such complications is required. Currently, there is no substantial information regarding this novel procedure. This study aims to define the potentially safe method of injection based on assessment of anatomical measurements.

Materials and Methods: We examined distances between the puncture sites and adjacent structures in Thiel-embalmed human cadavers (n=20) to propose an alternative technique for BoTX injection. Parameters were examined for the medial and lateral approaches at the fifth and sixth cervical vertebral levels. We compared each variable between the two different vertebral levels and the two different approaches to evaluate statistical differences.

Results: Comparing distances between the puncture sites and neck anatomical structures in each of the two approaches, results were statistically significant. Similarly, we found using the medial approach statistical significance when comparing the measurements at the fifth with the sixth cervical vertebral level of the distances between the puncture sites and the thyroidal arteries and recurrent laryngeal nerve ($p < 0.05$).

Conclusion: The present study results provide initial guidelines for the safe technique for BoTX injection into LCo. Our findings suggest that the medial approach at the C6 vertebral level is preferable with minimal injury to vital structures. Thus, it may provide an optional method and can be used as guidance to improve surgical practice. Ethical approval was not required for this study.

Keywords: Botulinum toxin (BoTX) injection; Cervical dystonia (CD); Longus Colli (LCo); Thiel-embalmed human cadavers (Siriraj Med J 2022; 74: 409-424)

INTRODUCTION

Cervical dystonia (CD) is the most frequent primary dystonia and is characterized by an involuntary contraction of neck muscle, causing abnormal head and neck motion and posture. The chemical de-innervation by intramuscular injection of botulinum toxin (BoTX) has been used as the standard treatment to improve the quality of a patient's life by reducing accompanying symptoms, such as continuous pain or repetitive and uncontrollable muscle contraction.[1-3] Anterocollis type is one of the clinical spectrums of this condition presented with abnormal flexion deformity due to inevitable repeated contraction of anterior neck

Corresponding author: Napakorn Sangchay
E-mail: napakorn.sac@mahidol.ac.th
Received 7 February 2022 Revised 31 May 2022 Accepted 9 June 2022
ORCID ID: https://orcid.org/ 0000-0001-9250-3702
http://dx.doi.org/10.33192/Smj.2022.50

muscles. The longus colli muscle (LCo) is the pathogenesis of this clinical presentation. Botulinum toxin (BoTX) injection into LCo is ideal for treating a specific type of cervical dystonia, especially the treatment of anterocollis-typed dystonic patients.[1,4] Localization of this muscle is crucial in clinical practice since this process serves as an essential step for achieving a desirable outcome. As part of the critical step, this process requires experience and accurate anatomical knowledge. A reliable and less harmful technique for targeting this muscle should be proposed and established to improve the accuracy of needle placement.[5]

Various techniques have been established to locate the targeted dystonic muscles for injections, such as the blind technique based on clinical examination. The ultimate goal of treatment for CDs is to completely de-innervate the causative muscles.[6] Deep muscles, such as longus colli, can also be involved. Many studies have concentrated on the more accessible causative muscle, such as the sternocleidomastoid. In general, this muscle selection is preferable because it is superficially located in the cervical region, and it can be easily identified on clinical examination. In contrast, placing a needle into LCo, one of the causative muscles, is more challenging because this muscle is profoundly located in the pre-vertebral area within the cervical region.[1] The recommendation of imaging modality techniques, such as ultrasonography and electromyography, has been introduced for the BoTX injection because of the difficulty in locating this muscle in clinical practice, especially for the CD patient with abnormal flexion deformity.[7-9] These techniques could reduce the misplacement of the needle and indicate the proper injection area.[6,8,10,11] However, such techniques do not apply to deep cervical areas, especially the LCo. Under those circumstances, a blind technique becomes the method of choice. For it to be safe to conduct a blind intramuscular BoTX injection into this muscle, the recognition of cervical topographic anatomical variation is crucial in perceiving the depth from the anterior surface of the neck. Variation of posterior neck muscles has been documented, such as splenius capitis and semispinalis capitis.[12] Nonetheless, some remaining deep anterior neck muscles, for example, LCo, which are difficult to access from the anterior aspect of the neck, require more investigation.

We hypothesize that incomplete chemical de-innervation of the deep cervical muscle with BoTX injection may be one cause of treatment failures in patients with anterocollis. Most research being established to identify the safe position for BoTX injection in CDs is mainly focused on superficial and more robust cervical muscles including sternocleidomastoid, splenius capitis, trapezius, semispinalis capitis, levator scapulae, and scaleni. However, complicated cases of anterocollis-type CDs who presented with deep neck muscle spasm, such as LCo, remain unexplored. LCo is not generally injected because there is scant research being conducted targeting this muscle to confirm the safest technique for BoTX injection. Furthermore, the reported clinical outcomes are usually based on a small sample size. It seems that guidance indicates safe and effective BoTX injections into this muscle should be established to reduce potentially harmful incidents.[6,13]

LCo is located on the anterior surface of the C1-T3 vertebrae, and it is innervated by the anterior rami of the second (C2) to the sixth (C6) cervical spinal nerves. This muscle can be divided into three anatomic compartments: the superior oblique part, vertical intermediate part, and inferior oblique (the smallest element). LCo is gracile and is located adjacent to essential vital structures, such as great vessels, cranial nerves, trachea and oesophagus.[14] LCo extends from the cervical region to the upper thoracic region. It is difficult to complete de-innervation this muscle using the conventional blind technique of BoTX injection. It can cause complications such as injury to the thyroidal artery or phrenic nerve. Dissemination of this toxin into nearby structures due to needle displacement can cause life-threatening adverse effects, including weakness of mistargeted muscles leading to dysphagia, dysphonia, or ptosis.[15] This means that the degree of preferable treatment outcome is reduced. Therefore, considering a potential technique based on anatomical topographic landmarks to improve accuracy and minimize unfavourable complications of this procedure is essential, primarily when localizing the LCo.

There are two approaches based on a conventional blind technique to inject botulinum toxin into LCo, the medial and the lateral approach.[6,16,17] The better approach can be selected after considering the position of the carotid artery in each patient. There is currently no substantial research comparing these approaches in cadaveric-based dissection studies. In the absence of a standard guideline regarding an anatomical landmark for this novel technique, BoTX injection into LCo was recommended at the anterior surface of the neck utilizing the sternocleidomastoid as a landmark at the C3 or C6 vertebral levels, known as the medial approach.[18] This approach is preferable due to identifiable anatomical landmarks and avoids injury to the neurovascular bundle that locates more laterally. When comparing medial and lateral approaches, it is clear that great vessels and nerves located laterally have a high possibility of being injured by

needle puncture. As a result, it can be more challenging to access LCo via the lateral approach. However, in the anterocollis-type clinical setting, the accessible area for the medial approach could be diminished due to the flexion deformity in CD patients. Considering this problem, localization of LCo at the lateral area of the neck should be explored as an option for approaching this deep cervical causative muscle.

The medial approach using the blind technique for BoTX injection in anterocollis-typed CD patients at C3 and C6 vertebral levels was reported to be the clinically acceptable safe zones in most current publications.[1] Some critical remarks also question the superiority of medial approach in BoTX injection over the lateral approach in anterocollis-typed CD patients. It has to be taken into account that positioning of the needle for medial and lateral approaches in blind technique is performed according to palpable cervical anatomical landmarks to determine the precise needle insertion location. Observation from reported case studies mentioned the injury to external carotid arteries and sympathetic trunk when the needle placement using medial approach at the C3 level was performed. In addition, an increase in injury to structures occupied within the carotid sheath and an internal hemorrhage in the thyroid gland due to the injury of superior and inferior thyroidal arteries are mentioned when the needle placement using the medial approach at the C6 level was performed.

Recent researches focused on identifying the best method to target desirable muscle in CD patients by comparing the accurate needle placement between the blind injection method based on detectable anatomical landmarks and the image-facilitated method.[5] It appears that image-guided injections may produce the favourable treatment outcome but did not appear to improve overall better accuracy for the anatomical needle placement to target LCo. This method might prevent unintended injury due to the misplacement of BoTX needle insertion. Current investigations suggested an image-facilitated method, such as EMG, is more suitable for localizing the contracting muscles during injection.[19] This method is suitable for injecting muscles differing in size, and the deep-localized muscle requires a different approach compared to superficial ones. It can be noticed that the advantages and preferable treatment outcome of image-guided BoTX injection were reported, in most studies, were analyzed and interpreted utilizing a small sample size. In addition, most recommendations for anterocollis-type CDs regarding the use of device-guided injection to enhance anatomic precision are basically established with these selected muscles which are superficially located, such as splenius capitis or sternocleidomastoid. For these reasons, this aspect should be considered when conducting treatment in CD patients using this technique in the more difficult accessible, gracile, or deeply located muscles such as the LCo.

Complications associated with BoTX injection into this muscle depend on the following criteria: mode of injection (medial or lateral approach), anatomical level of injection, posture, and sex differences. There have been no substantial studies or reports attempting to establish the adequate depth of the needle insertion for a practical approach into LCo without complication or injury to the adjacent structures. When a conventional blind technique is employed, the thickness of LCo musculature at different vertebral levels needs to be considered to ensure the accurate position of the needle and the specific cervical vertebral level to achieve the total de-innervation of the LCo. For this reason, appreciation of the depth of insertion at the various cervical vertebral levels becomes crucial to the safe conduct of the procedure. Indeed, this method is usually recommended at C3 and C6 levels in parallel with an imaging-assisted modality, such as ultrasonography or computerized tomography, to facilitate and enhance precision. However, research regarding needle placement for both medial and lateral approaches rather than those cervical levels has not been conducted. Variation of cervical and pre-vertebral anatomical contour, the difference in cervical soft tissue component, head and neck posture, cervical neurovascular variations, neck muscular dystrophy, and sex differences may also impact the risk of injury.[20-26] Consideration should be given to sex differences in cervical anatomical structures and their effect on the treatment outcomes. Current literature has reported sex dimorphism and cervical muscle differences, both shape and size. Males tend to have larger cervical musculatures than females. It can suggest a close relationship between sexual dimorphism and the risk of injury to vital cervical organs.[27]

This present study will concentrate on the accuracy of needle placement used to target the LCo by determining the safe anatomical landmark for BoTX injection using the conventional blind technique in Thiel-embalmed human cadavers. Medial and lateral approaches were used, from two different neck positions, flexion and supine, at the two different cervical vertebral levels, C5 and C6. We plan to propose the potential injection site associated with the topographic anatomy of the neck and related structures to reduce the risk of the Botulinum toxin injection into LCo. In addition, the effects of sex differences on the risk of adjacent vital structure injury will be examined.

MATERIALS AND METHODS

Experimental model and subject details

This study was conducted on 20 Thiel-embalmed human cadavers (male, n=10 and female, n=10). The study samples were cadavers used for educational purposes in the Department of Anatomy, Faculty of Medicine Siriraj Hospital, and approved by the Institutional Review Board from this faculty (Si 621/2020). All the cadavers have Thai origins, ranging from 60 to 70 years of age. The sex, cause of death and age at death were recorded. The cadavers were used by postgraduate surgical trainees for practical surgical sessions from June 2020 to February 2021. The structures of the neck region are intact and were not damaged by previous surgical practices.

Method details and rationale

This study used two approaches to define the most secure way for BoTX injection (Fig 1). First, the EMG needle (size 25 gauge, 25 mm.) was medially applied to the carotid sheath for the medial approach on the right side of the neck, passed through the thyroid gland, and then reached the LCo. Before performing the needle's puncture at the beginning of this study, each cadaver was set in the supine position. The anterior neck region was dissected to determine the needle placement in LCo (Fig 1). For the lateral approach, the needle was applied at the posterior border of the sternocleidomastoid muscle, traversed through the anterior scalene muscle and then reached LCo. In addition to this, we performed these two methods on different vertebral levels. We used the superior border of thyroid cartilage as a landmark for C5 (Fig 2) and the inferior border of cricoid cartilage for C6 vertebral level (Fig 3). The cadaveric dissections were performed after the needle was placed and fixed using the spinal needle fixator. Then, each cadaver was set in a neck flexion position using the cadaveric fixator. Every step was performed on the left side of the neck resembling the protocol that had been previously performed on the right side of the neck to determine the effect of neck posture. Images were taken from the sample for a specific region of interest.

Subsequently, distances between the puncture sites and adjacent structures were measured to define the safest injection method for the longus colli (LCo) muscle. A sliding vernier caliper was used to measure distances on each side to determine the potential anatomical landmark for BoTX injection into LCo for the medial and lateral approaches at the two different cervical vertebral levels of the two positions (Fig 1). Six parameters were measured for the medial approach, including the distance from the skin to the anterior surface of LCo and the distances between the puncture sites and carotid sheath, trachea, superior thyroid artery, inferior thyroid artery, and recurrent laryngeal nerve. Three parameters were measured for the lateral approach, including the distance from the skin to the lateral border of LCo, the distances between the puncture sites and carotid sheath, and the distances between the puncture sites and phrenic nerve. Anatomical landmarks and measurements were described as shown in Table 1.

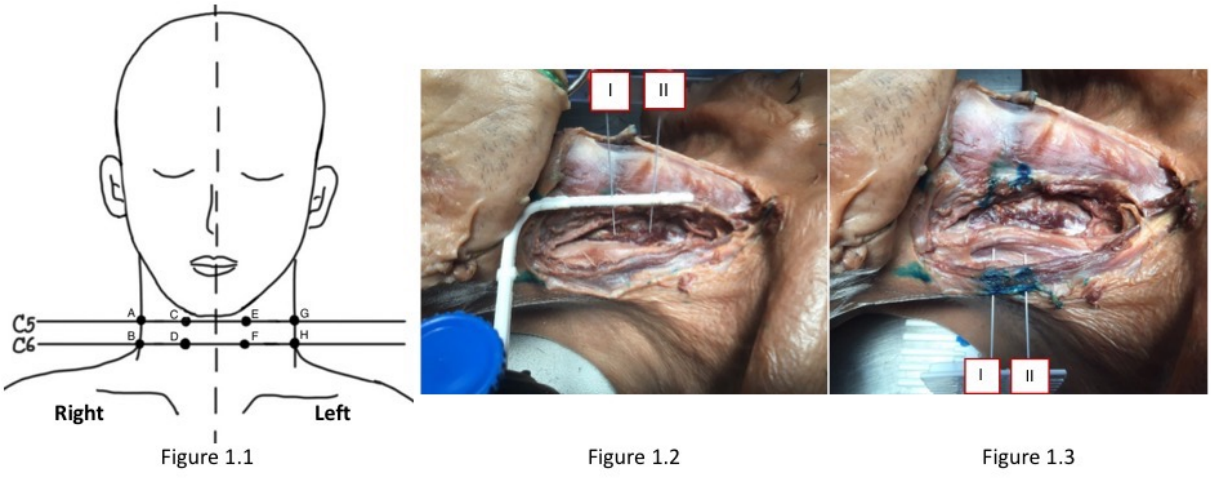

Fig 1. Anatomical landmarks represent puncture site in human cadaver. (1.1-Diagram illustrated landmarks of all approaches of botulinum toxin (BoTX) injection into longus colli (LCo) muscle in Thiel-embalmed embalmed cadavers (A- Lateral approach C5 supine position, B-Lateral approach C6 supine position, C-Medial approach C5 supine position, D-Medial approach C6 supine position, E-Medial approach C5 neck flexion position, F-Medial approach C6 neck flexion position, G- Lateral approach C5 neck flexion position, , and H-Lateral approach C6 neck flexion position, 1.2-Demonstrating medial approaches of BoTX injection into LCo in Thiel-embalmed cadaver in supine position (I-Medial approach, cervical vertebral level C5 and II-Medial approach, cervical vertebral level C6, and 1.3-Demonstrating lateral approaches of BoTX injection into LCo in Thiel-embalmed cadaver in supine position (I- lateral approach, cervical vertebral level C5 and II- lateral approach, cervical vertebral level C6).

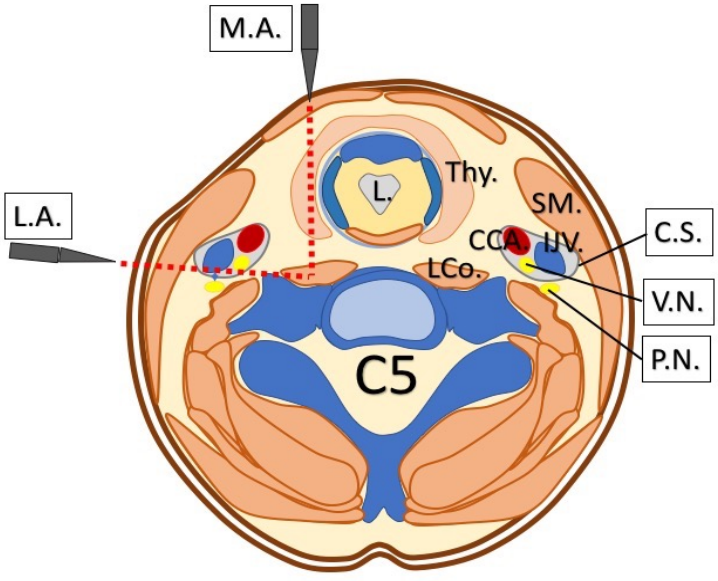

Fig 2. Schematic illustrated the topographic anatomy and related structures of the neck region at the C5 vertebral levels; red dot lines indicated the direction of the needle to target the longus colli muscle.
Abbreviations: M.A.; Medical approach, L.A.; Lateral approach, L.; Larynx, Thy.; Thyroid gland, SM.; Sternocleidomastoid muscle, C.S.; Carotid sheath, CCA.; Common carotid artery, IJV.; Internal jugular vein, V.N.; Vagus nerve, P.N. Phrenic nerve, C5; 5th cervical vertebral level

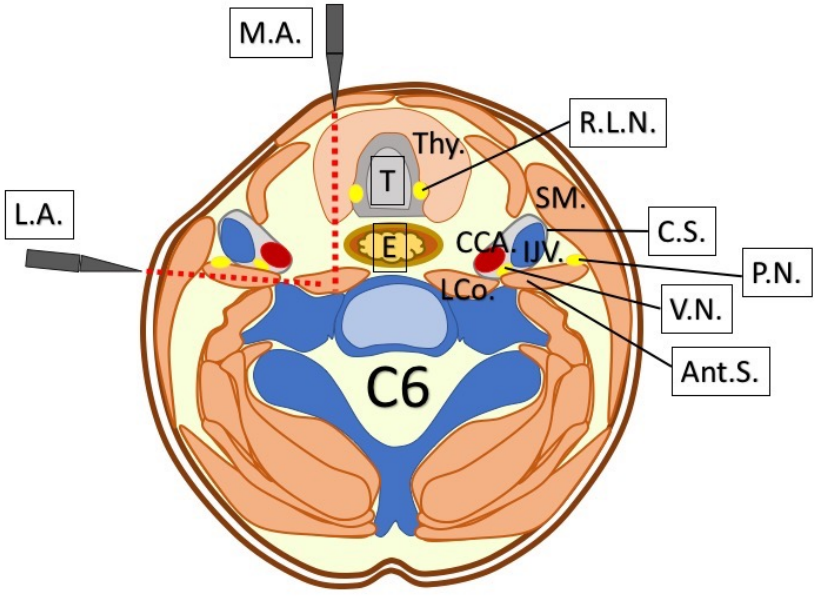

Fig 3. Schematic illustrated the topographic anatomy and related structures of the neck region at the C6 vertebral levels; red dot lines indicated the direction of the needle to target the longus colli muscle.
Abbreviations: M.A.; Medical approach, L.A.; Lateral approach, T.; Trachea, E.; Esophagus, Thy.; Thyroid gland, SM.; Sternocleidomastoid muscle, LCo.; Longus colli muscle, Ant.S.; Anterior scalene muscle, C.S.; Carotid sheath, CCA.; Common carotid artery, IJV.; Internal jugular vein, V.N.; Vagus nerve, P.N. Phrenic nerve, R.L.N.; Recurrent laryngeal nerve, C6; 6th cervical vertebral level

Statistical analyses

The mean and the standard deviation were calculated using the IBM SPSS version 27.0 for each measurement. A two-sample t-test was used to compare the outcomes between medial and lateral approaches in different vertebral levels, positions, and sexes. Comparison using one-way ANOVA was used to determine statistical differences between each dataset with normal distribution. The median and the standard deviation were calculated for datasets with non-normal distribution. The paired stepwise comparison analysis was used to examine all the measured parameters to determine statistical differences between each subgroup. Such analysis included all variables that were systematically added and removed from the list of

TABLE 1. Description of anatomical landmarks and all measurements (N.A. = Not applicable).

Anatomical structures	Measurement (Distances from needle to)	
	Medial approach (M.A.)	Lateral approach (L.A.)
Carotid sheath (C.S.)	Medial border	Posterior border
Superior thyroid artery (Sup.Thy.A.)	Inferior border	Inferior border
Inferior thyroid artery (Inf.Thy.A.)	Superior border	Superior border
Recurrent laryngeal nerve (R.L.N.)	Lateral border	N.A.
Phrenic nerve (P.N.)	N.A.	Anterior border
Trachea (T.)	Lateral border	N.A.

measurement. The first variable was removed from the analysis after the initial comparison between the first and second variables from the list was completed. The remaining parameters were selected and subsequently compared. The Kruskal-Wallis test and post-hoc analysis were used to determine statistical differences between each dataset. A p-value of <0.05 was considered statistically significant.

RESULTS

The summary of anatomical landmarks and all measurement descriptions is presented in Table 1. Descriptive statistics of all measurements is presented in Table 2. Comparing the outcome between male and female human cadavers by paired student t-test showed no statistical differences between the two sexes in all adjacent anatomical structures to the injection site for both medial and lateral approaches (Table 3).

The distances between puncture sites and the carotid sheath and between medial and lateral approaches are presented in Fig 4. The median distances between the puncture sites and carotid sheath of all lateral approaches were 0.00 mm indicating the needle injury to carotid sheath. As shown in Fig 5.2, the lateral approach at C5 or C6 revealed no significant difference in the distances between the puncture sites and the carotid sheath in different subjects' positions. The paired comparison of distances between the puncture sites and the carotid sheath (Table 4) showed a statistically significant difference in all comparisons between medial and lateral approaches (except the comparison between C5-M-S and C5-L-F). Our findings suggest that the lateral approach may cause injury to neurovascular structures adjacent to the sternocleidomastoid muscle, which clinicians should be aware of when performing BoTX injection with the lateral approach.

Comparisons of distances between the puncture sites and the vital structures among all medial approaches are presented in Fig 6, and comparisons of the distances between the puncture sites and the vital structure among all lateral approaches are presented in Fig 7. As shown in Figs 5.1 & 6.1, the medial approach at C5 or C6 revealed no significant difference in the distances between the puncture sites and the carotid sheath or trachea in different subjects' positions, respectively. However, we found that the distances between the puncture sites and the thyroid arteries were significantly greater in the neck-flexed position compared to the supine position (Figs 6.2 & 6.3). This also applies to the distances between puncture sites and the recurrent laryngeal nerve (Fig 6.4). Our findings suggest that the subjects' positions may affect the accuracy of the surface landmark on those neurovascular structures adjacent to the thyroid gland, which clinicians should be aware of when performing BoTX injection with the medial approach.

Paired stepwise comparison in Table 5 shows statistically significant differences in the distances between the puncture sites and the superior thyroid artery between C5 and C6 vertebral levels. These findings indicate that the needle placement at the C5 level using a medial approach tends to injure the superior thyroid artery without effect from the neck position.

There were statistically significant differences in distances between the puncture sites and the inferior

TABLE 2. The summary of descriptive statistics of all measurements, n = 20 (C5 = C5 vertebral level, C6 = C6 vertebral level, N.A. = Not applicable, S.D. = Standard deviation).

Parameters	Supine position								Neck flexion							
	Medial approach				Lateral approach				Medial approach				Lateral approach			
	C5		C6		C5		C6		C5		C6		C5		C6	
	Mean	S.D.	Mean	S.D.	Mean	S.D.	Mean	S.D.	Mean	S.D.	Mean	S.D.	Mean	S.D.	Mean	S.D.
Carotid sheath	3.84	2.06	4.64	2.07	1.56	2.23	0.73	1.16	4.82	2.82	5.01	2.13	1.44	1.94	0.73	1.36
Trachea	6.14	2.97	5.43	3.30	N.A.	N.A.	N.A.	N.A.	7.60	2.77	6.61	2.18	N.A.	N.A.	N.A.	N.A.
Superior thyroid a.	4.22	7.09	11.77	5.57	N.A.	N.A.	N.A.	N.A.	3.15	3.15	10.06	5.27	N.A.	N.A.	N.A.	N.A.
Inferior thyroid a.	21.28	7.25	12.19	5.86	N.A.	N.A.	N.A.	N.A.	13.15	6.79	8.77	12.14	N.A.	N.A.	N.A.	N.A.
Recurrent laryngeal n.	7.41	2.63	8.93	11.42	N.A.	N.A.	N.A.	N.A.	6.57	2.31	5.20	1.91	N.A.	N.A.	N.A.	N.A.
Phrenic n.	N.A.	N.A.	N.A.	N.A.	1.26	1.49	1.67	1.92	N.A.	N.A.	N.A.	N.A.	2.37	1.71	1.94	2.02

TABLE 3. Comparisons of the outcome between male (n = 10) and female (n = 10) human cadavers (C5 = C5 vertebral level, C6 = C6 vertebral level, n. = nerve, a. = artery, N.A. = Not applicable, S.D. = Standard deviation).

Parameters	Male (n=10)								Female (n=10)							
	Supine position								Supine position							
	Medial approach				Lateral approach				Medial approach				Lateral approach			
	C5 (C)		C6 (D)		C5 (A)		C6 (B)		C5 (C)		C6 (D)		C5 (A)		C6 (B)	
	Mean	S.D.	Mean	S.D.	Mean	S.D.	Mean	S.D.	Mean	S.D.	Mean	S.D.	Mean	S.D.	Mean	S.D.
Carotid sheath	3.45	2.44	4.31	2.40	1.14	1.81	0.98	1.45	4.23	1.62	4.97	1.75	1.97	2.62	0.47	0.77
Trachea	6.65	3.41	5.40	3.31	N.A.	N.A.	N.A.	N.A.	5.62	2.54	5.46	3.48	N.A.	N.A.	N.A.	N.A.
Superior thyroid a.	3.15	3.43	10.57	4.64	N.A.	N.A.	N.A.	N.A.	5.29	9.58	12.97	6.39	N.A.	N.A.	N.A.	N.A.
Inferior thyroid a.	22.19	7.90	12.37	7.09	N.A.	N.A.	N.A.	N.A.	20.37	6.83	12.00	4.72	N.A.	N.A.	N.A.	N.A.
Recurrent laryngeal n.	8.38	2.94	7.24	3.03	N.A.	N.A.	N.A.	N.A.	6.43	1.95	10.62	16.12	N.A.	N.A.	N.A.	N.A.
Phrenic n.	N.A.	N.A.	N.A.	N.A.	0.94	1.67	1.20	1.81	N.A.	N.A.	N.A.	N.A.	1.58	1.30	2.14	2.00
Parameters	**Neck flexion**								**Neck flexion**							
	Medial approach				Lateral approach				Medial approach				Lateral approach			
	C5 (E)		C6 (F)		C5 (G)		C6 (H)		C5 (E)		C6 (F)		C5 (G)		C6 (H)	
	Mean	S.D.	Mean	S.D.	Mean	S.D.	Mean	S.D.	Mean	S.D.	Mean	S.D.	Mean	S.D.	Mean	S.D.
Carotid sheath	4.53	3.16	4.89	2.22	1.99	2.18	1.07	1.48	5.10	2.57	5.13	2.14	0.89	1.59	0.38	1.20
Trachea	6.95	2.58	6.33	2.04	N.A.	N.A.	N.A.	N.A.	8.24	2.94	6.89	2.39	N.A.	N.A.	N.A.	N.A.
Superior thyroid a.	3.60	3.47	11.81	6.45	N.A.	N.A.	N.A.	N.A.	2.70	2.92	8.30	3.18	N.A.	N.A.	N.A.	N.A.
Inferior thyroid a.	11.05	6.47	10.13	16.68	N.A.	N.A.	N.A.	N.A.	15.24	6.76	7.40	5.38	N.A.	N.A.	N.A.	N.A.
Recurrent laryngeal n.	6.57	2.15	5.15	2.05	N.A.	N.A.	N.A.	N.A.	6.56	2.58	5.25	0.59	N.A.	N.A.	N.A.	N.A.
Phrenic n.	N.A.	N.A.	N.A.	N.A.	1.92	1.73	1.44	1.29	N.A.	N.A.	N.A.	N.A.	2.82	1.66	2.44	2.53

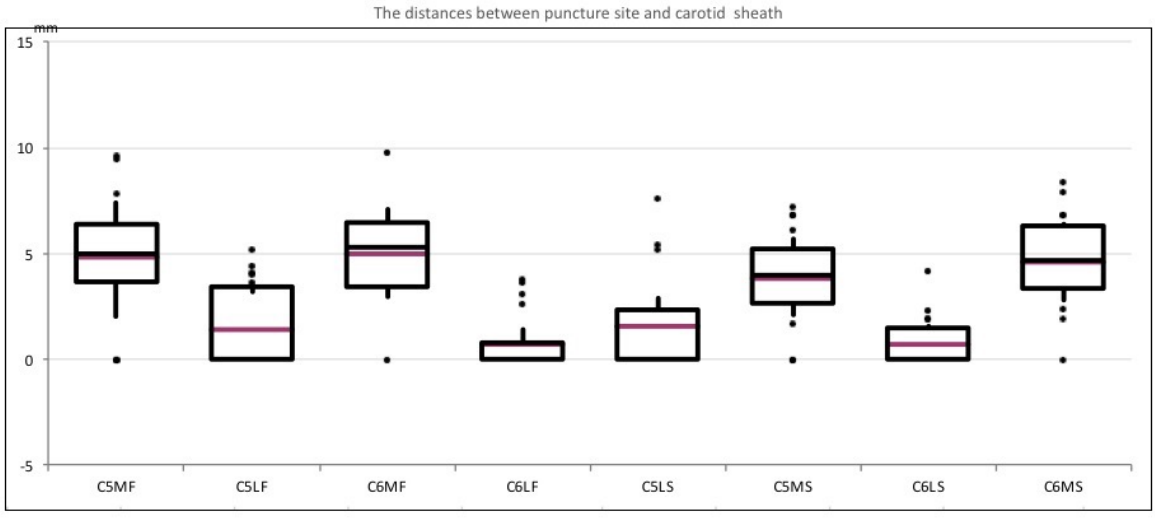

Fig 4. Distances between puncture site and carotid sheath of medial and lateral approaches in different vertebral levels and positions represented as boxplots. Each boxplot summarized all measurements taken per one anatomical landmark as shown in Fig 1.1, n = 20. (Medial approach C5 neck flexion position = C5-M-F, Lateral approach C5 neck flexion position = C5-L-F, Medial approach C6 neck flexion position = C6-M-F, Lateral approach C6 neck flexion position = C6-L-F, Lateral approach C5 supine position = C5-L-S, Medial approach C5 supine position = C5-M-S, Lateral approach C6 supine position = C6-L-S, and Medial approach C6 supine position = C6-M-S). Important distribution information, such as means (solid red lines within box), median (solid black lines within box), interquartile ranges (boxes), and outliers (solid black dots) are presented. Error bars represents means ± SD.

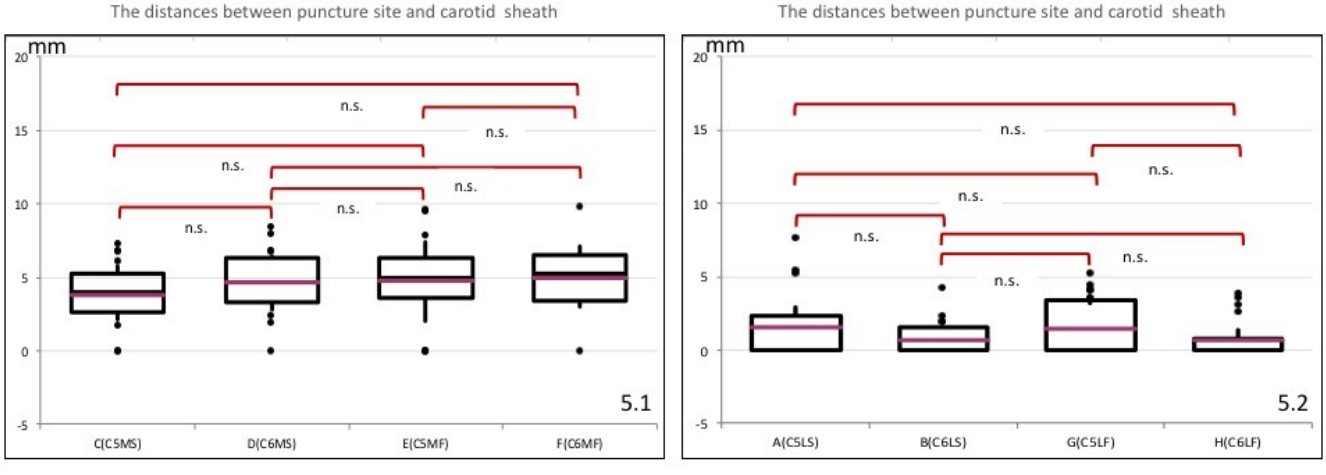

Fig 5. Distances between puncture site between puncture site and carotid sheath from the medial approach (5.1) and from the lateral approach (5.2) between two different vertebral levels and positions represented as boxplots. Each boxplot summarized all measurements taken per one anatomical landmark referred Fig 1.1, n = 20. Important distribution information, such as means (solid red lines within box), median (solid black lines within box), interquartile ranges (boxes), and outliers (solid black dots) are presented. Error bars represents means ± SD. Red bars represented comparison between subgroups. The n.s. above boxplots under significant bar mark measurements showed no statistical significances, according to one-way ANOVA tests performed at a 0.05 significance levels. (n.s. = no statistical significance; Medial approach C5 supine position = C5-M-S, Medial approach C6 supine position = C6-M-S, Medial approach C5 neck flexion position = C5-M-F, Medial approach C6 neck flexion position = C6-M-F, Lateral approach C5 supine position = C5-L-S, Lateral approach C6 supine position = C6-L-S, Lateral approach C5 neck flexion position = C5-L-F, and Lateral approach C6 neck flexion position = C6-L-F).

TABLE 4. Summary of stepwise comparison of distances between the puncture sites and the carotid sheath according to one-way ANOVA tests performed at a 0.05 significance levels. (Medial approach C5 supine position = C5-M-S, Medial approach C6 supine position = C6-M-S, Medial approach C5 neck flexion position = C5-M-F, Medial approach C6 neck flexion position = C6-M-F, Lateral approach C5 supine position = C5-L-S, Lateral approach C6 supine position = C6-L-S, Lateral approach C5 neck flexion position = C5-L-F, and Lateral approach C6 neck flexion position = C6-L-F).

Paired stepwise comparison		P-value	Paired stepwise comparison		P-value
C5-M-S (C)	vs C6-M-S (D)	0.98	C5-M-F (E)	vs C6-M-F (F)	1
	vs C5-M-F (E)	0.94		vs C5-L-S (A)	< 0.01
	vs C6-M-F (F)	0.85		vs C6-L-S (B)	< 0.001
	vs C5-L-S (A)	0.09		vs C5-L-F (G)	< 0.001
	vs C6-L-S (B)	< 0.01		vs C6-L-F (H)	< 0.001
	vs C5-L-F (G)	0.058	C6-M-F (F)	vs C5-L-S (A)	< 0.001
	vs C6-L-F (H)	< 0.01		vs C6-L-S (B)	< 0.001
C6-M-S (D)	vs C5-M-F (E)	1		vs C5-L-F (G)	< 0.001
	vs C6-M-F (F)	0.99		vs C6-L-F (H)	< 0.001
	vs C5-L-S (A)	< 0.01	C5-L-S (A)	vs C6-L-S (B)	0.97
	vs C6-L-S (B)	< 0.001		vs C5-L-F (G)	1
	vs C5-L-F (G)	< 0.01		vs C6-L-F (H)	0.97
	vs C6-L-F (H)	< 0.001	C6-L-S (B)	vs C5-L-F (G)	0.98
C5-L-F (G)	vs C6-L-F (H)	0.98		vs C6-L-F (H)	1

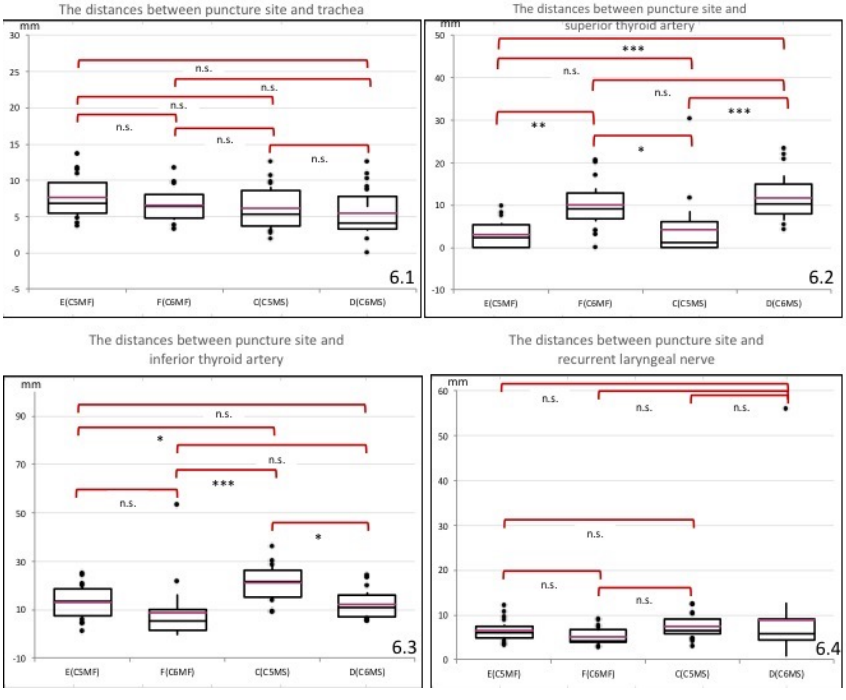

Fig 6. Distances between puncture site between puncture site and trachea (6.1), superior thyroid a. (6.2), inferior thyroid a. (6.3), and recurrent laryngeal nerve (6.4) from the medial approach between two different vertebral levels and positions represented as boxplots. Each boxplot summarized all measurements taken per one anatomical landmark as shown in Fig 1.1, n = 20. Important distribution information, such as means (solid red lines within box), median (solid black lines within box), interquartile ranges (boxes), and outliers (solid black dots) are presented. Error bars represents means ± SD. Red bars represented comparison between subgroups. Asterisks above boxplots under significant bar mark measurements show statistical significances, according to one-way ANOVA tests performed at a 0.05 significance levels. (* = p <0.05, ** = p < 0.01, *** = p <0.001, and n.s. = no statistical significance; Medial approach C5 supine position = C5-M-S, Medial approach C6 supine position = C6-M-S, Medial approach C5 neck flexion position = C5-M-F, and Medial approach C6 neck flexion position = C6-M-F).

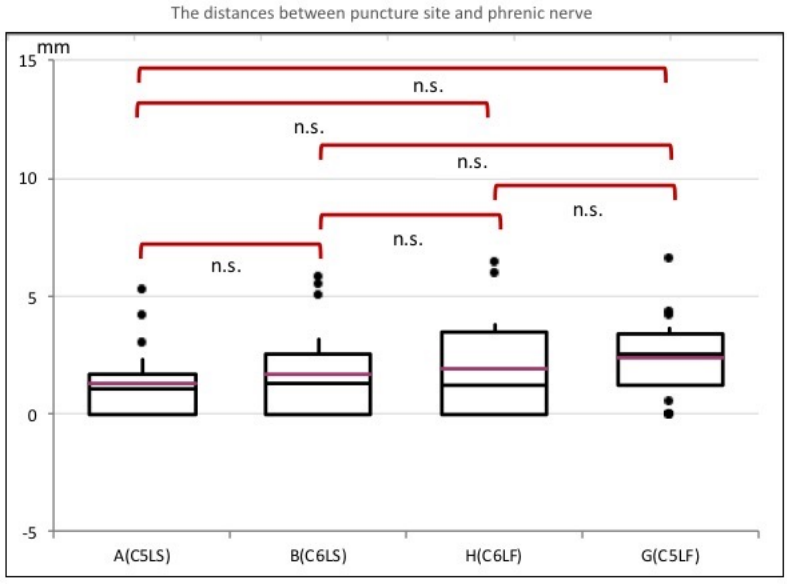

Fig 7. Distances between puncture site and phrenic nerve from the lateral approach between two different vertebral levels and positions represented as boxplots. Each boxplot summarized all measurements taken per one anatomical landmark as shown in Fig 1.1, n = 20. Important distribution information, such as means (solid red lines within box), median (solid black lines within box), interquartile ranges (boxes), and outliers (solid black dots) are presented. Error bars represents means ± SD. Red bars represented comparison between subgroups. The n.s. above boxplots under significant bar mark measurements showed no statistical significances, according to Kruskal-Wallis tests performed at a 0.05 significance levels. (n.s. = no statistical significance; Lateral approach C5 supine position = C5-L-S, Lateral approach C6 supine position = C6-L-S, Lateral approach C5 neck flexion position = C5-L-F, and Lateral approach C6 neck flexion position = C6-L-F).

TABLE 5. Summary of stepwise comparison of the trachea, superior thyroid artery, inferior thyroid artery and recurrent laryngeal nerve according to one-way ANOVA tests performed at a 0.05 significance levels. (Medial approach C5 supine position = C5-M-S, Medial approach C6 supine position = C6-M-S, Medial approach C5 neck flexion position = C5-M-F, and Medial approach C6 neck flexion position = C6-M-F).

Parameter	Paired stepwise comparison		P-value	Parameter	Paired stepwise comparison		P-value
Trachea	C5-M-S (C)	vs C6-M-S (D)	0.89	Superior thyroid a.	C5-M-S (C)	vs C6-M-S (D)	< 0.001
		vs C5-M-F (E)	0.45			vs C5-M-F (E)	0.94
		vs C6-M-F (F)	0.96			vs C6-M-F (F)	< 0.05
	C6-M-S (D)	vs C5-M-F (E)	0.13		C6-M-S (D)	vs C5-M-F (E)	< 0.001
		vs C6-M-F (F)	0.63			vs C6-M-F (F)	0.8
	C5-M-F (E)	vs C6-M-F (F)	0.75		C5-M-F (E)	vs C6-M-F (F)	< 0.01
Inferior thyroid a.	C5-M-S (C)	vs C6-M-S (D)	< 0.05	Recurrent laryngeal n.	C5-M-S (C)	vs C6-M-S (D)	0.89
		vs C5-M-F (E)	< 0.05			vs C5-M-F (E)	0.98
		vs C6-M-F (F)	< 0.001			vs C6-M-F (F)	0.72
	C6-M-S (D)	vs C5-M-F (E)	0.98		C6-M-S (D)	vs C5-M-F (E)	0.67
		vs C6-M-F (F)	0.65			vs C6-M-F (F)	0.29
	C5-M-F (E)	vs C6-M-F (F)	0.44		C5-M-F (E)	vs C6-M-F (F)	0.91

thyroid artery in medial approaches (except the comparison between C6-M-S vs C5-M-F, C6-M-S vs C6-M-F, and C5-M-F vs C6-M-F) from paired stepwise comparison in Table 5. There was no statistically significant difference in the distances between the puncture sites and recurrent laryngeal nerve (Table 5). Unlike the medial approach at the C5 level, these findings indicate that the needle placement at the C6 level using the medial approach tends to injure the inferior thyroid artery without any effect from the neck position. It means that the needle placement using a medial approach either at C5 or C6 level can cause an injury to the recurrent laryngeal nerve. Neck position may also alter the risk of injury to this structure.

We found that the distances between the puncture sites and the thyroid arteries were significantly greater in the neck-flexed position compared to the supine position (Figs 6.2 & 6.3). Our findings suggest that the subjects' positions may impact injury to thyroidal vessels, which clinicians should be aware of when performing BoTX injection with the neck flexion deformity CD patients.

There were no differences of the median between distances from the puncture sites and carotid sheath using the lateral approach (C5-L-S, C6-L-S, C5-L-F and C6-L-F were 0.00 mm, as shown in Fig 4). These findings indicate that the needle placement using a lateral approach at either cervical level can cause an accidental injury to the carotid sheath. This was also the pattern showed when comparing the medians of the distances between the puncture sites and the phrenic nerve between two cervical vertebral levels in both neck positions. There was no statistically significant difference in the distances between the puncture sites and the vital structures among all lateral approaches (Figs 5.2 & 7). Our findings suggest that the subjects' positions may not alter the risk of injury to the carotid sheath and phrenic nerve, which clinicians should consider when performing BoTX injection using the lateral approach in CD patients.

DISCUSSION

This study provides anatomical references to the longus colli (LCo) muscle. To reduce complications, it proposes the potential alternative technique for BoTX injection to LCo in terms of an anatomical-based approach using human cadavers compared with the current technique. Results from different injection approaches with various parameters are compared at the fifth and sixth cervical vertebral levels.[28]

Although most current publications recommend that the injection should be performed at the C3 and C6 vertebrae levels, we chose C5 and C6 vertebral levels for this present study.[1,6] The objective in selecting these two different vertebral levels is to avoid the bifurcation of the common carotid artery and reduce the possibility of accidental injury to the vertebral artery.[5] These two landmarks also have the palpable bony landmark to facilitate the identification of the precise cervical vertebral level.[29,30] The authors could not find any information about the recommendation regarding the specific site for complete chemical de-innervation of LCo at the C5 vertebral level. Concerning anatomic compartments of the LCo, this muscle may have distinct functions because it has three distinctive parts, representing the unique function of the neck biomechanical property. Oblique parts may act as the lateral neck flexor, while the inferior oblique part functions as the neck rotator. These functional aspects should be a consideration regarding the treatment outcome in patients with cervical dystonia (CD) and applying BoTX injections into this muscle.

In anterocollis-typed CD, the abnormal posture in anterior neck flexion can affect the anatomical relation. This study indicates that the different methods of BoTX injection into LCo in Thiel-embalmed cadavers led to different outcomes. Two percutaneous approaches were used to collect the data: medial and lateral. We examine the possible technique to target LCo to avoid damaging adjacent structures at C5 and C6 vertebral levels (Figs 2 & 3). Selection of the cadaveric position, supine and neck flexion, replicates the patient's clinical presentation and follows most research scenarios. By accessing the LCo from the medial approach, we are utilizing the bony landmark of the thyroid cartilage, which is well known for indirectly indicating the structures of the anterior cervical region. The thyroidal arteries are located anterolateral to the LCo at the C5 and C6 vertebral levels (Fig 8). They are at risk of being injured using this approach in neck flexion and supine positions. It should be considered that the possibility of superior thyroid artery injury is higher in the medial approach at the C5 vertebral level than at the C6 vertebral level (Fig 8.1). The inferior thyroid artery was more likely to be injured at a C6 vertebral level than a C5 vertebral level from the medial approach in the same neck position. Locating the cricoid cartilage at C6 and inserting the needle immediately next to the trachea can avoid an injury to the carotid artery within the carotid sheath. Awareness of the potential possibility of neurovascular complications is considered. However, our observation has not detected such injuries from the medial approach.

Previous studies described a medial or lateral approach relative to the carotid sheath when targeting

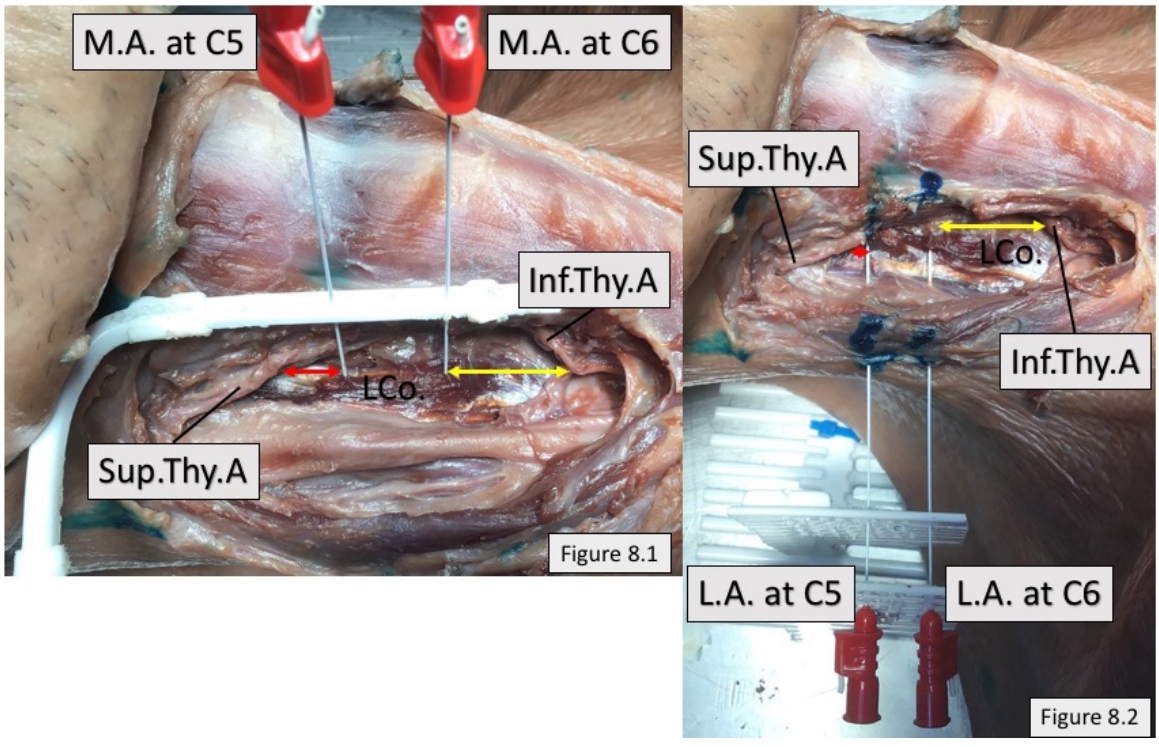

Fig 8. Measurements of distance between the needle placement into longus colli muscle in Thiel-embalmed cadavers and thyroidal arteries. (8.1-Medial approach and 8.2-Lateral approach; M.A.at C5 = Medial approach at C5, M.A. at C6 = Medial approach at C6, L.A.at C5 = Lateral approach at C5, L.A. at C6 = Lateral approach at C6, Lco. = Longus colli muscle, Sup.Thy.A. = Superior thyroid artery, Inf.Thy.A. = Inferior thyroid artery, Double-headed red arrow = Measurement from the needle to inferior border of superior thyroid artery, and double-headed yellow arrow = Measurement from the needle to superior border of inferior thyroid artery)

the LCo muscle using the position of the patient's neck as an anatomical reference. The disadvantage of the medial approach is that the needle is inserted into and penetrates the thyroid gland, with an increased risk of puncturing the thyroid arteries. The lateral approach has the disadvantage of the needle passing through a narrow space between the anterior tubercle and carotid sheath (Figs 2 & 3). As a result, the lateral approach is more likely to cause injury to the carotid sheath than the medial approach. In addition, puncture through the anterior scalene muscle is unavoidable and may increase the tendency of phrenic nerve injury. An additional limitation of both selected approaches at C5 and C6 levels is that they only allow injection of the most distal portion of LCo. This means that the cephalic part of this muscle may only be incompletely de-innervated.

Our proposed lateral approach at C5 and C6 can avoid penetrating injury to the thyroid gland and reduce the potential risk of accidental injury to thyroidal vessels. However, injury to the carotid sheath is inevitable with this approach at both cervical levels. We were performing needle insertion at the C5 and C6 levels; at either level, the needle trajectory provides access to the LCo (Fig 8.2). After performing cadaveric dissection, it was realized that needle placement for BoTX injection using a lateral approach at C5 was close to the superior thyroid artery. The needle placement below the C6 level should not be done due to the position of LCo being deeply located in the upper thoracic region. This approach is more likely to cause injury to the carotid sheath than the medial one. This study successfully targeted the muscle with the blind technique for medial and lateral approaches in supine and neck flexion positions. During the cadaveric dissection study, direct measurements were made, providing the confirmation that this is indeed the LCo. Localization of LCo in the lateral approach was analyzed following the identification of the posterior border of the sternocleidomastoid muscle, which accounts for its usefulness in the actual clinical circumstance and may reduce the degree of uncertainty regarding our protocol.

Publications about the complications of BoTX injection into LCo are sparse regarding procedures using tools not designated for medial and lateral approaches at C5 and C6 vertebral levels. None of the previous studies reported differences in structural complications between the medial and lateral approach at C5 and C6 vertebral levels concerning sex dimorphism or neck posture, confirming the necessity of this present research. Various complications,

such as pain, hoarseness of voice or dysphagia, have been reported, without mentioning a recommendation of a safe position to avoid those complications. It can be noticed that the lateral puncture may contribute to more severe complications than the medial approach, and the advancement of the needle to approach LCo may be more traumatic for the neurovascular bundle than the currently recommended technique, the medial approach at C3 and C6 vertebral levels. In this study, we did not observe any significant laryngeal damage when performing cadaveric dissection following the needle insertion. However, on cadavers, hemorrhage or structural swelling cannot be observed, and therefore only significant noticeable damage such as accidental puncture or laceration could be observed and documented. Nevertheless, using the proposed technique of introducing a needle into the LCo through the skin at the C5 level, any complications should be similar to those of the recommended method, except the injury to the superior thyroid artery. Moreover, this technique maybe practised on a human cadaver to enhance these clinical skills for BoTX injection.

One of the main concerns regarding BoTX injection into the LCo is the recurrent laryngeal nerve injury, which may lead to laryngeal complications such as the weakening of the laryngeal muscles. Laryngeal injury has occasionally happened following the blind technique. However, due to the possibility of severe disability, risk using this technique should be determined. The medial approach at the C5 vertebral level has a higher chance of injuring the recurrent laryngeal nerve than the medial approach at the C6 vertebral level. However, this complication is not observed in the present study. Using our technique, the tip of the needle was placed above the C6, avoiding the recurrent laryngeal nerve. We also determine the injury to the phrenic nerve regarding lateral approach at two different levels. In the present study, injury of the phrenic nerve was not detected in two different cervical vertebral levels.

Inserting the needle at the lower part of the neck increases the likelihood of traversing the thyroid gland during the injection; in our study, we used C5 and C6 vertebral levels.[17] However, previous research recommended the injection of BoTX at the C3 level. In patients with severe neck flexion deformity with a limited area to insert the needle, this recommended approach at the C3 vertebral level is inapplicable. We have not observed any complications related to the thyroidal vessels when attempting the medial approach for this neck posture at the C6 vertebral level. In contrast, attempting to insert the needle through the thyroid gland at the C5 level showed a high tendency to injure the superior thyroidal artery (Figs 8.1 & 8.2). Publications have reported various degrees of anatomical variation of the superior thyroid artery, either the location where this structure originates from the external carotid artery or their branches and the relation between this vessel and thyroid cartilage.[25] Despite this study, the needle penetrated the thyroid gland in all cases and there was no association with vascular puncture. However, it should be noted that this present study, primarily at the C5 level, was conducted utilizing human cadavers. As a result, visible hemorrhage from these vessels and within the thyroid gland may be obscured.

Determination of sex differences and their effect on the variation of cervical anatomical landmarks for the BoTX injection should be considered in clinical practice.[31] Current literature reports observe the anatomical variation of cervical structures between the two sexes.[12,26,32-34] Although we examined all parameters from cadaveric samples, it was clinically relevant to discuss previous studies on the effects of musculoskeletal conditions and therapeutic interventions. The LCo acts as a local spine stabilizer and facilitates neck flexor and contralateral rotator. From a clinical perspective, the anatomical orientation, musculature and robusticity of this muscle, functional component and zonal innervation of LCo muscle should be further explored for its clinical relevance in individuals with CD. Based on the present results, the different injection techniques can alter the outcomes and risk of complications after interventions. Such complications may alter the functional compartment of this muscle and affect neck motion after BoTX injection. The present study also validated the sex difference concerning the location of the newly proposed landmark for BoTX injection and demonstrated no effects of sex differences on anatomical-related complications. Previous studies reported differences of subcutaneous tissue between the two sexes that may impact on the depth from the skin to approach the LCo. The present study was conducted on Thiel-embalmed cadavers where subcutaneous fat is not well preserved and usually dissolves over time. Despite the distances measured from the skin to the LCo, we decided to exclude these variables from statistical analyses due to the reason previously mentioned. For all of these reasons, the results being observed and determined in this study regarding the relationship between sex dimorphism and cervical structures might be inapplicable to the general human population. Future research should examine the optimization between subject-specific study samples in the present study and the actual clinical situation regarding sex dimorphism and cervical musculature in the CD patient.

Thiel-embalmed cadavers were used in this present study to preserve the biomechanics of the soft tissue and the joint mobility of the human body, unlike normal embalmed cadavers that have a limitation on tissue integrity and joint flexibility.[35,36] Thiel's cadaveric-based experiments in terms of anatomical significance are recognizable for their life-like preservation. This cadaveric type provides favourable conditions for the image-facilitated procedure and excellent tissue preservation and is also found to help explore anatomical structures.[37] This embalming method provides the advantage of tissue plasticity and flexibility that cannot be achieved in formalin-embalmed cadavers.[38] In addition, such a method of embalming has been reported to reduce the potential risk of biosafety compared with studies conducted on a fresh frozen cadaver.[39] Furthermore, the Thiel-embalming process can lend itself to preliminary surgical skills training in a highly realistic and life-like setting.[40] Coupled with the challenge of reducing serious complications and undesirable consequences of BoTX injection, rehabilitation practitioners are confronted with a requirement to exercise and develop their skills. Thiel-embalmed cadavers meet these demands utilizing a highly anatomically accurate training model. Current studies highlighted the benefit of training courses, such as the training of prevertebral BoTX injection utilizing this type of human cadaver. This particular type of human cadaver provides life-like tissue quality, muscular consistency, and sensible perception of anatomical landmarks, which are ideally suitable for training courses similar to fresh frozen cadavers.

This proposed technique provides reliable, consistent access to a difficult-to-target muscle and is helpful for CD patients who experience treatment failure after a BoTX injection into superficial neck muscles has been administered.

This technique demonstrates some limitations and shows the clinicians who perform these techniques following our results should exercise caution. Further investigations are required. First, it was conducted in Thiel-embalmed cadavers; therefore, the anatomical distances could be different when performed in humans. Additional research should be conducted to establish the cervical anatomy in real clinical situations, especially further studies in humans using an imaging modality. It was challenging to conduct a study utilizing imaging modality in Thiel-embalmed cadavers because of the difficulty locating vital structures precisely. Second, recent research conducted in a small group of human cadavers on injections of deeply located muscles where the approach is challenging, the longus colli, has led to different methodologies being proposed. Although most results obtained were statistically significant, the literature surrounding the treatment of CD is sparse, possibly because CD itself is relatively rare and the utilization of BoTX to treat this clinical condition remains controversial. As clinical trials were only established in the late 1990s, the fact that this study lacks randomized-controlled clinical trials may limit the dependability of the results. Third, the majority of the human cadavers in our department is mainly confined to the elderly aged group. As a result, the effect of age and the outcome utilizing our proposed technique has not been examined. Future research being conducted across the age range should be considered to determine this aspect. Last, there were no intra- and inter-observer technical measurement errors in this present study, limiting the generalizability and application of BoTX injection in patients with different characteristics.

Our approach provides some beneficial aspects compared to previously described approaches-first, the possibility of utilizing the thyroid cartilage as landmark to identify the LCo. Second, the neck position in supine and neck flexion impacts the risk of injury to the neurovascular bundle. Third, variation of the thyroidal vessel, especially the superior thyroidal artery and its branch, should be considered when inserting the needle using a medial approach at C5 and C6 vertebral levels. Last, the medial approach tends to injure the recurrent laryngeal nerve, while the lateral approach can cause injury to the phrenic nerve. For these reasons, the medial approach at the C6 vertebral level would be the potential safest landmark for BoTX injection to target the LCo muscle in the anterocollis-type CD patients.

CONCLUSION

Combining anatomical-based knowledge and clinical practices utilizing cadaver simulator training is the key to performing accurate botulinum toxin (BoTX) injections without direct visualization into the longus colli (LCo), especially when the standard guidelines remain unavailable. This study proposes an alternative approach for injecting the LCo. We conclude that the medial approach at the C6 vertebral level is more precise, safer and demonstrates a more beneficial outcome in surgical practices than the lateral approach. This study also emphasises the importance of the topographic anatomical dimension of the neck region using a cadaveric approach, allowing proper planning for practical skill development utilizing a human cadaver and preventing life-threatening injury to the neurovascular bundle.

ACKNOWLEDGEMENT

None

Declaration: Part of the results from this study was presented at the 43rd Annual Conference of the Anatomy Association of Thailand, 5th -7th May 2021

Conflicts of interests: None

Funding: None

REFERENCES

1. Bahroo LB. Anterocollis posture and deep cervical muscle injections with BoNT. Toxicon. 018;156:S5. Available from: https://www.neurotoxins.org/toxins/2019/posters/058.pdf
2. Papapetropoulos S, Tuchman A, Sengun C, Russell A, Mitsi G, Singer C. Anterocollis: Clinical features and treatment options. Med Sci Monit. 2008;14(9):CR427-30.
3. Mittal SO, Lenka A, Jankovic J. Cervical dystonia: an update on therapeutics. Vol. 7, Expert Opinion on Orphan Drugs. 2019; 7(4):199-209.
4. Kojovic M, Caronni A, Bologna M, Rothwell JC, Bhatia KP, Edwards MJ. Botulinum toxin injections reduce associative plasticity in patients with primary dystonia. Mov Disord. 2011; 26(7):1282-9.
5. Ko YD, Yun SI, Ryoo D, Park J, Chung ME. Accuracy of Ultrasound-Guided and Non-guided Botulinum Toxin Injection Into Neck Muscles Involved in Cervical Dystonia: A Cadaveric Study. Ann Rehabil Med. 2020;44(5):370-7.
6. Kaymak B, Kara M, Gürçay E, Özçakar L. Sonographic Guide for Botulinum Toxin Injections of the Neck Muscles in Cervical Dystonia. Phys Med Rehabil Clin N Am. 2018;29(1):105-23.
7. Lee IH, Yoon YC, Sung DH, Kwon JW, Jung JY. Initial experience with imaging-guided intramuscular botulinum toxin injection in patients with idiopathic cervical dystonia. Am J Roentgenol. 2009;192(4):996-1001.
8. Walter U. Botulin toxin infiltration under ultrasound guidance. Cerebrovasc Dis. 2014;37:8-9.
9. Razaq S, Kaymak B, Kara M, Özkan S, Özçakar L. Ultrasound-Guided Botulinum Toxin Injections in Cervical Dystonia Needs Prompt Muscle Selection, Appropriate Dosage, and Precise Guidance. Vol. 98, Am J Phys Med Rehabil. 2019;98(3): e21-e23.
10. Allison SK, Odderson IR. Ultrasound and electromyography guidance for injection of the Longus Colli With Botulinum toxin for the treatment of cervical dystonia. Ultrasound Q. 2016;32(3): 302-6.
11. Herting B, Wunderlich S, Glöckler T, Bendszus M, Mucha D, Reichmann H, et al. Computed tomographically controlled injection of botulinum toxin into the longus colli muscle in severe anterocollis. Mov Disord. 2004;19(5):588-90.
12. Rankin G, Stokes M, Newham DJ. Size and shape of the posterior neck muscles measured by ultrasound imaging: Normal values in males and females of different ages. Man Ther. 2005;10(2): 108-15.
13. Hicklin LA, Kocer S, Watson NA, Marion MH. Ultrasound study to validate the anterior cervical approach to the longus colli muscle using electromyography control alone. Tremor and Other Hyperkinetic Movements. 2020;10(1)35:1-6.
14. Noussios G, Chatzis I, Konstantinidis S, Filo E, Spyrou A, Karavasilis G, et al. The Anatomical Relationship of Inferior Thyroid Artery and Recurrent Laryngeal Nerve: A Review of the Literature and Its Clinical Importance. J Clin Med Res. 2020; 12(10):640-6.
15. Mustalampi S, Ylinen J, Korniloff K, Weir A, Häkkinen A. Reduced Neck Muscle Strength and Altered Muscle Mechanical Properties in Cervical Dystonia Following Botulinum Neurotoxin Injections: A Prospective Study. J Mov Disord. 2016;9(1):44-49.
16. Glass GA, Ku S, Ostrem JL, Heath S, Larson PS. Fluoroscopic, EMG-guided injection of botulinum toxin into the longus colli for the treatment of anterocollis. Park Relat Disord. 2009;15(8): 610-3.
17. Tyślerowicz M, Jost WH. Injection into the longus colli muscle via the thyroid gland. Tremor and Other Hyperkinetic Movements. 2019;9:1-4.
18. Kreisler A, Defebvre L. Clinical guidance of botulinum toxin injections in cervical dystonia: How accurate is needle placement? Toxicon. 2018;156:S64.
19. Marion MH, Hicklin LA. Botulinum toxin treatment of dystonic anterocollis: What to inject. Park Relat Disord. 2021;88:34-39.
20. Toni R, Della Casa C, Castorina S, Roti E, Ceda G, Valenti G. A meta-analysis of inferior thyroid artery variations in different human ethnic groups and their clinical implications. Ann Anat. 2005;187(4):371-85.
21. Toni R, Della Casa C, Castorina S, Malaguti A, Mosca S, Roti E, et al. A meta-analysis of superior thyroid artery variations in different human groups and their clinical implications. Ann Anat. 2004;186(3):255-62.
22. Shao T, Qiu W, Yang W. Anatomical variations of the recurrent laryngeal nerve in Chinese patients: A prospective study of 2,404 patients. Sci Rep. 2016;6:25475.
23. Makay O, Icoz G, Yilmaz M, Akyildiz M, Yetkin E. The recurrent laryngeal nerve and the inferior thyroid artery - Anatomical variations during surgery. Langenbeck's Arch Surg. 2008;393(5): 681-5.
24. Taytawat P, Viravud Y, Plakornkul V, Roongruangchai J, Manoonpol C. Identification of the external laryngeal nerve: Its anatomical relations to inferior constrictor muscle, superior thyroid artery, and superior pole of the thyroid gland in Thais. J Med Assoc Thail. 2010;93(8):961-8.
25. Amarttayakong P, Woraputtaporn W, Munkong W, Sangkhano S. Cadaveric and angiographic studies of superior thyroid artery: Anatomical variations in origin and distance to carotid bifurcation. Asia-Pacific J Sci Technol. 2018;23(4):1-7.
26. Thomas AM, Fahim DK, Gemechu JM. Anatomical variations of the recurrent laryngeal nerve and implications for injury prevention during surgical procedures of the neck. Diagnostics. 2020;10(9):670.
27. Yi KH, Choi YJ, Cong L, Lee KL, Hu KS, Kim HJ. Effective botulinum toxin injection guide for treatment of cervical dystonia. Clin Anat. 2020;33(2):192-8.
28. Fujimoto H, Mezaki T, Yokoe M, Mochizuki H. Sonographic guidance provides a low-risk approach to the longus colli muscle. Vol. 27, Movement Disorders. 2012;27(7):928-9.
29. Yan Y zhao, Huang C an, Jiang Q, Yang Y, Lin J, Wang K, et al. Normal radiological anatomy of thyroid cartilage in 600 Chinese individuals: Implications for anterior cervical spine surgery. J Orthop Surg Res. 2018;13(1):31.
30. Won SY. Anatomical considerations of the superior thyroid artery: Its origins, variations, and position relative to the hyoid

bone and thyroid cartilage. Anat Cell Biol. 2016;49(2):138-42.
31. Islam MR, Begum T, Islam N, Islam MM. Anatomical Variation of Recurrent Laryngeal Nerve with Inferior Thyroid Artery: A Cross Sectional Study in Bangladeshi People. J Sci Found. 2021; 18(1):7-12.
32. Hong JT, Park DK, Lee MJ, Kim SW, An HS. Anatomical variations of the vertebral artery segment in the lower cervical spine: Analysis by three-dimensional computed tomography angiography. Spine (Phila Pa 1976). 2008;33(22):2422-6.
33. Graves M, Henry B, Sanna B, Pękala P, Taterra D, Witczak K, et al. Anatomical variations of the inferior thyroid artery : a cadaveric examination. Przegl Lek. 2017;74(12):633-5.
34. Nagai T, Schilaty ND, Krause DA, Crowley EM, Hewett TE. Sex differences in ultrasound-based muscle size and mechanical properties of the cervical-flexor and -extensor muscles. J Athl Train. 2020;55(3):282-8.
35. Boaz NT, Anderhuber F. The Uses of Soft Embalming for Cadaver-Based Dissection, Instruction in Gross Anatomy, and Training of Physicians. FASEB J. 2009;23(S1). Available from: https://doi.org/10.1096/fasebj.23.1_supplement.480.3
36. Kennel L, Martin DMA, Shaw H, Wilkinson T. The Uses of Soft Embalming for Cadaver-Based Dissection, Instruction in Gross Anatomy, and Training of Physicians. Anat Sci Educ. 2018;11(2):166-174.
37. De Brito Marco Zanuto E, De Souza MCCMI, Ribeiro AACM, Matera JM. Cadaver preservation for surgical skill training: Comparison of two embalming formulations. Cienc Anim Bras. 2019;20:1-11.
38. Eisma R, Wilkinson T. From "Silent Teachers" to Models. PLoS Biol. 2014;12(10):1-5.
39. Sangchay N. The Soft Cadaver (Thiel's Method) : The New Type of Cadaver of Department of Anatomy, Siriraj Hospital. Siriraj Med J. 2014;66(Suppl 6):S228-S231.
40. Rueda-Esteban RJ, Camacho FD, Rodríguez C, McCormick JSL, Cañón D, Restrepo JDH, et al. Viability and characterization trial of a novel method as an alternative to formaldehyde and Walter-Thiel cadaveric preservation for medical education and surgical simulation. Cir Esp (Engl Ed). 2021;S0009-739X(21) 00221-9.

Quantification of Bending Tolerance of the Cartilaginous Nasal Septum: Computer-Based Measurements

Suphalerk Lohasammakul, M.D.*, Chaiyawat Suppasilp, M.D., Sompol Tapechum, M.D.***, Sorawuth Chu-Ongsakul, M.D.****, Rosarin Ratanalekha, M.D.***

**Department of Anatomy, Faculty of Medicine Siriraj Hospital, Mahidol University, Bangkok, Thailand, **Department of Clinical Epidemiology and Biostatistics, Faculty of Medicine, Ramathibodi Hospital, Mahidol University, Bangkok, Thailand, ***Department of Physiology, Faculty of Medicine Siriraj Hospital, Mahidol University, Bangkok, Thailand, ****Division of Plastic and Reconstructive Surgery, Department of Surgery, Faculty of Medicine Siriraj Hospital, Mahidol University, Bangkok, Thailand.*

ABSTRACT

Objective: Nose deformity, including nasal deviation, is conspicuous since it locates in central face area. Regarding this and its prevention, nasal septum is one of the important supporting structures. Understand bending tolerance of the cartilaginous septum not only helps mitigate secondary deformity from surgical intervention, but also provides baseline information for further study regarding the nasal septum.

Materials and Methods: Nineteen fresh cadavers were dissected to expose the cartilaginous nasal septum. It was connected with the set-up computer system for detection of electrical signal at 1-mm septal bending from the midline. Mechanical load (bending load) was applied over the dorsal septum to quantify its bending tolerance. The data of bending tolerance and Pearson's correlation were reported.

Results: The mean of septal thicknesses is 1.5 ± 0.4 with the average bending load of 19.0 ± 11.2 g. The majority of the septal thicknesses (15/19; 78.9%) of the dissections are within the range of 1.1 – 2.0 mm with bending load of 18.2 ± 8.9 g on average. There is a moderately positive association between septal thickness and bending load, the Pearson's correlation coefficient is 0.602 (95%CI from 0.204 to 0.830) with p-value of 0.006.

Conclusion: The overall nasal septum and the septum with thickness between 1.1 – 2 mm are able to tolerate loading over distal part of caudal septum about 19.0 and 18.2 g, respectively. Septal thickness shows moderately positive correlation with bending load.

Keywords: Nasal septum; nasal deformity; bending tolerance; mechanical load; quantification (Siriraj Med J 2022; 74: 425-430)

INTRODUCTION

Nose is one of the central face structures, so any nasal deformity is conspicuous.[1] In current era, there are many nasal procedures for aesthetic and functional purposes. The majority of them, such as nasal tip augentation, increase mechanical load to the nasal septum and other midline supports. These procedures therefore require sufficiently strong support to maintain the structures in the midline. Improving nasal stability in weak septum is possible, but its drawbacks are longer operative time and

Corresponding author: Rosarin Ratanalekha
E-mail: rosarin.rat@mahidol.edu
Received 22 February 2022 Revised 19 April 2022 Accepted 20 April 2022
ORCID ID: https://orcid.org/0000-0001-9468-5976
http://dx.doi.org/10.33192/Smj.2022.51

more procedure complexity.[2-5] Understanding baseline strength of the septum to tolerate the mechanical load is beneficial especially in Asian population, whom commonly undergo augentation nasal tip procedure. As far as we know, there is no study regarding bending tolerance of septal cartilage to mechanical load. This study is therefore conducted to clarify this aspect in Asian population.

MATERIALS AND METHODS

Nineteen fresh cadavers without history of nasal dissection or pre-existing weakness of nasal septum detected by palpation before experimental processes were included in this study. These included 12 males and 7 females within the age of 16 – 97 years. This study was approved by the ethical committee of the Faculty of Medicine Siriraj Hospital, Mahidol University, Thailand.

Skin envelope, lower lateral cartilage, and upper lateral cartilage were dissected to expose the midline bony-cartilaginous framework of the nose. Parameters of the nasal septum, including thickness, length of caudal septum, and length of dorsal septum, were recorded. The thickness of caudal septum was measured at midpoint between anterior nasal spine (ANS) to anterior septal angle (ASA). Lengths of dorsal side and caudal side of the septum are defined as the distance from rhinion to ASA and from ANS to ASA, respectively. Surrounding soft tissue was removed as needed to facilitate setting up of the instruments for measurement in later process.

Two force transducers connected to nasal septum using non-elastic thread. Another end of each transducer connected to bridge amplifier, which subsequently connected to MacLab, an Analog-to-digital converter, that connected to the computer. This system with Chart 5 software (AdInstruments, Dunedin, New Zealand) convert mechanical load into electrical signal. The third force transducer was set over the septal area to apply mechanical load (unit of gram). This load created bending of the nasal septum, observed on the caudal view (Fig 1). The overall system is shown in Fig 2. For consistent results and measurements, additional test was done repeatedly before the main experiment. This showed that any mechanical load applied over the dorsal septum generated electrical signal of +/-0.1 mV from either arm of force transducers is consistent with septal bending of 1 mm from the midline. This mechanical load is defined as "bending load". In each cadaver, the bending load was quantified 3 times in each cadaver to find average for statistical analyses.

Statistical analyses

Mean with standard deviation (SD) and median with interquartile range (IQR) will be used for descriptive statistics. To determine magnitude of association between two variables, we used use Pearson's correlation coefficient with 95% confidence intervals (95%CI) calculated by using Fisher's z transformation due to rather normal distribution of the data, but will interpret along with rank correlation coefficients; Spearman's and Kendall's tau-b. The level of significance is set at 0.05 for all statistical testing.

RESULTS

There were 19 cadaveric subjects in this observational study with 12 males (63.16%) and the average age of 73.84 years (SD 10.68, median 72, IQR 9). Thickness of nasal septum, length of dorsal septum, and length of caudal septum were within range of 0.7 – 2.2 mm, 1.7 – 2.7 cm, and 1.5 – 2.6 cm, respectively. There was

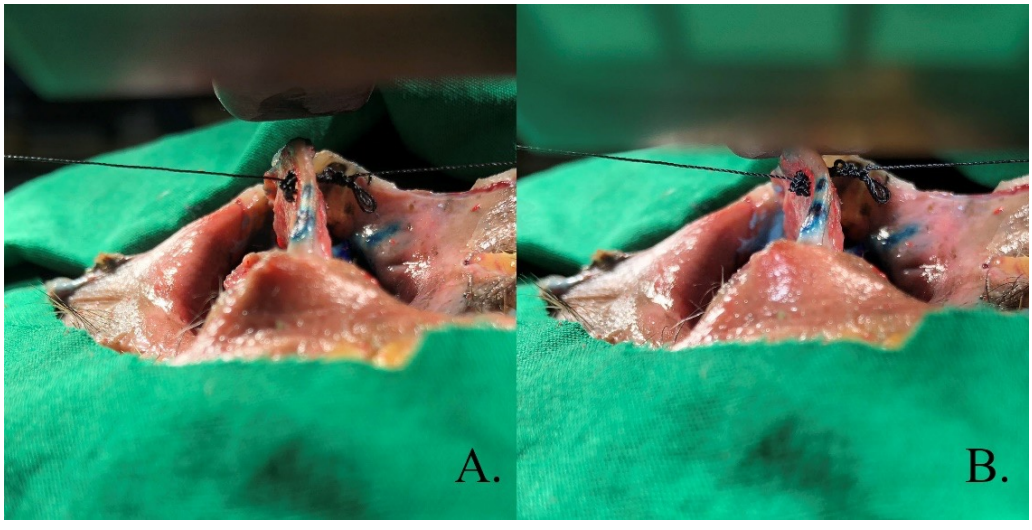

Fig 1. Bended nasal septum (1 mm from the midline), observed on the caudal view.

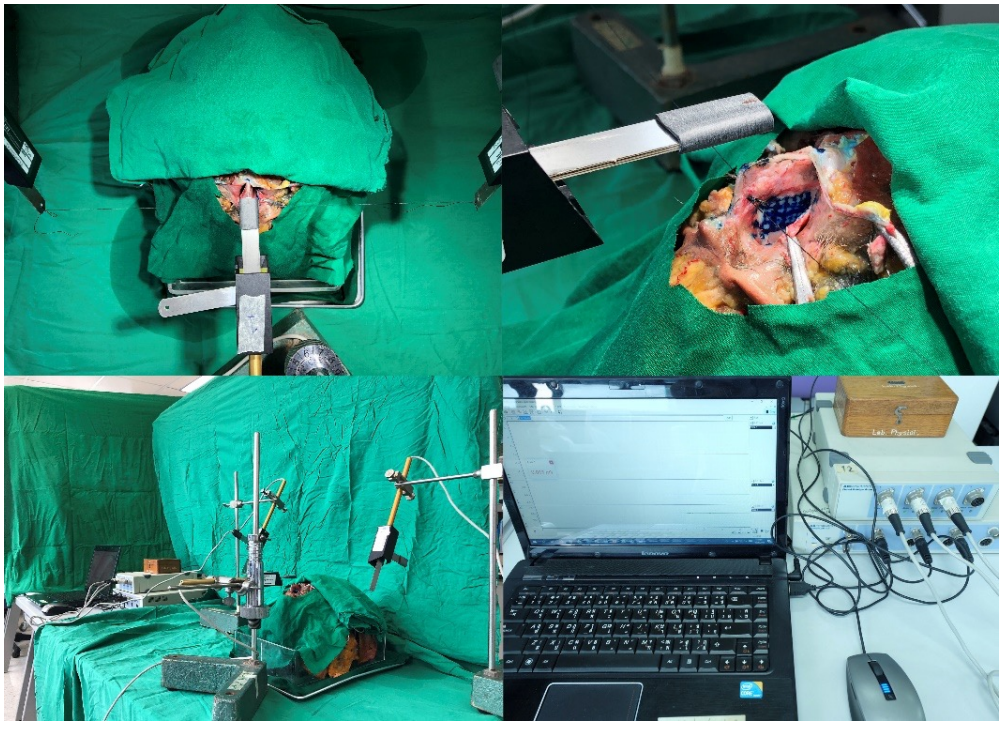

Fig 2. The overall system.

no correlation between lengths of dorsal septum and caudal septum (correlation coefficient of -0.014, p-value 0.953). The majority of the thickness (15/19; 78.9%) of the dissections were within the range of 1.1 – 2.0 mm (Table 1).

Overall, average mechanical load creating bending nasal septum of 1 mm was 19.0 ± 11.2 g. This average of the load was 18.2 ± 8.9 g in the group with thickness between 1.1 – 2.0 g. The average loads related to subgroups of thickness are shown in Table 1.

Correlations between bending loads and parameters of nasal septum, including thickness, length of dorsal septum, and length of caudal septum, are shown in Figs 3, 4, and 5, respectively. The bending load showed moderately positive association with septal thickness, Pearson's correlation coefficient is 0.602 (95%CI from 0.204 to 0.830) with p-value of 0.006 corresponding with rank correlation coefficients of 0.562 for Spearman's and of 0.467 for Kendall's with p-value of 0.012 and 0.007, respectively. The length of dorsal septum was moderately correlated with the bending load with statistical significance (coefficient of 0.564, p-value = 0.012), but the rank correlation coefficients showed no significance (Spearman's of 0.402 with p-value = 0.088 and Kendall's of 0.322 with p-value = 0.073).

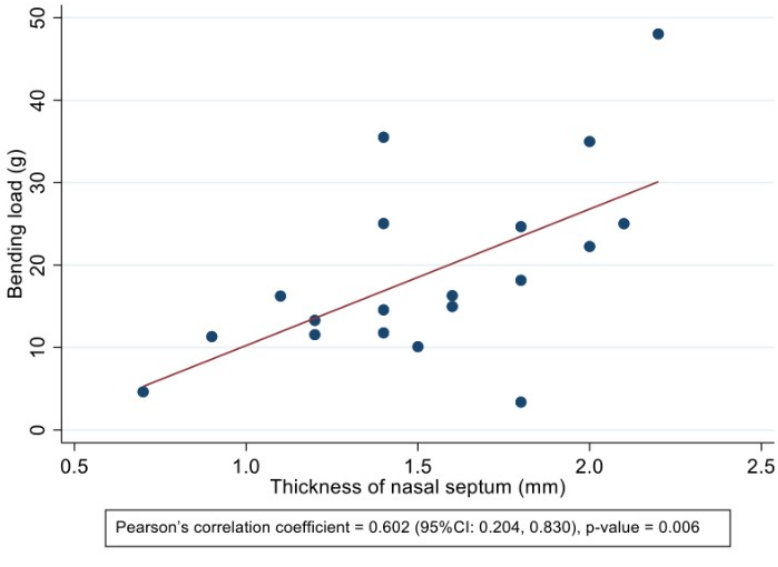

Fig 3. Pearson's correlation between bending load and thickness of nasal septum.

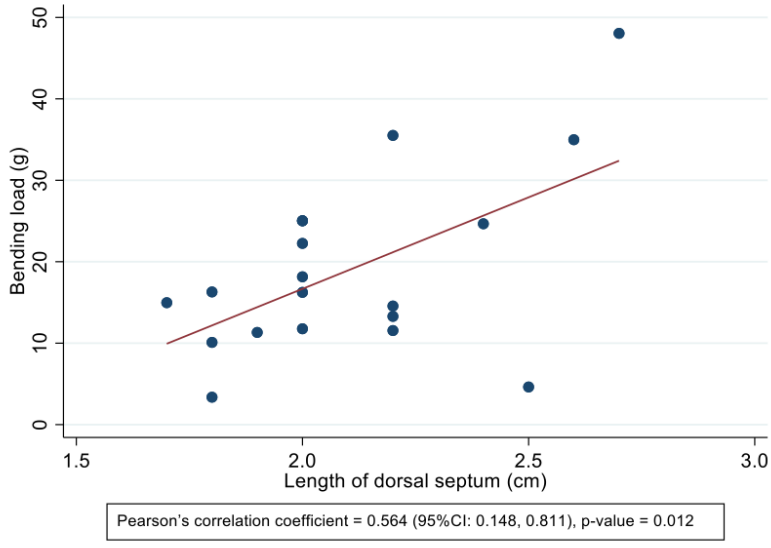

Fig 4. Pearson's correlation between bending load and length of dorsal septum.

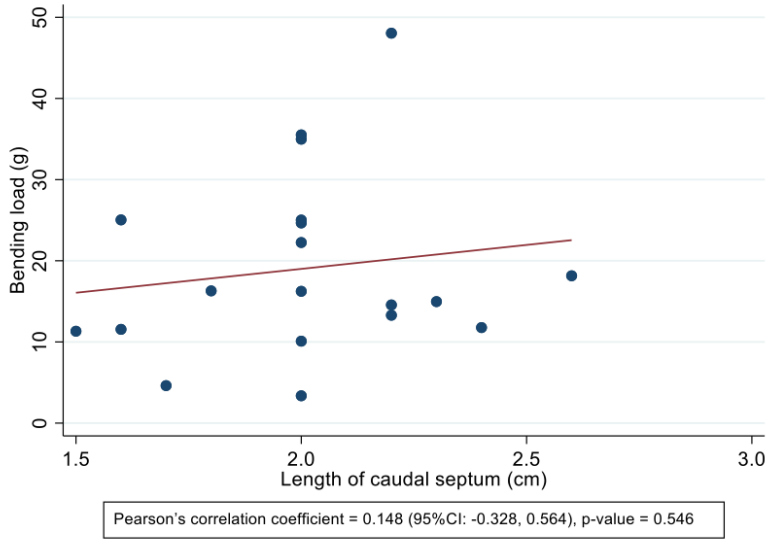

Fig 5. Pearson's correlation between bending load and length of caudal septum.

TABLE 1. Average of bending load by subgroups of septal thickness.

Septal thickness	n (%)	Bending load (g)	
		Mean (SD)	Median (IQR)
Overall	19 (100.0)	19.0 (11.2)	16.2 (13.5)
Subgroups			
1.1 to 2.0 mm (majority)	15 (78.9)	18.2 (8.9)	16.2 (12.9)
1 mm or less	2 (10.5)	8.0 (4.7)	8.0 (6.7)
1.1 to 1.5 mm	8 (42.1)	17.3 (8.7)	13.9 (9.0)
1.6 to 2.0 mm	7 (36.9)	19.2 (9.7)	18.2 (9.7)
2.1 mm or more	2 (10.5)	36.5 (16.3)	36.5 (23.0)
1.5 mm or less	10 (52.6)	15.4 (8.8)	12.5 (4.9)
1.6 mm or more	9 (47.4)	23.1 (12.7)	22.3 (8.7)

DISCUSSION

Nose is a crucial organ as it is a part of the upper respiratory system. In addition to this function, the nose also serves as an aesthetic structure of the face due to its location within central face area.[1] This comes with the concern that any nasal deformity is commonly noticeable. Anatomically, the nose consists of nasal skin envelope and osteocartilaginous framework. The framework is the foundation of the nose. There are 3 pairs and 3 midline structures. The former are nasal bones, upper lateral cartilages, and lower lateral cartilages. The midline structures are cartilaginous nasal septum, perpendicular plate of ethmoid bone, and vomer. Among these midline structures, surgical application is frequently focused on the nasal septum since its common deformity and capability to serve as cartilage donor.[6,7] Understanding anatomy of the septal cartilage is therefore crucial for surgical application to minimize the complications.

Septoplasty is one of the most commonly performed procedures. Each surgery comes with possible complications and the most commonly cited ones are saddle nose deformity and supratip depression.[8-10] These results from weakness of septal cartilage. To reduce these complications, it has been recommended to leave width of the septal L-strut of more than 10-15 mm.[9-13] In some cases, additional procedures of septal modification are required to strengthen the weak septum.[2-5] In severe scenarios of septal deformity, total reconstruction of the septum (extracorporeal septal reconstruction) is needed.[14-16] These 2 main operations share common principle of providing strong support to create a good foundation for the nose. However, powerful support comes at the exchange stiff nose appearance due to loss to pliability of the distal nose.[17] Balance between these 2 ends are crucial to provide aesthetically strong nose.

In this study, we quantify bending load to the nasal septum, one of the supporting midline nasal structures. Overall, nasal septum can tolerate force applied over its distal part of dorsal side approximately 19.0 g. This parameter can be applied as a baseline value of nasal septum in future studies to mimic native septum providing sufficiently strong support and aesthetic pliability. In addition, there is moderate correlation between the thickness and bending load with statistical significance. This is also helpful in application for septal reconstruction by increasing thickness of the septum to provide better support. This bending load varies by dividing thickness subgroups. In clinical practice, the difference of 1.9 g of bending loads between the thickness of 1.1 – 1.5 mm (17.3 g) and 1.6 – 2 mm (19.2 g) seems to be not significant. On the other hand, bending loads in septal thickness of 1 mm or less and 2.1 mm or more tend to show clinically significant difference, but their statistical differences require additional study with larger sample size. Average bending load of 36.5 g in thickness of more than 2.1 mm is comparable to one study reported nasal tip support in Caucasian population.[18] Although the research methodology is different, this number is worth mentioned due to probability that septal thickness of more than 2 mm able to tolerate bending load of more than 30 g on average. This finding assertively supports the positive correlation between the thickness and bending load.

The clinical implication of the findings in this study should be customization of the material using in nasal reconstruction to achieve comparable strength to native septal cartilage for aesthetically durable framework without stiff nose appearance. In addition, the bending load reported in our study can be applied in simulation of further nasal septum studies. However, larger sample size is required to quantify the average bending load in the population with septal thickness of less than 1 mm and more than 2 mm for clinical implication, and to possibly find the explanation of correlation between dorsal septum and bending load.

In case of septal deviation, findings from previous study[19] revealed the statistically significant decrease in air flow and increase in resistance of the nasal cavity ipsilateral to the deviating direction of the septum therefore this deviated septum, especially in the severe cases, seems to require surgical intervention for relieving its clinical symptom caused by such structural drawbacks. Nonetheless, further study on the load-bearing strength of septum with varying degree of deviation and thickness before and after L-strut septoplasty would be necessary for application in weighing the clinical advantage in each patient case prior to decision for operational correction.

CONCLUSION

Septal thickness shows moderately positive correlation with bending load. The nasal septum and the septum with thickness between 1.1 – 2 mm are able to tolerate loading over distal part of caudal septum about 19.0 and 18.2 g, respectively.

REFERENCES

1. FJ M. Aesthetic nasal reconstruction. In: Rodriguez ED LJ, Neligan PC, editor. Plastic surgery 4th ed Vol 3, Craniofacial, head and neck surgery and pediatric plastic surgery. Philadelphia: Elsevier; 2018. p. 126-80.e2.
2. Kridel RW, Scott BA, Foda HM. The tongue-in-groove technique in septorhinoplasty. A 10-year experience. Arch Facial Plast Surg. 1999;1(4):246-56; discussion 57-8.

3. Toriumi DM. Structure approach in rhinoplasty. Facial Plast Surg Clin North Am. 2005;13(1):93-113.
4. Ha RY, Byrd HS. Septal extension grafts revisited: 6-year experience in controlling nasal tip projection and shape. Plast Reconstr Surg. 2003;112(7):1929-35.
5. Pham AM, Tollefson TT. Correction of caudal septal deviation: use of a caudal septal extension graft. Ear Nose Throat J. 2007; 86(3):142, 144.
6. Sancho BV, Molina AR. Use of septal cartilage homografts in rhinoplasty. Aesthetic Plast Surg. 2000;24(5):357-63.
7. Yoon SH, Kim CS, Oh JW, Lee KC. Optimal harvest and efficient use of septal cartilage in rhinoplasty. Arch Craniofac Surg. 2021;22(1):11-6.
8. Yanagisawa E, Ho SY. Unintended middle turbinectomy during septoplasty. Ear Nose Throat J. 1998;77(5):368-9.
9. Yeo NK, Jang YJ. Rhinoplasty to correct nasal deformities in postseptoplasty patients. Am J Rhinol Allergy. 2009;23(5): 540-5.
10. Ketcham AS, Han JK. Complications and management of septoplasty. Otolaryngol Clin North Am. 2010;43(4):897-904.
11. Planas J. The twisted nose. Clin Plast Surg. 1977;4(1):55-67.
12. Moche JA, Palmer O. Surgical management of nasal obstruction. Oral Maxillofac Surg Clin North Am. 2012;24(2):229-37, viii.
13. Kim DW, Gurney T. Management of naso-septal L-strut deformities. Facial Plast Surg. 2006;22(1):9-27.
14. Gubisch W. The extracorporeal septum plasty: a technique to correct difficult nasal deformities. Plast Reconstr Surg. 1995; 95(4):672-82.
15. Gubisch W. Twenty-five years experience with extracorporeal septoplasty. Facial Plast Surg. 2006;22(4):230-9.
16. King ED, Ashley FL. The correction of the internally and externally deviated nose. Plast Reconstr Surg (1946). 1952;10(2): 116-20.
17. Toriumi DM. New concepts in nasal tip contouring. Arch Facial Plast Surg. 2006;8(3):156-85.
18. Beaty MM, Dyer WK, 2nd, Shawl MW. The quantification of surgical changes in nasal tip support. Arch Facial Plast Surg. 2002;4(2):82-91.
19. Assanasen P, Jareoncharsri P, Bunnag C. The Relationship between deviated nasal septum and middle ear pressure. Siriraj Med J. 2002;54(8):439-54.

A Pilot Comparative Study of Submerge vs. Non-Submerg Saturated Salt Solution Human Cadavers Embalming Method by Gross, Histological, and Microbiological Evaluation

Anuch Durongphan, M.D.*,, Warit Chongkolwatana, M.D.*, Popchai Ngamskulrungroj, M.D., Ph.D. ***, Thanaphat Pochnasomboon, B.Sc.*, Jatupong Pinkaew, B.Sc.*, Benjaporn Pamornpol, Ph.D.*, Rosarin Ratanalekha, M.D.* Mathee Ongsiriporn, M.D.***

**Department of Anatomy, Faculty of Medicine Siriraj Hospital, Mahidol University, Bangkok, Thailand, **Department of Otorhinolaryngology, Faculty of Medicine Siriraj Hospital, Mahidol University, Bangkok, Thailand, ***Department of Microbiology, Faculty of Medicine Siriraj Hospital, Mahidol University, Bangkok, Thailand.*

ABSTRACT

Objective: To investigate and develop the saturated salt embalming method and evaluate the cadavers.

Materials and Methods: Eight cadavers were embalmed with a saturated salt solution (SSS) by submerged (SG, N=2) and non-submerged (NSG, N=6), then evaluated by gross dissection, which compared to living humans, fresh and Thiel's cadavers. The histological evaluation was compared to textbook pictures. The assessments were recorded on a Likert scale from 0 (no resemblance) to 5 (most resemblance). Pre-and post-embalming swabs were collected for bacterial and fungal cultures and lung tissues for acid-fast staining and mycobacterial cultures. Comparisons between the evaluated items were performed using the Kruskal–Wallis test. The Likert scale results were reported by percentage.

Results: The submerge method (N=2) was terminated after three months of embalming because it showed insufficient quality for dissection. Six cadavers in NSG had gross tissue qualities that resembled living humans or fresh cadavers on a scale of 3 or 4. NSG had excellent joint flexibility. The histological tissues showed similarity to textbook pictures, with a scale of 4 or 5. There were bacterial and fungal cultures at the end of embalming. The pathogenic bacteria were *Clostridium perfringens* and *Pseudomonas aeruginosa*. Mycobacterium cultures were negative.

Conclusion: Injected SSS, 80% total body water volume, is a promising embalming method that yields cadavers with high tissue quality, flexible joints, and good histological structures. However, this technique cannot eliminate bacteria and normal flora. It may result from the tropical climate setting.

Keywords: Saturated salt solution; embalming; cadaver; dissection (Siriraj Med J 2022; 74: 431-439)

INTRODUCTION

Well-known cadaver preservation methods were fresh frozen, Thiel's, and formalin embalming cadavers. Fresh cadavers are non-chemically treated. Their color, consistency, and flexibility resemble living patients.[1,2] However, they have a short usage time, need to be stored in a freezer, and may host infectious organisms. Thiel's cadavers have excellent joint flexibility and soft tissue

Corresponding author: Mathee Ongsiriporn
E-mail: mathee.ong@mahidol.edu
Received 7 March 2022 Revised 18 April 2022 Accepted 20 April 2022
ORCID ID: https://orcid.org/0000-0001-9513-4252
http://dx.doi.org/10.33192/Smj.2022.52

consistency.[1] Their weaknesses are a poorly preserved brain, muscular disintegration, complex preparation, and expensive.[3-6] Conventional embalmed cadavers have hard tissue consistency and inflexible joints. Also, the high formaldehyde content in conventional embalming solution is toxic because of its carcinogenicity.[7,8]

Coleman and Kogan introduced a saturated salt solution embalming cadaver (SSS). The cadaver had excellent dissection properties and well-preserved histological structures.[9] Hayashi et al. published a study of SSS made from Coleman and Kogan's solution, comparing this solution with 20% formaldehyde and Thiel's solution. Cotton swabs were taken at the pharynx and rectum for pre-and 14-day post-embalming bacterial and fungal cultures. Body cavities fluid were collected during dissection for cultures. The post-embalming results showed the solution had a bactericidal effect.[10] The SSS had flexible joints and high tissue quality and were equally suitable for surgical simulations as Thiel's cadavers.[10] However, their study assessed only two cadavers per embalming type. Coleman's publication did not mention the number of cadavers. Hayashi et al.'s embalming technique differed from Coleman's. They injected 6 liters (L) of SSS with an undetermined amount afterward, while Coleman and Kogan used 21 L for a small cadaver. Hayashi et al. had stored a cadaver in a plastic body bag and kept it at room temperature, but they did not report the storage time duration. In contrast, Coleman and Kogan placed cadavers in thick polyethylene sheeting and stored them in an embalming solution at 18 °C for at least three months and up to 1 year or longer.[9,10]

The present study aimed to investigate, develop, and clarify the saturated salt embalming method. Furthermore, we radically evaluated SSS in all possible aspects: gross anatomy, applicability, histology, microbiology, and period of use.

MATERIALS AND METHODS

This study took place at the Faculty of Medicine Siriraj Hospital, Mahidol University, Thailand. The university institutional review board granted documentary proof of exemption, SIRB Protocol No. 500/2018 (Exemption). The study design is a descriptive study.

Eight legally donated cadavers with negative serologic tests for HIV, hepatitis B, hepatitis C, and venereal disease research laboratory (VDRL) were recruited. The cadavers were randomized into two groups: the submerged group (SG) and the non-submerged group (NSG), with equal gender distribution. The groups indicated the method of embalming. In case of embalming method failure, such as putrefy cadaver, unsuitable for dissection, observed along the process, the soon-to-be embalmed cadaver would be processed with the better method. Hence, the total number of recruited cadavers was eight (Table 1).

Oral and rectal swabs under sterile technique for bacterial, fungal culture and identification had been performed before embalming. The embalming solution contained 40% formaldehyde 0.5 L, isopropyl alcohol 4 L, phenol 0.2 L, glycerin 0.5 L, tab water 19.8 L, and 20 kilograms (kg) of sodium chloride resulting in a 25 L solution.[10] The solution was injected into a cadaver via the femoral artery with a pressure pump at 10 pounds/

TABLE 1. Demographic data and injected solution volumes.

Cadaver type	Code	Sex	Age (years)	Height (cm)	Weight (kg)	Cause of death	Death time to embalming		Embalming solution	
							Hours	Minutes	Planned amount (mL)	Injectable amount (mL)
Submerged cadavers`	SS6101	Female	83	149	70	Pulmonary Embolism	11	22	16	16
	SS6102	Male	68	150	60	Respiratory failure	24	0	17	17
Non-submerged cadavers	SS6103	Male	69	167	70	Cardiopulmonary failure	67	16	30	30
	SS6104	Female	74	150	70	Aging	92	10	26	26
	SS6105	Male	63	165	55	Hypertension	34	30	26	20
	SS6106	Male	86	150	45	Pulmonary infection	35	30	17	17
	SS6107	Female	64	170	70	Heart failure	70	30	26	24
	SS6108	Female	58	158	55	Asphyxia	57	10	23	23

inch.[3] The injected amount was based on the total body water, which was calculated by Watson's formula using the average height for Thai males (171 cm) and females (161 cm).[11,12] The mean ages came from the Siriraj cadavers' database, collected between 2012-2015 A.D. (70.5 years old from 805 males and 71.5 years old from 615 females). The NSG were injected with solution equal to 80% of their total body water, while the SG were injected with fluid equal to 50%. The actual injected amounts are presented in Table 1. Then the NSG were stored in a polyethylene bag, one bag per cadaver, at room temperature, the same method as Hayashi et al.[10] The SG were placed in a tank containing the embalming solution with the same composition as the injected. The storing process stopped after six months. Then, post-embalming oral and rectal swabs were taken for bacterial and fungal cultures.

Each cadaver underwent gross anatomy evaluation by randomly invited five physicians or anatomists in our department, who would be asked about their prior experiences regards experiences in the operating room as an assistant or a surgeon, experiences with each cadaver type, and cadaver number they have encountered for dissecting, instructing, and teaching. The pre-dissection evaluation assessed general appearance, joint flexibility, and consistency compared to living humans, fresh cadavers, and embalmed cadavers. The post-dissection evaluation items were the resemblance of tissues/body regions/organs compared to living humans or fresh cadavers; eye/nose/skin/hand irritation during dissection; odor; and suitability (e.g., for medical student dissection or surgical training). The evaluations results used a Likert scale, where 0 = no resemblance/no symptom/unpleasant odor/unsuitable for use, up to 5 = most resemblance/severe irritation/acceptable odor/most suitable for use.

Additional swabs for culture assessment were performed during dissection at the ileum (2 inches proximal to the ileocecal valve) and sigmoid (2 inches proximal to the rectum). Lung tissues were sent for acid-fast bacilli (AFB) staining and mycobacterial culture. Histological specimens were also collected in this process, including skin, skeletal muscle, smooth muscle, cardiac muscle, artery, nerve, ligament, heart, liver, intestines, and kidney. After performing hematoxylin and eosin (H&E) staining, the histological structures were evaluated on a Likert scale of zero (no resemblance) to five (most resemblance) by a pathologist comparing the specimens with standard textbook descriptions and photos.[13]

Statistical analysis

Data analysis was done using PASW Statistics software, version 18 (SPSS Inc.). Comparisons between evaluated items used the Kruskal–Wallis Test. P values <0.05 were defined as statistically significant. The Likert scale results were reported as frequency percentages.

RESULTS

Eight cadavers were recruited for the study: two cadavers in the SG and six in the NSG. Because after embalming for three months, the SG showed an insufficient quality for dissection due to stiffening, shrinkage, and distorted hands and feet (supplementary material). Consequently, the submerged method was then terminated.

Most of the evaluations (87%) were done by evaluators who have experience as surgeon assistants or surgeons (Total N = 30, five evaluators per cadaver). They had encountered more than 40 embalmed cadavers before this study. Eighty-three percent of them had dissected 1-10 fresh cadavers, and 97% had experienced 1-10 Thiel's cadavers. They mostly rated the NSG's consistency resemblance to living humans with a Likert scale of 3 (43.3%), fresh cadavers with a scale of 3 (70%), and Thiel's cadavers with a scale of 4 (56.7%). Kruskal–Wallis H test showed a statistically significant difference of $\chi2(2) = 8.081$, $p = 0.018$, comparing these three consistency evaluations. There was no statistically significant difference, $\chi2(2) = 3.531$, $p = 0.171$, comparing the NSG general appearance to a living human, fresh cadavers, and Thiel's cadavers. Table 2 shows the gross anatomy resemblance post-dissection evaluation results compared to living humans or fresh cadavers of various organs and body regions.

Fig 1 shows the thoracic region, abdominal region, and joint flexibility of the NSG. This method excellently preserved subcutaneous fat and muscles. The skin darkness was seen only in the superficial layer. After peeling this off, the dermis color was like a Thiel's cadavers skin color. The small and large NSG joints could be moved like in living humans. The selected Likert scales of the internal organs were mainly 3 and 4. However, cadavers SS6105 and SS6107 had putrefied thoracoabdominal organs. SS6105's ascending colon was perforated. Tumors were seeding in the intestinal wall, and there were numerous blood clots in the thorax. While SS6107's abdominal organs were thin and fluffy. There were tumors on both sides of the SS6107's lungs.

Forty-three percent of the evaluations showed no eye or nose irritation during dissection. Thirty-three percent were rated on a scale of 3, and the others scale of 2. Forty-seven percent had no hand irritation, thirty-three percent reported on scale 3, and the others on scale 2. The odor during dissection was highly acceptable (70% selected scale 4). The odor was an anchovy-like odor. However, it became more intense as time passed.

TABLE 2. The gross anatomy resemblance post-dissection evaluation compared to living humans or fresh cadavers of various organs and body regions.

Tissue resemblance to living humans or fresh cadavers	Selected likert scale (%)					
	0	1	2	3	4	5
Skin	0	10	63.3	23.3	3.3	0
Subcutaneous tissue	0	0	0	46.7	46.7	6.7
Vessel	0	0	0	30	60	10
Nerve	0	0	0	66.7	26.7	6.7
Fascia	0	0	0	13.3	76.7	10
Muscle	0	0	3.3	33.3	56.7	6.7
Cartilage	0	0	0	46.7	46.7	6.7
Ligament	0	0	0	60	36.7	3.3
Lymphatic tissue	0	0	0	56.7	40	3.3
Heart	0	0	3.3	30	63.3	3.3
Lung	0	3.3	0	60	33.3	3.3
Stomach	0	3.3	0	30	60	6.7
Small intestine	0	3.3	0	0	90	6.7
Large intestine	0	3.3	0	3.3	86.7	6.7
Kidney	0	3.3	0	70	20	6.7
Spinal cord	0	3.3	0	16.7	23.3	56.7
Brain	13.3	3.3	6.7	70	6.7	0
Body wall region	0	0	16.7	53.3	23.3	6.7
Head neck region	0	0	20	36.7	40	3.3
Pharynx and larynx region	0	0	6.7	36.7	53.3	3.3
CNS and organ of special senses region	0	0	13.3	43.3	43.3	0
Upper and lower limb region	0	0	0	66.7	23.3	10
Thorax region	0	0	3.3	53.3	36.7	6.7
Abdominal region	0	0	0	36.7	56.7	6.7
Perineum and pelvic region	0	0	16.7	36.7	40	6.7

Likert scale 0 = No resemblance, 5 = Most resemblance

The suitability for medical student anatomy class was a scale of 3 (53.3%) and 4 (46.7%), whereas suitability for surgical training was scale 4 (60%) and 3 (30%). The NSG brains were very soft and liquefied in most areas.

Table 3 shows the results from the pathologist who compared histological structure quality with textbook pictures. The tissues had some autolysis and pale nuclear staining but had identifiable structures. The captured histological slides are shown in the supplementary materials.

Before embalming, there were organisms in both the mouth and rectum, mostly microbiota. After embalming, the organisms were still present (Table 4). But all the intestinal and rectal swabs were negative for *Salmonella, Shigella, Vibrio, Aeromonas,* and *Plesiomonas shigelloides.* There was no mycobacterium in the AFB stains and no mycobacterial growth in the lung specimens. After dissection was finished, we observed the possible period that these cadavers could be used by leaving them in the laboratory at room temperature. After 4-6 weeks, we found fungal colonies growing on all the cadavers.

Fig 1. The thoracic region, abdominal region, and joint flexibility of the NSG.

TABLE 3. The histological resemblance compared to the reference picture in the standard textbook.

Tissue	Selected likert scale (%)					
	0	1	2	3	4	5
Skin (epidermis, dermis, subcutis)		0	60	0	40	0
Skin (basal layer)	40	0	0	0	60	0
Skin (melanocyte)	40	0	0	0	60	0
Skeletal muscle geography	0	0	0	40	60	0
Skeletal muscle	0	0	0	40	60	0
Smooth muscle	0	20	0	0	80	0
Cardiac muscle	0	40	20	40	0	0
Cardiac muscle: intercalated disc	80	20	0	0	0	0
Muscular artery	0	0	0	0	60	40
Small-sized artery	0	0	0	0	20	80
Medium-sized vein	0	0	0	0	40	60
Small-sized vein	0	0	0	0	0	100
Peripheral nerve	20	0	0	0	0	80
Ligament	0	0	0	0	40	60
Heart geography	0	0	0	0	60	40
Liver geography	0	20	0	0	0	80
Portal area	20	0	40	40	0	0
Duodenum	0	0	0	100	0	0
Jejunum	0	20	40	40	0	0
Ileum	0	40	40	20	0	0
Colon	0	20	40	40	0	0
Kidney geography	0	20	0	0	80	0
Renal Cortex	0	20	20	40	20	0
Renal Medulla	0	60	40	0	0	0

Likert scale 0 = No resemblance, 5 = Most resemblance

TABLE 4. Pre-embalming and post-embalming culture results

Organ	Culture type	SS6103		SS6104		SS6105		SS6106		SS6107		SS6108	
		Pre-embalming	Post-embalming	Pre-embalming	Post-embalming	Pre-embalming	Post-embalming	Pre-embalming	Post-embalming	Pre-embalming	Post-embalming	Pre-embalming	Post-embalming
Oral	Bacteria	Numerous mixed bacteria	Few mixed bacteria	Moderate microbiota	Rare microbiota	Numerous microbiota	Few microbiota	Numerous microbiota	Few microbiota	Numerous microbiota, Moderate Yeasts	Numerous microbiota	Numerous mixed bacteria, Numerous *Pseudomonas aeruginosa*, Numerous *Prevotella* spp.	Few microbiota
	Fungus	*Candida albicans*	Bacterial overgrowth	*Candida albicans*	Yeast seen in direct examination but no growth on culture	No growth	Bacterial overgrowth	*Candida albicans*	Bacterial overgrowth	Candida albicans	Bacterial overgrowth	*Candida tropicalis, Candida krusei*	Bacterial overgrowth
Rectum	Bacteria	Moderate microbiota	No growth	Numerous microbiota	No growth	Microbiota	*Clostridium perfringens, Clostridium* spp.	Moderate microbiota	No growth	Numerous microbiota	No growth	Numerous microbiota	*Clostridium perfringens, Clostridium* spp.
	Fungus	Bacterial overgrowth	No growth	Bacterial overgrowth	No growth	Bacterial overgrowth	Bacterial overgrowth	*Candida albicans*	No growth	Bacterial overgrowth	No fungal detected due to bacterial overgrowth	*Candida albicans, Candida species* (non-albicans, non-tropicalis, non-krusei)	No growth
Ileum	Bacteria	N/A	Microbiota	N/A	*Costridium perfringens*	N/A	No growth	N/A	No growth	N/A	No growth	N/A	No growth
	Fungus	N/A	No growth	N/A	Yeast seen in direct examination but no growth on culture	N/A	No growth	N/A	Bacterial overgrowth	N/A	Yeast seen in direct examination but no growth on culture.	N/A	Bacterial overgrowth
Sigmoid	Bacteria	N/A	No growth	N/A	*Clostridium perfringens*	N/A	*Clostridium perfringens*	N/A	*Clostridium perfringens*	N/A	No growth	N/A	No growth
	Fungus	N/A	No growth	N/A	Yeast seen in direct examination but no growth on culture	N/A	Bacterial overgrowth	N/A	Bacterial overgrowth	N/A	Bacterial overgrowth	N/A	Hyphae seen in direct examination but no growth on culture.
Lung	AFB	N/A	No AFB observed	N/A	No AFB observed	N/A	No AFB observed	N/A	No AFB observed	N/A	No AFB observed	N/A	No AFB observed
	Mycobacterium	N/A	No growth	N/A	No growth	N/A	No growth	N/A	No growth	N/A	No growth	N/A	No growth

DISCUSSION

Embalming technique and the gross evaluations

There are few publications concerning the human embalming technique with the saturated salt solution.[9,10,14] There is no standardization. Apart from Coleman and Kogan's and Hayashi et al.'s studies, Burns et al. injected 15-20 L of embalming fluid on the embalming day with an additional 1-5 L on the next day.[9,10,14] We hypothesized the volume should be at least 80% of the total body fluid in the NSG. Because in a 50 kg male cadaver, the injected fluid amount is 24.8 L by our calculation method, which is close to Coleman's study.[9] Our NSG storage technique was different from that of Coleman and Kogan. Their method involved storing a wrapped embalmed cadaver in the solution. Despite these differences, the gross evaluation of the NSG showed consistency, resembling Thiel's cadavers on a scale of 4 (56.7%) and fresh cadavers on a scale of 3 (70%). The gross tissue qualities resembled that of living humans or fresh cadavers on scales of 3 and 4 (Table 2). The NSG had excellent joint flexibility (Fig 1). These results are similar to previous studies performed in both human cadavers and rats.[6,10,14-16]

The NSG's brains were soft and mostly liquefied. This finding is similar to Thiel's solution embalming method, which has been shown to poor preserve the brain.[3,17] There is no prior report of brain morphology. However, a study of different salt concentration solutions to preserve human brain and liver slices found that saturated salt fluid can preserve brain slices without signs of decomposition.[18] This discordancy suggests there is room for further study.

We also tested the submerged method by directly placing cadavers in the fluid and decreasing the injected fluid amount. However, this was unsuccessful, which could have resulted from the cadavers' body fluids diffusing into the higher osmotic embalming fluid.

Histological evaluations

Coleman and Kogan reported the saturated salt method preserved adipose tissue, striated muscles, liver, and spinal cord microanatomy.[9] Beger et al. compared seven preservative methods on rat cadavers. They found that Thiel's and the saturated salt method had the same qualities as freshly preserved assessed by appearance, joint flexibility, and consistency. But Thiel's solution skin and internal organs were too pliable. The saturated salt method's skeletal muscles and tendons had similar properties to the fresh. But Thiel's solution muscles had less nuclear prominence and muscle fiber integrity.[16] We used another way to assess histological quality by comparing H&E-stained tissues to textbook pictures. Most of them were rated on Likert scales 4 and 5 (Table 3). It is presumed that the saturated salt with the non-submerged technique has preservative properties for the histological structures.

Microbiological evaluations

At 25 °C, 1 L of water can dissolve 360 grams of sodium chloride. The saturated salt solution molarity was 6.2 molar (M).[19] A study of pathogenic bacterial inoculated natural sheep casing showed that no non-spore-forming bacteria could be identified in the casing from brine at 6.2 M. The pathogenic bacteria in that study were *Escherichia coli, Salmonella typhimurium, Listeria monocytogenes, Staphylococcus aureus, Clostridium perfringens,* and *E. coli* O157:H7. The results showed that Gram-positive and spore-forming bacteria were more resistant to high osmotic pressure than the others, resulting in a need for at least 30-day preservation to eliminate the pathogens.[20]

Our study findings contradicted Hayashi et al.'s results. We found bacteria and fungus at the end of the embalming. The post-embalming pathogenic bacteria were *Clostridium perfringens* and *Pseudomonas aeruginosa*. Burns et al.'s study found fungal growth on SSS after using them for 15 days. There was no microbiological evidence of putrefaction in Burn et al.'s report. But we found bacteria in every NSG's intestine since the first dissection. We speculated that the climate in our country (Thailand) plays a role in microorganism growth since no prior SSS studies have been done in a tropical country.[6,9,10,14,21]

The putrefied cadavers

We found that the death records and post-mortem signs in cadavers SS6105 and SS6107 were mismatched. Both cadavers' internal organs had disrupted surfaces, whereby microbiomes could leak into the body cavities and ingest tissue right after death.[22] This also may have caused the lower injected fluid amount than planned in these two cadavers (Table 1). The cadavers might have entered the bloated stated before we embalmed.[22]

Application

A questionnaire-based study asking medical students, residents, and specialists from five Israel medical schools about how anatomy should be taught showed 87.8% of participants (Total N = 678) thought anatomy is relevant to general practitioners even in the age of the imaging and 68.8% agreed that dissection should be taught based on dissection, while only 13% agreed with image-based.[23] A preclinical education study found active learning enhanced learning outcomes and soft skills such as responsibility,

honesty, and kindness.[24] Cadaveric dissection is one way of active learning, which needs teamwork, responsibility, and intention to complete the assignment. Moreover, longitudinal integration such as cadaveric biopsy during dissection is helpful in pathology learning correlation, and practice suturing during dissection makes medical students at ease in the clinical year.[25,26] Recent research shows cadaver-based simulation also increases resident confidence and augments operative autonomy.[26] From previously studies and this research, saturated salt cadaver shows good quality for all these applications, but the embalming technique is still in need of perfection.[9,10,14,15,18]

Limitation

We have a limited cadaver number in this study since it's a pilot study. Moreover, the gross anatomy evaluators were randomly invited to avoid bias. In future research, more cadaver numbers and randomly selected staff forming an evaluator team to evaluate every cadaver may yield a different result.

CONCLUSION

The embalming technique by injecting the saturated salt solution at up to 80% total body water volume is a promising embalming method that yields cadavers with high gross tissue quality, flexible joints, and good histological structures. However, this technique cannot eliminate bacteria and normal flora. It may result from the tropical climate setting. Further study of this technique adjustment, such as changing the solution composition and storing cadavers in low-temperature conditions, is advised.

ACKNOWLEDGEMENT

This research project was supported by Faculty of Medicine Siriraj Hospital, Mahidol University, Grant Number (IO) R016232004.

REFERENCES

1. Balta JY, Cronin M, Cryan JF, O'Mahony SM. Human preservation techniques in anatomy: A 21st century medical education perspective. Clinical Anatomy. 2015;28(6):725-34.
2. Macchi V, Munari PF, Brizzi E, Parenti A, De Caro R. Workshop in clinical anatomy for residents in gynecology and obstetrics. Clin Anat. 2003;16(5):440-7.
3. Yiasemidou M, Roberts D, Glassman D, Tomlinson J, Biyani S, Miskovic D. A Multispecialty Evaluation of Thiel Cadavers for Surgical Training. World J Surg. 2017;41(5):1201-7.
4. Benkhadra M, Gerard J, Genelot D, Trouilloud P, Girard C, Anderhuber F, et al. Is Thiel's embalming method widely known? A world survey about its use. Surgical and radiologic anatomy : SRA. 2011;33(4):359-63.
5. Hammer N, Loffler S, Bechmann I, Steinke H, Hadrich C, Feja C. Comparison of modified Thiel embalming and ethanol-glycerin fixation in an anatomy environment: Potentials and limitations of two complementary techniques. Anat Sci Educ. 2015;8(1):74-85.
6. Homma H, Oda J, Sano H, Kawai K, Koizumi N, Uramoto H, et al. Advanced cadaver-based educational seminar for trauma surgery using saturated salt solution-embalmed cadavers. Acute Med Surg. 2019;6(2):123-30.
7. Durongphan A, Amornmettajit N, Rungruang J, Nitimanee E, Panichareon B. One academic year laboratory and student breathing zone formaldehyde level, measured by gas-piston hand pump at gross anatomy laboratory, Siriraj Hospital, Thailand. Environ Sci Pollut Res Int. 2020.
8. Durongphan A, Panichareon B, Ongsiriporn M, Piumpook N, Roongruangchai J. A Pilot Study of Measures Enhancing Local Ventilation System to Decrease Formaldehyde Level at Siriraj's Gross Laboratory. Siriraj Med J. 2019;71:S33-S8.
9. Coleman R, Kogan I. An improved low-formaldehyde embalming fluid to preserve cadavers for anatomy teaching. J Anat. 1998;192(Pt 3):443-6.
10. Hayashi S, Homma H, Naito M, Oda J, Nishiyama T, Kawamoto A, et al. Saturated salt solution method: a useful cadaver embalming for surgical skills training. Medicine (Baltimore). 2014;93(27):e196.
11. Watson PE, Watson ID, Batt RD. Total body water volumes for adult males and females estimated from simple anthropometric measurements. Am J Clin Nutr. 1980;33(1):27-39.
12. Collaboration NCDRF. A century of trends in adult human height. Elife. 2016;5.
13. Young B, O'Dowd G, Woodford P. Wheater's functional histology : a text and colour atlas. 6th ed. Philadelphia, PA: Churchill Livingston, Elsevier; 2014.
14. Burns DM, Bell I, Katchky R, Dwyer T, Toor J, Whyne CM, et al. Saturated Salt Solution Cadaver-Embalming Method Improves Orthopaedic Surgical Skills Training. J Bone Joint Surg Am. 2018;100(15):e104.
15. Shirai T, Hayashi S, Itoh M. Experience of Raising Flaps Using Cadavers Embalmed by Saturated Salt Solution Method. Plast Reconstr Surg Glob Open. 2015;3(10):e543.
16. Beger O, Karagul MI, Koc T, Kayan G, Cengiz A, Yilmaz SN, et al. Effects of different cadaver preservation methods on muscles and tendons: a morphometric, biomechanical and histological study. Anat Sci Int. 2020;95(2):174-89.
17. Miyake S, Suenaga J, Miyazaki R, Sasame J, Akimoto T, Tanaka T, et al. Thiel's embalming method with additional intra-cerebral ventricular formalin injection (TEIF) for cadaver training of head and brain surgery. Anat Sci Int. 2020;95(4):564-70.
18. Jumlongkul A TP. Comparison between formaldehyde and salt solutions for preservation of human liver and brain slices. Chula Med J. 2017;61(1):17-30.
19. Burgess J. Metal ions in solution. Chichester New York: Ellis Horwood; distributed by Halsted Press; 1978. p. 481.
20. Wijnker JJ, Koop G, Lipman LJ. Antimicrobial properties of salt (NaCl) used for the preservation of natural casings. Food Microbiol. 2006;23(7):657-62.
21. Pinheiro J. Decay process of a cadaver. In: Schmitt A CE, Pinheiro J, editor. Forensic anthropology and medicine. Totowa:

Humana Press; 2006. p. 85-116.
22. Lee Goff M. Early post-mortem changes and stages of decomposition in exposed cadavers. Exp Appl Acarol. 2009;49(1-2):21-36.
23. Marom A, Tarrasch R. On behalf of tradition: An analysis of medical student and physician beliefs on how anatomy should be taught. Clin Anat. 2015;28(8):980-4.
24. Imwattana K DY, Ngamskulrungroj P. Active learning classes in a preclinical year may help improving some soft skills of medical students. Siriraj Med J. 2020;72(5):415-23.
25. Lavezo JL BE, Lacy NL, Hogg T, Padilla O, Manglik N, et al. Cadaver biopsies positively impact the Medical Student Educational Experience. Medical Science Educator. 2017;27(3):543-7.
26. Manning EP, Mishall PL, Weidmann MD, Flax H, Lan S, Erlich M, et al. Early and prolonged opportunities to practice suturing increases medical student comfort with suturing during clerkships: Suturing during cadaver dissection. Anat Sci Educ. 2018;11(6):605-12.

Deep Peroneal Nerve: Orientation and Branching at the Ankle and Proximal Part of the Foot

Chairat Turbpaiboon, M.D., Ph.D.*, Rungsarit Sunan, M.Sc., Darunee Rodma, M.Sc.**, Sukrit Promtang, M.Sc.***, Anup Pandeya, M.Sc.****, Rosarin Ratanalekha, M.D.*, Woratee Dacharux, M.D.***

**Department of Anatomy, Faculty of Medicine Siriraj Hospital, Mahidol University, Bangkok 10700, Thailand, **Division of Basic and Medical Sciences, Faculty of Allied Health Sciences, Pathumthani University, Pathum Thani 12000, Thailand, ***Molecular Medicine Program, Faculty of Science, Mahidol University, Bangkok 10400, Thailand, ****Department of Anatomy, Devdaha Medical College and Research Institute, Kathmandu University Extended Program, Rupandehi, Nepal.*

ABSTRACT

Objective: This study investigated the frequency and types of 1) orientation of the deep peroneal nerve (DPN) and its branches relative to the dorsalis pedis artery (DPA) and the extensor hallucis longus tendon (EHLT) and 2) branching site and pattern of DPN at the distal area of leg and the proximal zone of the foot.

Materials and Methods: One-hundred and sixty specimens from the lower extremities of 80 formalin-embalmed cadavers were investigated for anatomical position, orientation and the branching pattern of DPN by manual dissection, starting from the anterior side of lower extremity just proximal to ankle joint down to the area distal to inferior extensor retinaculum.

Results: The most prevalent medial-to-lateral orientation of structures in the area anterior to ankle joints was the EHLT/DPA/DPN. Comparing DPA with the branching of DPN in the areas inside anterior tarsal tunnel (ATT) and distal to ATT, the most common type was an orientation of DPA that was lateral to both the DPN main trunk and its medial terminal branch. Regarding branching sites and patterns of DPN in the intermalleolar and ATT areas, nearly half of the studied specimens had DPN bifurcation at the intermalleolar level and more than half of the bifurcations were inside the ATT.

Conclusion: This study establishes novel data regarding type variation and prevalence of DPN in areas of ankle and proximal part of foot in the Thai population which could be helpful in clinical practice.

Keywords: Deep peroneal nerve; inferior extensor retinaculum; anterior tarsal tunnel; dorsalis pedis artery; extensor hallucis longus tendon (Siriraj Med J 2022; 74: 440-447)

INTRODUCTION

The deep peroneal nerve (DPN) is composed of both sensory and motor components that innervate certain regions of the lower extremity.[1] At the neck of fibula, DPN branches from the common peroneal nerve, which is one division of the sciatic nerve, and distally terminates as dorsal digital nerves (cutaneous nerves) at the first interdigital cleft of the dorsum of foot. While passing through the anterior compartment of the leg, DPN provides muscular branches and runs downward along the anterior tibial vessels laterally. At the distal part of the leg, DPN runs superficially in companion with the dorsalis pedis artery (DPA, the artery continuing from the anterior tibial artery) and the extensor hallucis

Corresponding author: Woratee Dacharux
E-mail: woratee.dah@mahidol.edu
Received 22 March 2022 Revised 16 April 2022 Accepted 25 April 2022
ORCID ID: https://orcid.org/0000-0003-1038-7002
http://dx.doi.org/10.33192/Smj.2022.53

longus tendon (EHLT). Before passing the dorsum of the foot, the course of DPN is beneath both the superior and inferior extensor retinacula (IER) and is part of the anterior tarsal tunnel (ATT, the roof of which is the IER). After running over the talus bone, DPN bifurcates into the medial terminal branch (MTB) and lateral terminal branch (LTB). The MTB and LTB then accompany the DPA and the lateral tarsal artery, respectively.[2]

Typically, DPN and MTB are located laterally to the DPA. However, variations in DPN orientation and branching have been reported and this reveals their inconsistency.[3,4] These variations mostly concern certain surgical approaches in the leg and foot areas involved with the courses of DPN and also structures supplied by DPN, e.g. ankle arthroscopy, ultrasound-guided DPN block and neurovascular flap surgery. The aim of this study was to investigate 1) the types and frequencies of orientation of DPN and its branches (MTB and LTB) relative to its neighboring structures (DPA and EHLT) and 2) the types and frequencies of the branching site and pattern of DPN at the distal area of the leg and the proximal zone of foot. These findings play a crucial role in providing safety information for surgeons and anesthetists to ensure high accuracy and effectiveness of clinical practice with DPN and to reduce the risk of nearby structures.

MATERIALS AND METHODS

This study was conducted in 80 formalin-embalmed cadavers donated to the Department of Anatomy, Faculty of Medicine Siriraj Hospital, Mahidol University, Thailand for academic and research purposes. This research project was approved by the Siriraj Institutional Review Board (Si 186/2020). One-hundred and sixty specimens of lower extremities were investigated for anatomical position, orientation and branching pattern of DPN by manual dissection starting from the area of anterior side of lower extremity just proximal to ankle joint down to the area distal to IER. The dissected zone was horizontally enlarged to adequately visualize the related anatomical information. Results from the right-sided and left-sided specimens were compared for correlation.

RESULTS

Each Thai cadaver was studied for orientation of DPN, DPA and EHLT in the areas anterior to both ankles. Branching of DPN to MTB and LTB and their courses were also compared with orientation of DPA. The DPN branching site was identified to determine its location in relation to an imaginary line, connecting medial and lateral malleoli, and ATT. The demographic data of 80 cadavers were as follows: age range = 36-104 (mean = 73.6; SD = 14.4) and gender (male/female = 44/36).

Numbers and percentages of the medial-to-lateral orientation of DPN, DPA and EHLT in the area anterior to the ankle joint are summarized in Table 1. All six possible types of orientations were identified in this study. Type O1 (EHLT/DPA/DPN) was the most common and type O4 (DPA/EHLT/DPN) was the least prevalent. Examples of the common types are shown in Fig 1. The course of the DPA was investigated by comparing the branching of DPN to MTB and LTB in areas inside the ATT and distal to ATT (Table 2). The most common type was the orientation of DPA lateral to both DPN main trunk and MTB (type A4). This type was identified in nearly 40% of the studied specimens. Moreover, complex orientation of DPA and DPN as multiple crossings over each other (type A5) was low in prevalence at about 3.1%. However, one specimen was identified as having no MTB and thus, DPA was found to be medial to LTB below ATT (type A6). Three most-common types of orientation are shown in Fig 2.

Branching sites and patterns of DPN were studied in the intermalleolar and ATT areas (Table 3). Almost half of the studied specimens had bifurcation of DPN at the same vertical level as the intermalleolar line (type L2), while the majority of the remaining specimens had bifurcation distal to this line (type L3). Being relative to IER, more than half of DPN bifurcations were localized inside the ATT (type R2) whereas the bifurcations distal to the ATT (type R3) were the least identified. However, 1.3% of the studied specimens had multiple DPN branching (type M) and 0.6% of the studied specimens had no DPN branching (type N). The most and the least prevalent types of DPN bifurcation sites are demonstrated in Figs 3A-3D and multiple branching of DPN visualized in Fig 3E.

Correlations between results from right-sided and the left-sided specimens in this study were similar among different investigated parameters. The percentages of side correlation in the DPN, DPA and EHLT orientations were slightly higher than the orientation between DPA and DPN trunks and branches.

DISCUSSION

As this study focused on the DPN at the lower area of the leg, near the proximal part of the foot, the orientation of the DPN main trunk together with its companions anterior to the ankle was examined first (Table 1). The classic medial-to-lateral orientation of EHLT/DPA/DPN (type O1) was found in about half of all observations. The second-most prevalent type was the EHLT/DPN/

TABLE 1. Numbers and percentages of types of medial-to-lateral orientation of DPN (*N*), DPA (*A*) and EHLT (*T*) at the area anterior to ankle joint.

	Type O1: *T-A-N*	Type O2: *T-N-A*	Type O3: *A-N-T*	Type O4: *A-T-N*	Type O5: *N-A-T*	Type O6: *N-T-A*	Side correlation
No. of specimens detected	81	61	6	2	5	5	48 cadavers
(percentage)	(50.6)	(38.1)	(3.8)	(1.3)	(3.1)	(3.1)	(60)

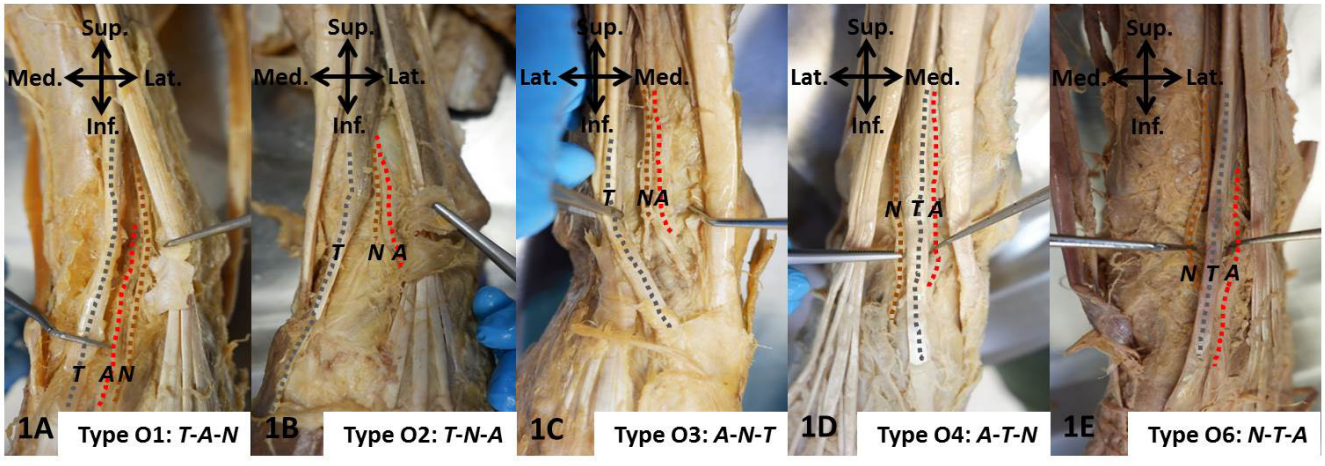

Fig 1. Examples of common types of medial-to-lateral orientation of DPN (*N*, brown dashed line), DPA (*A*, red dashed line) and EHLT (*T*, gray dashed line) at the area anterior to ankle joint.

TABLE 2. Course of DPA compared with the branching of DPN to MTB and LTB in the areas of ATT and distal to ATT.

	Type A1: DPA was medial to DPN in ATT and medial to MTB of DPN below ATT	Type A2: DPA was medial to DPN in ATT and lateral to MTB of DPN below ATT	Type A3: DPA was lateral to DPN in ATT and medial to MTB of DPN below ATT	Type A4: DPA was lateral to DPN in ATT and lateral to MTB of DPN below ATT	Type A5: DPN and DPA crossed over each other at multiple levels	Type A6: No MTB of DPN, DPA was medial to LTB of DPN below ATT	Side correlation
No. of specimens detected	38	40	16	60	5	1	46 cadavers
(percentage)	(23.8)	(25)	(10)	(37.5)	(3.1)	(0.6)	(57.5)

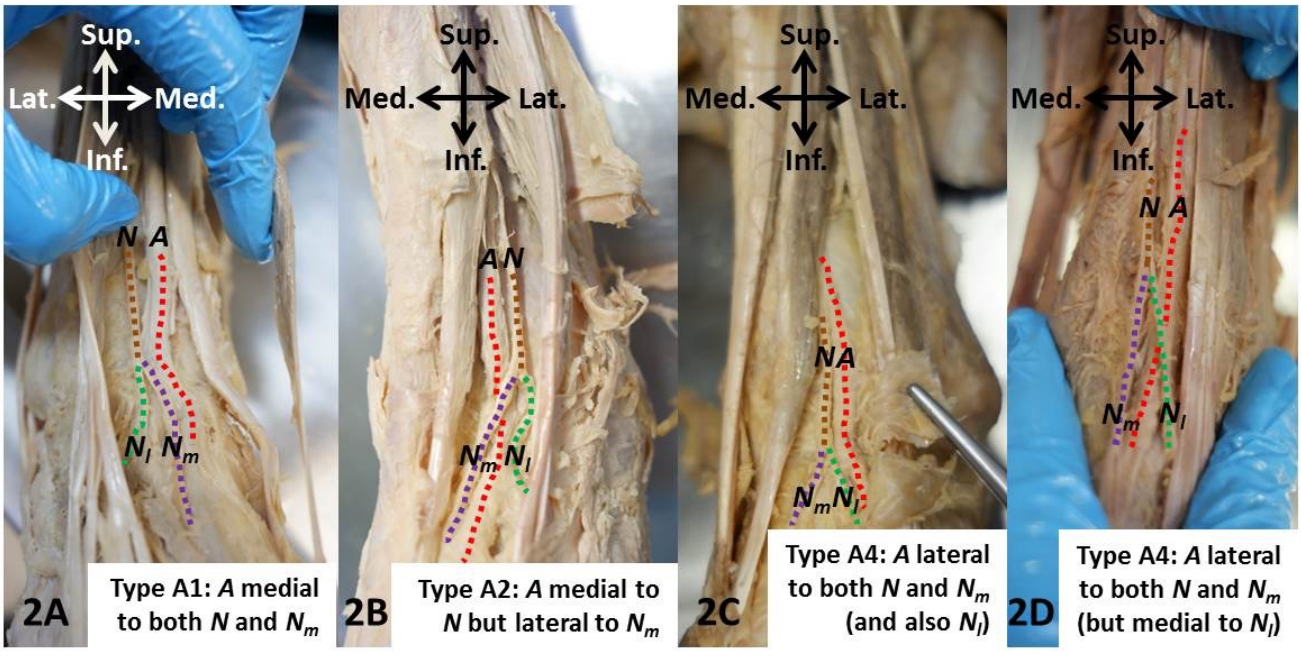

Fig 2. The three most-common types of the course of DPA compared with the branching of DPN to MTB and LTB in ATT and areas distal to ATT. (*N*, brown dashed line = DPN main trunk; *A*, red dashed line = DPA; *Nm*, purple dashed line = MTB; *Nl*, green dashed line = LTB)

TABLE 3. Branching sites and patterns of DPN in the intermalleolar and ATT areas.

	Presence of bifurcation to MTB and LTB						Type M: Presence of multiple branching of DPN	Type N: Absence of branching
	Compared with imaginary line connecting medial and lateral malleoli			Compared with IER (or ATT)				
	Type L1: Proximal to imaginary line	Type L2: Midway between medial and lateral malleoli	Type L3: Distal to imaginary line	Type R1: Proximal to IER (above ATT)	Type R2: Posterior to IER (in ATT)	Type R3: Distal to IER (below ATT)		
No. of specimens detected	17	65	55	45	69	9	2	1
(percentage)	(12.4)	(47.4)	(40.2)	(36.6)	(56.1)	(7.3)	(1.3)	(0.6)

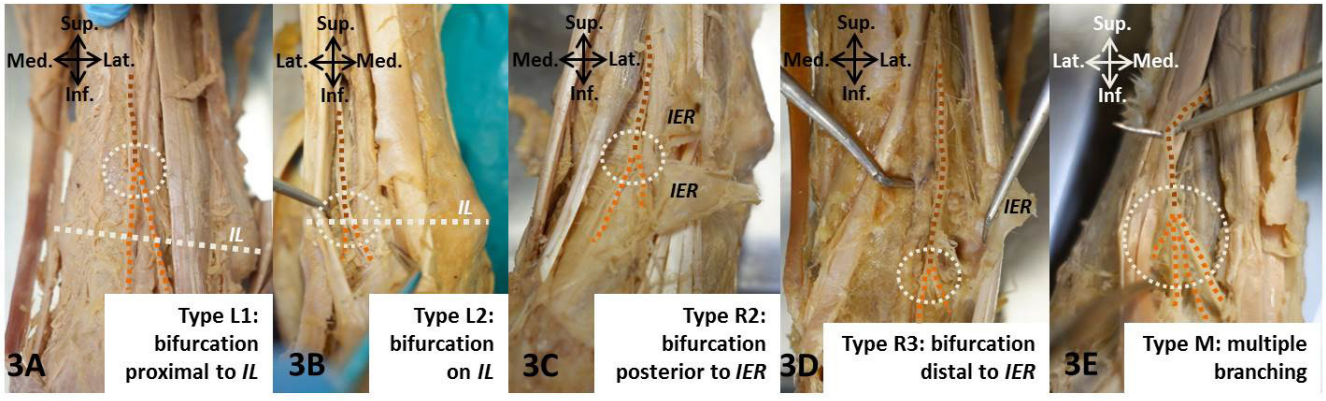

Fig 3. The most and the least prevalent types of DPN bifurcation site (3A-3D) in the intermalleolar and ATT areas, and the multiple branching of DPN (3E). (*IL*, white dashed line = imaginary line connecting medial and lateral malleoli; white dashed circle = area of DPN branching; brown dashed line = DPN main trunk; orange dashed line = branches of DPN)

DPA orientation (type O2) in about 40% of all cases. This means that EHLT was mostly found as the medial-most structure while DPN and DPA could be interchangeable. By using EHLT as a fixed medial landmark, this is useful for clinical procedures involving the area anterior to the ankle joint (e.g. ultrasound-guided DPN block and ankle arthroscopy). Nonetheless, orientation similarity of both sides can be implemented in only about 60% of cases.

A further investigation was performed to observe patterns of orientation of DPN at the branching level (MTB and LTB). A total of six patterns were found in this study (Table 2). Surprisingly, the classic orientation type (type A1: DPA was medial to DPN in ATT and medial to MTB of DPN below ATT) was not the most prevalent but rather type A4 (DPA located laterally). This result contrasts previous studies which show DPA located medially to MTB (types A1 and A3) and medially to DPN (types A1 and A2) being most prevalent (76% and 92.9%, respectively).[2,5] Nevertheless, the prevalence of DPA types located medially to the DPN main trunk in ATT (type A1: 23.8% and type A2: 25%) were not much different than the previous study (type A1: 36.1% and type A2: 25%).[3] The observation of DPN and DPA crossing over each other at multiple levels (type A5: 3.1%) was slightly less than in one previous study (8.4%)[4] and significantly less frequent than in another study (30.6%).[3] The prevalence of instances of no MTB found (type A6: 0.6%) was low, and much rarer than in a previous observation (8.3%).[3] To use these six types in practice, side similarity can be implied with a confidence level of nearly 60%.

Variations of the DPN branching level was also observed in our specimens. There were two stable landmarks used for positional reference. The first was an imaginary line connecting the medial and lateral malleoli as an intermalleolar line, the vertical level of which was approximately assumed as the level of ankle mortise. The other was the IER, which superficially covers the ATT. These two landmarks were independently located, so the IER was equally proximal, anterior, and distal to the ankle mortise.[2] In this study, bifurcation of DPN, either proximal to (type L1) or at the intermalleolar level (type L2), was high in frequency, or about 60%, but a significantly lower frequency was reported in a previous study (23%).[2] When considered in separate categories, DPN bifurcations at the intermalleolar line (type L2) and distal to it (type L3) were twice as high in prevalence than a previous study (47.4% vs 21% and 40.2% vs 27%, respectively).[4] In the case of an IER landmark, specimens with DPN bifurcation in the ATT observed in this study (type R2) gave the highest prevalence similar to a previous report. However, the prevalence was to a much different extent (56.1% vs 86.1%).[6] Interestingly, DPN bifurcation proximal to IER (type R1) has not been previously observed at high frequency as reported in this study (36.6%). Meanwhile, bifurcation below ATT (type R3) was comparable to a prior study (7.3% vs 5.6%).[6] The absence of branching (type N) and multiple branching (type M) was also found in this study at a low frequency like other studies.[4,6]

In addition to the studies aforementioned, there still have been a number of studies regarding the structural variation of both DPN and DPA by presenting significantly diverse data on type and prevalence which depended on either numbers of studied specimen or cadaveric ethnicity. For example, a study on DPA course compared to DPN branching performed in an Asian population revealed the different levels of variation prevalence from our current study.[7] The most- and least-common types found in

this study were the types A1 and A6 at 36.7% and 6.7%, respectively, in prevalence while the types A2 and A5 were about 30% and 26.7%, respectively. Interestingly, there was no existence of types A3 and A4 in this study. Not only the courses of DPN and DPA that have been widely investigated but the branching pattern of DPN has also been focused. For instance, it has been found for many decades in other ethnic groups that the termination of DPN can also exist in multiple branching similar to the type M reported in our current study, not only the bifurcation into MTB and LTB.[8] In terms of positional variation for applying in clinical entrapment of DPN, various etiologies has been discovered other than the ATT syndrome caused by IER entrapment.[9] Compression by the extensor hallucis brevis muscle can be a cause that has been reported.[10] Likewise, fascia around the areas of tarsal and metatarsal bones were also considered as the possible structural constraint for DPN.[11] Therefore, further variation study in our population to demonstrate the incidence of each etiology causing the ATT syndrome in the patients is required.

Another structural variation that has been commonly found in other populations and is worth determining its prevalence in our population is the accessory deep peroneal nerve (ADPN) which branches from the superficial peroneal nerve. It carries the motor component to supply several muscles including certain or total parts of the extensor digitorum brevis (EDB)[12,13] and the sensory innervation for areas of fibula periosteum, lateral zone of ankle and metatarsal area.[14,15] ADPN has been previously investigated by either manual dissection in cadaveric specimens or electrophysiological study in plenty of studies. According to the meta-analysis of these studies[16], the pooled prevalence of ADPN existence and EDB innervation by ADPN once existing were about 18.8% and 79.5%, respectively. No significant difference between the males and females in ADPN prevalence was detected.[17] By investigating the inheritance among the family members of the ADPN presence, the autosomal dominant mode was suggested.[18]

Besides the variations detected in DPN course and branching, the arterial system that runs parallelly with DPN also displays its variation in several patterns as encountered in several cadaveric and angiographic studies. Starting from the constant anterior tibial artery (ATA) that mostly lies medially to the DPN except for the middle-third of this nerve, leading to another name of DPN as nervus hesitans, the distal part (DPA) inconstantly varies in its orientation into several types as described in Table 1. In some studies, 8% of investigated DPA were found to arise from arteries other than the single direct extension from ATA.[19] At the level of ankle joint, only 58% of studied specimens were found to branch medially (36%), laterally (55%) or even bilaterally (9%) in previous study.[20] These findings are useful for being aware of the risk in pseudoaneurysm formation during ankle arthroscopy or anterior hindfoot surgery. Apart from the orientation variation of the distal part of DPA described in Table 2, there have been additional variations in terms of number, location and also its branching pattern.[21-23] For example, distance variation due to DPA location in relation to the tarsal navicular bone was established to provide the practical data for the midfoot surgery.[21] In the sense of number, this artery itself can be found in double or even the increase in distal branching as atypical trifurcation.[23] Furthermore, the branching patterns on the dorsum of foot were surprisingly various as classified up to 9 types with the typical pattern at only 36.4% in prevalence.[22] All of these knowledge play an important role in reducing the risk of complications from intervention dealing with this artery or the structures nearby, eg., nerves, bones and joints.

DPN is a nerve that courses profoundly among the muscular tissue in the leg compartment and superficially beneath the cutaneous tissue as found in 1) the neck of the fibula as the part branching from the common peroneal nerve and 2) the area anterior to the ankle joint before running down to the ATT. Anatomical variations of the former part of DPN in Thais has been studied by Chompoopong *et al.* to avoid an iatrogenic injury caused during fibular biopsy[24] while variations in the latter were examined in this study. However, our findings are in agreement and disagreement with previous studies. This can be elucidated by two explanations: the difference in ethnicities of the investigated cadavers and the numbers of cadavers used in each study. A sufficient number of specimens were included in this study in order to achieve high reliability of the results and to reach

Variability in type and prevalence in the course of DPN and its branching pattern found in this study can be used in clinical practice under various contexts such as population-specific treatment. The main application of this research is the direct procedures on DPN and its branches, eg. nerve block[25,26], nerve stimulation and conduction study[27,28], surgical nerve transfer[29] and flap surgery for lower extremity reconstruction which is commonly operated on in a tertiary-care center.[30] In addition, another useful aspect is to minimize iatrogenic injuries of structures surrounding the DPN during certain procedures such as ankle arthroscopy and surgery in the ankle and foot areas.[31] Likewise, certain natures of the

DPN unveiled in this study can also correlate to clinical imaging information[32,33] and be used to predict clinical neurovascular consequences following a traumatic injury or treatment in the ankle and foot region.[34]

CONCLUSION

Based on the specimens, this study provides novel information on the type of variation and prevalence of DPN in the ankle and proximal part of the foot in the multiracial population inhabiting in Thailand. Therefore, this information can be used to help update population-specific clinical databases in this region. Due to significant differences found in our study when compared with data from other studies in other population groups, our study confirms that population-specific studies on structural variation is required before application in practice.

ACKNOWLEDGEMENTS

The authors are grateful to Dr. Supin Chompoopong, Dr. Pawinee Pangthipampai and Dr. Prae Plansangkate for their guidance and suggestions in this study. The authors would also like to thank the teaching assistants (departmental interns) from the Department of Anatomy, Faculty of Medicine Siriraj Hospital for their help during this study. CT, RR and WD were supported by the Siriraj Chalermphrakiat Grant, Faculty of Medicine Siriraj Hospital, Mahidol University.

Conflict of interest: The authors declare no conflicts of interest.

REFERENCES

1. Standring S. Gray's anatomy: the anatomical basis of clinical practice. 41st ed. Philadelphia: Elsevier; 2016.
2. Lawrence SJ, Botte MJ. The deep peroneal nerve in the foot and ankle: an anatomic study. Foot Ankle Int. 1995;16(11):724-8.
3. Ikiz ZAA, Ucerler H, Uygur M. The clinical importance of the relationship between the deep peroneal nerve and the dorsalis pedis artery on the dorsum of the foot. Plast Reconstr Surg. 2007;120(3):690-6.
4. Ranade AV, Rajanigandha V, Rai R, Ebenezer DA. Relationship between the deep peroneal nerve and dorsalis pedis artery in the foot: a cadaveric study. Clin Anat. 2008;21(7):705-12.
5. Rab M, Ebmer J, Dellon AL. Innervation of the sinus tarsi and implications for treating anterolateral ankle pain. Ann Plast Surg. 2001;47(5):500-4.
6. Aktan Ikiz ZA, Ucerler H, Uygur M. Dimensions of the anterior tarsal tunnel and features of the deep peroneal nerve in relation to clinical application. Surg Radiol Anat. 2007;29(7):527-30.
7. Chitra R. The relationship between the deep fibular nerve and the dorsalis pedis artery and its surgical importance. Indian J Plast Surg. 2009;42(1):18-21.
8. Geller M, Barbato D. Nervus peronaeus profundus. Terminal branches and their variations. Hospital (Rio J). 1970;77(2):679-98.
9. Andresen BL, Wertsch JJ, Stewart WA. Anterior tarsal tunnel syndrome. Arch Phys Med Rehabil. 1992;73(11):1112-7.
10. Reed SC, Wright CS. Compression of the deep branch of the peroneal nerve by the extensor hallucis brevis muscle: a variation of the anterior tarsal tunnel syndrome. Can J Surg. 1995;38(6):545-6.
11. Dellon AL. Deep peroneal nerve entrapment on the dorsum of the foot. Foot Ankle. 1990;11(2):73-80.
12. Lambert EH. The accessory deep peroneal nerve. A common variation in innervation of extensor digitorum brevis. Neurology. 1969;19(12):1169-76.
13. Murad H, Neal P, Katirji B. Total innervation of the extensor digitorum brevis by the accessory deep peroneal nerve. Eur J Neurol. 1999;6(3):371-3.
14. Kudoh H, Sakai T, Horiguchi M. The consistent presence of the human accessory deep peroneal nerve. J Anat. 1999;194 (Pt 1):101-8.
15. Prakash, Bhardwaj AK, Singh DK, Rajini T, Jayanthi V, Singh G. Anatomic variations of superficial peroneal nerve: clinical implications of a cadaver study. Ital J Anat Embryol. 2010;115(3):223-8.
16. Tomaszewski KA, Roy J, Vikse J, Pekala PA, Kopacz P, Henry BM. Prevalence of the accessory deep peroneal nerve: A cadaveric study and meta-analysis. Clin Neurol Neurosurg. 2016;144:105-11.
17. Sinanovic O, Zukic S, Muftic M, Tinjic N. Prevalence of Accessory Deep Peroneal Nerve in Sample of Bosnia and Herzegovina Subjects: an Electrophysiological Study. Acta Inform Med. 2021;29(3):193-6.
18. Crutchfield CA, Gutmann L. Hereditary aspects of accessory deep peroneal nerve. J Neurol Neurosurg Psychiatry. 1973;36(6):989-90.
19. George A, Alex L, George A. Variations in the origin of dorsalis pedis artery. Indian Journal of Clinical Anatomy and Physiology. 2021;7(4):354-62.
20. Parikh S, Dawe E, Lee C, Whitehead-Clarke T, Smith C, Bendall S. A cadaveric study showing the anatomical variations in the branches of the dorsalis pedis artery at the level of the ankle joint and its clinical implication in ankle arthroscopy. Ann R Coll Surg Engl. 2017;99(4):286-8.
21. Rimchala C, Chuckpaiwong B. Relationship of the dorsalis pedis artery to the tarsal navicular. J Foot Ankle Surg. 2015;54(1):66-8.
22. Ntuli S, Nalla S, Kiter A. Anatomical variation of the Dorsalis pedis artery in a South African population - A Cadaveric Study. Foot (Edinb). 2018;35:16-27.
23. Hemamalini, Manjunatha HN. Variations in the origin, course and branching pattern of dorsalis pedis artery with clinical significance. Sci Rep. 2021;11(1):1448.
24. Chompoopong S, Apinhasmit W, Sangiampong A, Amornmettajit N, Charoenwat B, Rattanathamsakul N, et al. Anatomical considerations of the deep peroneal nerve for biopsy of the proximal fibula in Thais. Clin Anat. 2009;22(2):256-60.
25. Johnston S, Kraus J, Tutton S, Symanski J. Ultrasound-guided diagnostic deep peroneal nerve blocks prior to potential neurectomy: a retrospective review. Skeletal Radiol. 2020;49(8):1313-21.
26. Fletcher T, Orgill BD, Barth B. Deep Peroneal Nerve Block. StatPearls. Treasure Island (FL)2022.

27. Lo YL, Leoh TH, Dan YF, Tan YE, Nurjannah S, Fook-Chong S. An electrophysiological study of the deep peroneal sensory nerve. Eur Neurol. 2003;50(4):244-7.
28. Kim KH, Kim DH, Yun HS, Park BK, Jang JE. Optimal stimulation site for deep peroneal motor nerve conduction study around the ankle: cadaveric study. Ann Rehabil Med. 2012;36(2):182-6.
29. Koshima I, Nanba Y, Tsutsui T, Takahashi Y. Deep peroneal nerve transfer for established plantar sensory loss. J Reconstr Microsurg. 2003;19(7):451-4.
30. Akaranuchat N. Lower Extremity Reconstruction with Vascularized Free-Tissue Transfer: 20 Years of Experience in the Faculty of Medicine Siriraj Hospital, Mahidol University, Bangkok, Thailand. Siriraj Med J. 2021;73(7):462-70.
31. Lui TH. Extensor tendons and deep peroneal nerve adhesion: Treated by complete anterior ankle arthroscopic capsulotomy. Foot Ankle Surg. 2012;18(1):e1-3.
32. Becciolini M, Pivec C, Riegler G. Ultrasound Imaging of the Deep Peroneal Nerve. J Ultrasound Med. 2021;40(4):821-38.
33. Sakci Z, Aydin F, Tuncer K, Ogul H. Demonstration With Three-Dimensional Volumetric Magnetic Resonance Sequences of Deep Peroneal Nerve Compression on Os Intermetatarseum Syndrome. Am J Phys Med Rehabil. 2021;100(8):e116-e7.
34. Meyerkort DJ, Gurel R, Maor D, Calder JDF. Deep Peroneal Nerve Injury Following Hardware Removal for Lisfranc Joint Injury. Foot Ankle Int. 2020;41(3):320-3.

Deep Peroneal Nerve: From an Anatomical Basis to Clinical Implementation

Chairat Turbpaiboon, M.D., Ph.D.*, Chapa Puprasert, M.D., Suphalerk Lohasammakul, M.D.*, Woratee Dacharux, M.D.*, Terasut Numwong, M.D.*, Anup Pandeya, M.Sc.***, Arin Pisanuwongse, M.D.****, Adisak Kasemassawachanont, M.D.***

Department of Anatomy, Faculty of Medicine Siriraj Hospital, Mahidol University, Bangkok 10700, Thailand, ** Department of Physical Medicine and Rehabilitation, Lerdsin Hospital, Bangkok 10500, Thailand, * Department of Anatomy, Devdaha Medical College and Research Institute, Kathmandu University Extended Program, Rupandehi, Nepal, **** Department of Radiology, Faculty of Medicine Siriraj Hospital, Mahidol University, Bangkok 10700, Thailand.*

ABSTRACT

The deep peroneal nerve (DPN) is considered one of the clinically significant nerves of the lower extremity since several clinical abnormalities can commonly be caused by its defects, either in its sensory or motor functions. Its derivatives, classified as muscular, cutaneous, and articular, mainly supply the muscles in the anterior fascial compartment of the leg and the dorsum of the foot, the 1st dorsal web space of the foot, the ankle joint, and certain joints of the foot. To improve the effectiveness of clinical practices involving the DPN, it is important to first understand its anatomical nature, including its typical characteristics and the variants (orientation, branching, and analogous structure), prior to applying such practices in clinical implementation. This review, therefore, aims to review the previously studied information of DPN on its fundamental anatomy and link it to the provided examples of current commonly used procedures, both non-invasive and invasive, e.g., nerve imaging, nerve block, neuro-electrophysiological study, and free autologous tissue transfer, thereby giving an integrated view in the translational medicine of DPN. Conclusively, the ultimate goal of this review is to help maximize the therapeutic effectiveness and to minimize the unanticipated complications of any clinical practices involving the DPN by inferring from its anatomical knowledge.

Keywords: Deep peroneal nerve; accessory deep peroneal nerve; nerve imaging; nerve block; electrophysiological study; surgical reconstruction (Siriraj Med J 2022; 74: 448-462)

Abbreviations: DPN; deep peroneal nerve, CPN; common peroneal nerve, PL; peroneus longus, EDL; extensor digitorum longus, ATA; anterior tibial artery, TA; tibialis anterior, EHL; extensor hallucis longus, SER; superior extensor retinaculum, IER; inferior extensor retinaculum, DPA; dorsalis pedis artery, MTB; medial terminal branch, LTB; lateral terminal branch, SPN; superficial peroneal nerve, LTA; lateral tarsal artery, EDB; extensor digitorum brevis, EHB; extensor hallucis brevis, ATT; anterior tarsal tunnel, ADPN; accessory deep peroneal nerve, PB; peroneus brevis, US; ultrasonography, MRI; magnetic resonance imaging, CMAP; compound muscle action potential, NCV; nerve conduction velocity, AUC; area under the curve, SNAP; sensory nerve action potential, MNAP; mixed nerve action potential, EMG; electromyography

Corresponding author: Adisak Kasemassawachanont
E-mail: adisakmd117@gmail.com
Received 11 April 2022 Revised 5 June 2022 Accepted 9 June 2022
ORCID ID: https://orcid.org/0000-0003-2754-6145
http://dx.doi.org/10.33192/Smj.2022.54

INTRODUCTION

DPN is recognized as one of the clinically significant nerves since several clinical manifestations can commonly be observed attributed to its defective components in either sensory or motor function. These abnormalities are caused by either intraneural (e.g., peripheral nerve sheath tumor or intraneural ganglion cyst from metatarsophalangeal joint distension) or extraneural (e.g., tumor, extensor retinaculum, bony spur, ganglion cyst or inadequate foot device) compressive lesions. In addition, they can also be due to the traumatic etiologies. For example, common injuries near the proximal part of the fibula, especially the iatrogenic ones after certain interventions around the lateral side of the knee and upper part of the leg, e.g., the proximal fibular osteotomy, percutaneous wire placement in the proximal tibia or total knee arthroplasty, can result in DPN dysfunction. Not only the proximal part, the clinical procedures near the distal part of DPN, e.g., ankle arthroscopy, may also cause the disturbance to this nerve and lead to the sensory impairment of the cutaneous area supplied by this nerve. Besides its clinical significance in terms of nerve injury, several clinical manipulations with this nerve, both non-invasive and invasive, are commonly employed in the medical practice nowadays, e.g., imaging, anesthetic procedure, functional study, or even surgical intervention. In this study, we, therefore, aimed to review its anatomical basis and variations reported in the previous literature and to link these to its current applications that are commonly used in clinical service, e.g., clinical imaging, nerve block, electrophysiological study, and employing this nerve in surgical procedures, to establish definitive translational knowledge for its clinical implementation.

The review process was carried out by using groups of keywords for searching on the standard online publication database, i.e., PubMed (https://pubmed.ncbi.nlm.nih.gov/). Certain keywords used for searching comprised "deep peroneal nerve", "deep fibular nerve", "anatomical variations and deep peroneal nerve", "dorsalis pedis artery", "accessory deep peroneal nerve", "accessory deep fibular nerve", "deep peroneal nerve imaging", "deep peroneal nerve block", "electrophysiological study and deep peroneal nerve", "surgical reconstruction and deep peroneal nerve". All searched records available on the PubMed database were screened for their relatedness to the aim of this review and only the full articles of the related ones were retrieved. The publication resource used in this review, starting from the latest ones in 2021, dates back to 1896 as the earliest one. All publication resource, after being categorized according to the disciplines (anatomy, radiology, rehabilitative medicine and plastic surgery), was then distributed to the authors with specialty corresponding to each discipline, i.e., anatomist, radiologist, rehabilitation physician and plastic surgeon. After reviewing all related resource, authors altogether conceptualized and drafted the contents of this review to propose the systematic knowledge of its anatomical nature linking to the application useful in current clinical practice.

Anatomical background of the DPN

General information and origination of the DPN

DPN, also known as the deep fibular nerve (L. nervus peroneus profundus, nervus fibularis profundus), is one of the nerves in the lower extremity that functions as combined sensory and motor fibers, mainly supplying the leg and foot area.[1] This nerve is a bifurcating branch of the common peroneal (fibular) nerve (CPN), which is one of the two divisions of the sciatic nerve (ventral rami of the 4th and 5th lumbar together with the 1st, 2nd, and 3rd sacral spinal nerves).

Continuing from the distal part of the CPN that passes posterior to the head of fibula, the bifurcation is located near the neck of the fibula and terminates as two branches: the superficial and deep peroneal nerves (Fig 1A). Traumatic/non-traumatic abnormalities of the proximal part of the fibula[2] or iatrogenic injuries around this zone[3], e.g., after fibular biopsy, high tibial osteotomy, or total knee arthroplasty, can result in dysfunction of the DPN. The superficial branch courses downward laterally along the length of the leg into the lateral fascial compartment while the deep one deviates medially, pierces through the anterior intermuscular septum, and then passes downward anteriorly into the anterior fascial compartment.

Proximal part of the DPN

The proximal part of the DPN runs deep to the peroneus (fibularis) longus (PL) and then the extensor digitorum longus (EDL) muscles to lie anterior to the interosseous membrane. It becomes laterally parallel to the anterior tibial artery (ATA, in the proximal third of leg) as the neurovascular supply for the surrounding extensor muscular tissue, i.e., the tibialis anterior (TA), EDL, extensor hallucis longus (EHL), and peroneus (fibularis) tertius muscles. Therefore, lower motor neuron disturbance or neuropathy of this nerve, e.g., complications of diabetes, intraneural ganglion cyst, compartment syndrome, or inflammatory problems, commonly causes the clinical sign of foot drop, which is the inability to achieve ankle dorsiflexion and toe extension.[4]

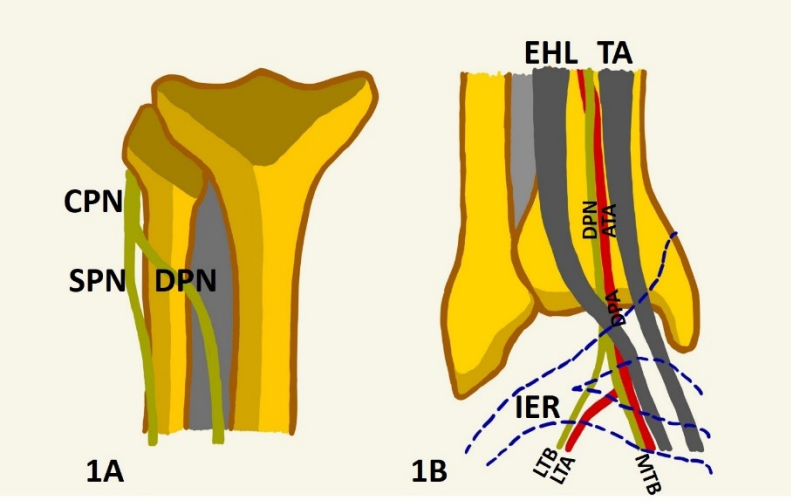

Fig 1. **1A:** Schematic demonstrating the right DPN originating from the bifurcation of CPN near the neck of fibula. **1B:** Schematic demonstrating the orientation and branching of the distal part of the right DPN at the lower leg and ankle areas. CPN = common peroneal nerve; DPN = deep peroneal nerve; SPN = superficial peroneal nerve; EHL = extensor hallucis longus (tendon); TA = tibialis anterior (tendon); ATA = anterior tibial artery; DPA = dorsalis pedis artery; MTB = medial terminal branch; LTB = lateral terminal branch; LTA = lateral tarsal artery; IER = inferior extensor retinaculum (borders represented by the blue curved dashed lines).

Distal part of the DPN

During its passage downwards through the distal part of the leg, these neurovascular structures course more superficially than the proximal part and lie posterior to the superior and inferior extensor retinacula (SER and IER, respectively) and in between the TA (medial) and EHL (lateral) muscles (Fig 1B). When the course of DPN passes anterior to the ankle joint, the tendon of the EHL crosses superficially over the descending neurovascular structures (DPN and dorsalis pedis artery, DPA) to lie medially to them (Fig 1B). The DPN is typically lateral to the DPA. At this level, the DPN shares an articular branch for the ankle joint and then divides into two terminal branches, i.e., the medial and lateral terminal branches (MTB and LTB, respectively), although division proximal or distal to this level can also be found as positional variations (Fig 1B).

Terminating branches of the DPN

The MTB runs dorsally along with the DPA and provides the articular branch for the 1st metatarsophalangeal joint and the muscular branch for the 1st dorsal interosseous muscle. Finally, the MTB communicates with the medial branch of the superficial peroneal nerve (SPN) in the 1st interosseous space and reaches the proximal zone of the 1st interdigital cleft to terminate as two digital cutaneous nerves supplying the 1st dorsal web space of the foot. This explains the sensory impairment of this cutaneous area in the case of DPN disturbance, even when it's due to the iatrogenic etiology, e.g., ankle arthroscopy.[5] Likewise, the LTB runs dorsolaterally along with the branch of the DPA, the lateral tarsal artery (LTA), and passes beneath the extensor digitorum brevis (EDB) and the extensor hallucis brevis (EHB) muscles (as a pseudoganglion enlargement) to supply them (Fig 1B). Moreover, the LTB also provides the articular branches for the tarsal and the middle three metatarsophalangeal joints.

Key takeaway

DPN is one of the lower extremity nerves supplying structures in the anterior fascial compartment, ankle region and dorsum of foot in both sensory and motor functions. Two superficial parts of DPN course, i.e., near the neck of the fibula and anterior to the ankle region, should be clinically focused as the common sites for iatrogenic and non-iatrogenic nerve damage. In addition, anatomical relations to its adjacent structures are the fundamental concept for implementing in various clinical applications.

Anatomical variations of the DPN

Proximal part of the DPN

Owing to the superficial lying of the proximal part of the DPN adjacent to the fibular head, the anatomical variation of this part is vulnerable to pathological disturbance by the surrounding structures.[6] Thus, understanding the positional variation of the proximal DPN plays an important role in clinical practice in order for physicians to find a safe area or angle for procedures that can avoid injury to the DPN. Iatrogenic injury caused by clinical procedures around the lateral side of the knee and upper part of the leg, e.g., proximal fibular osteotomy during high tibial osteotomy or percutaneous wire placement in the proximal tibia, significantly contributes to cases of DPN damage, and have prompted a number of studies into the variation of DPN in this region to find a safe area that can allow avoiding the risk of damage to the DPN.[7,8]

1. Variations of the DPN originating position and orientation of the proximal part

A study in Thai cadavers was performed to find the ethnic-specific distance from the tip of the fibular head to the DPN originating point (28.4 ± 4.8 mm).[9] Compared with the Thai study, a study in the Japanese

cadavers showed an approximate average of this distance of 26.0 ± 0.32 mm.[10] However, studies in cadavers of non-Thai ethnicity indicated a safe distance for fibular head procedures of only about 20 mm distal to the tip of the head of the fibula.[7,8] In terms of the angle of proximal DPN relative to the vertical axis of the fibula, it was reported to be about 28.1° ± 7.2° in the study of Thai cadavers.[9] Compared with the Thai study, the results from the Japanese cadavers showed a slightly narrower angle (23.5° ± 3.5°).[10]

2. CPN entrapment by the peroneal (fibular) tunnel

In addition to iatrogenic injury, the peroneal tunnel is one common cause of idiopathic entrapment of the CPN, which also affects the function of the DPN. A study in cadavers was carried out in Ireland and found that the compression site of DPN was about 3.2 ± 1.0 cm (at the entering point of the CPN into the tunnel) and 7.0 ± 1.5 cm (at the exit point of the DPN from the tunnel) from the apex of the fibula.[11] These results can be implemented in planning a procedure to release a nerve entrapment, but they need to confirm in Thai subjects to avoid the risk of existing ethnic-specific variations.

Distal part of the DPN

In contrast to the proximal part of the DPN, the distal part demonstrates a larger number of both positional and branching variations due to the larger possibility of diverse orientations relative to neighboring structures along the distal coursing and also the branching circumstances. As the DPN divides into the MTB and LTB at the approximate zone of the ankle joint without a particular location, the branching patterns and levels have been investigated in a number of studies with an aim to identify their distribution.

1. Variations of the DPN branching level and pattern

Based on the previous study using the ankle mortise as the landmark, only 23% of the studied specimens were found to be bifurcated either above or at this level (Fig 1B).[12] Likewise, using an imaginary line connecting the medial to the lateral malleoli as the landmark instead of the ankle mortise showed the prevalence of bifurcation at and distal to this level as about 21% and 27.1%, respectively (Fig 1B)[13] Further compared with the IER (the roof of the anterior tarsal tunnel, ATT), most of the bifurcation (86.1%) was observed in the ATT, while only a small number of the studied specimens (5.6%) showed bifurcation below the ATT, and no bifurcation above the ATT was seen (Fig 1B).[14] Nonetheless, the absence of bifurcation[14-16] and multiple branching[13] were found at low prevalence of 6.7-8.3% and 4.16%, respectively.

2. Positional variations of the DPN and its branches in relation to the DPA

Not only have branching variations of the distal part of DPN been significantly observed but the positional variations of the DPN and its branches in relation to the DPA have also been explored to reveal their orientation. Inside the ATT, Rab *et al.* reported that the DPN was found lying anterolaterally to the DPA in almost all of the studied specimens (92.9%) (Fig 2).[17] When combined with observations of the DPN branching level, the prevalence of the DPA orientation medial to the DPN in the ATT and medial to the MTB distal to the ATT was about 36.1%–36.7% (Fig 2A), whereas the prevalence of the DPA orientation lateral to the MTB was reported to be 25%–30% (Fig 2B).[15,16] Crossover of the DPN and DPA at multiple levels was also reported in wide-ranging frequency of about 8.4%–30.6%, which may depend on the ethnicity of the cadavers in each study (Fig 2C).[13,15,16]

Accessory deep peroneal nerve (ADPN)

1. General information and course of the ADPN

The accessory deep peroneal nerve (ADPN; L. nervus peroneus profundus accessorius), first reported in 1896[18], is a nerve variant emerging from the SPN, carrying both sensory and motor fibers, and descending along the anterior surface of the posterior intermuscular septum and the posterior border of the peroneus brevis (PB) muscle in the lateral fascial compartment of the leg until reaching the lateral malleolus, while some studies demonstrated its possible existence in the anterior fascial compartment.[19–21] The course of the ADPN can bifurcate to reunite at the proximal part of the PB muscle and can also be partially covered by the slip of PB muscle.[21] During passing inferior to the distal part of the fibula with the tendons of two peronei muscles, the ADPN runs through the superior peroneal tunnel and then the deep-anterior compartment of the inferior peroneal tunnel.[21] Finally, it courses anteriorly near the sural nerve and deep to the tendon of the PB muscle to the dorsum of the foot.

2. Structures innervated by the ADPN

As commonly reported for innervation of the EDB muscle, the ADPN was revealed to provide muscular branches for not only the PL and PB muscles (75%, 33.3%, and 100% of the studied cases for the EDB, PL and PB, respectively) but also for other small peronei muscles (peroneus quartus and peroneus digiti quinti).[21]

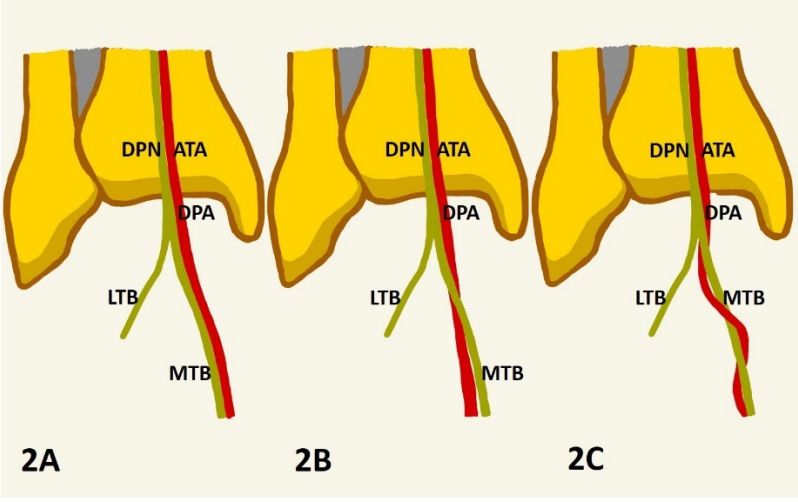

Fig 2. Schematic demonstrating the orientation of the right DPN and its branches at the ankle area and the dorsum of foot in comparison with the right ATA and DPA. **2A:** The vessel is medial to both DPN and MTB. **2B:** The vessel is medial to DPN but lateral to MTB. **2C:** Crossover of the DPN and the vessel at multiple levels. DPN = deep peroneal nerve; ATA = anterior tibial artery; DPA = dorsalis pedis artery; MTB = medial terminal branch; LTB = lateral terminal branch.

It commonly innervates the EDB muscle for the extensor part of the 4th toe rather than the 3rd and the 5th toes.[22] For the sensory component, the ADPN supplies the fibular periosteum, lateral region of the ankle (e.g., the ankle joint, ligaments, tarsal periosteum, and synovial sheath of the peroneal muscles), and the metatarsal region (37.5%, 100%, and 20.8% of the studied cases for each, respectively).[19,21,23]

3. Study methods for the occurrence of the ADPN

Study into the occurrence of the ADPN can be performed by two approaches, i.e., by direct dissection of cadaveric specimens and by electrophysiological study in living subjects. Nonetheless, the latter approach usually gives a lower prevalence than the former (13.6% vs. 39.3%)[24], as a positive verification of the ADPN by the latter requires the presence of a muscular branch to the EDB muscle. Identification of ADPN existence is crucial for clinical practice in cases with peroneal lesions that may involve a confused diagnosis. Furthermore, clinical procedures at the lateral side of the ankle, e.g., ankle arthroscopy, orthopedic procedures at the lateral malleolus, and sural nerve biopsy should raise some concern for iatrogenic complications that may occur to the ADPN. This risk can be reduced by performing a prior electrophysiological study to detect the existence of ADPN. Besides, the existence of ADPN may account for certain unexplained clinical conditions, such as EDB muscle atrophy and chronic ankle pain.

4. Prevalence of the ADPN and its branches

A number of ADPN studies, both cadaveric and electrophysiological, among different ethnicities have been conducted to find the prevalence of ADPN, prevalence differences between the sexes and sides, bilateral similarity, and the prevalence of a muscular branch to the EDB muscle. A meta-analysis was done to collect eligible published data from 19 ADPN studies.[24] The pooled ADPN prevalence was 18.8% (95% CI: 14.2–24.0%). Variability in the pooled prevalence among different ethnicities was also found (Asian = 50.3% (95% CI: 21.1–79.5%), North American = 17.6% (95% CI: 13.3–22.3%), and European = 12.1% (95% CI: 8.3–16.5%)).

The pooled prevalence on each side (from 4 out of 19 studies) was 6.4% (95% CI: 4.8–8.2%) for the right side and 8.5% (95% CI: 7.3–9.8%) for the left side. The pooled unilateral prevalence was two times higher (67%, 95% CI: 53.8–79.1%) than the pooled bilateral one (33%, 95% CI: 20.9-46.2%) in cases with ADPN present (from 11 out of 19 studies). The pooled prevalence of a muscular branch to the EDB muscle was 79.5% (95% CI: 53.5–97.4%) of all specimens with ADPN (from 4 out of 19 studies). There was no statistical significance in prevalence difference between the sexes.[25,26] Nevertheless, the occurrence of ADPN seems to run among family members as a hereditary trait with the proposed autosomal dominant mode of inheritance.[27]

Key takeaway

DPN is one of certain nerves that its anatomical variants can be found in all aspects, e.g., position, orientation, branching level and pattern or even additional accessory. For the proximal part, they are mostly about the positional and orientational variants, whereas the significant variabilities observed in the distal part are involved with aspects of branching and relations to its adjacent structures. These anatomical observations are the key translational knowledge to effectively practicalize the clinical approaches dealing with DPN.

Current clinical applications of the DPN

Application in radiology

1. General imaging characteristics of DPN

Diseases of the DPN are composed of many factors, including traumatic[28] and non-traumatic diseases, such as intraneural and extraneural compressive lesions.[29] Nowadays, imaging techniques play a major role in the diagnosis of peripheral nerve diseases, such as high-frequency ultrasonography (US) and magnetic resonance imaging (MRI).[30,31]

1.1 Ultrasonographic imaging

In US, the normal appearance of the nerve appears as a honeycomb pattern in the short axis, in which the hypoechoic nerve fiber is enveloped by the hyperechoic epineurium (Fig 3). In the long axis, it appears as a coarse hypoechoic longitudinal structure without anisotropy as in the tendon.[32] The landmark for the depiction of the DPN in US corresponds with its anatomy. First, in the proximal part, it continues on from the CPN after bifurcation at the peroneal tunnel, where the anterior one is the DPN and the other posterior one is the SPN. Second, in the leg region, it lies in the anterior fascial compartment of the leg, which is deep to the TA muscle and anterior to the interosseous membrane, and laterally accompanies the ATA (Fig 3). Last, in the ankle and foot regions, it lies between the EHL and EDL muscles and distally gives two terminal branches: the MTB, which accompanies the DPA until the 1st web space (Fig 4), and the LTB, which supplies the EDB muscle, tarsal joints, and 2nd to 4th metatarsophalangeal joints.[31,33]

1.2 Magnetic resonance imaging

In MRI, a normal appearance of the nerve is revealed with an iso-signal intensity (SI) in T1W and T2W as the SI of the muscles (or a slightly higher SI than that of the muscle in T2W), and it is surrounded by high SI fat (Figs 5&6).[34-36]

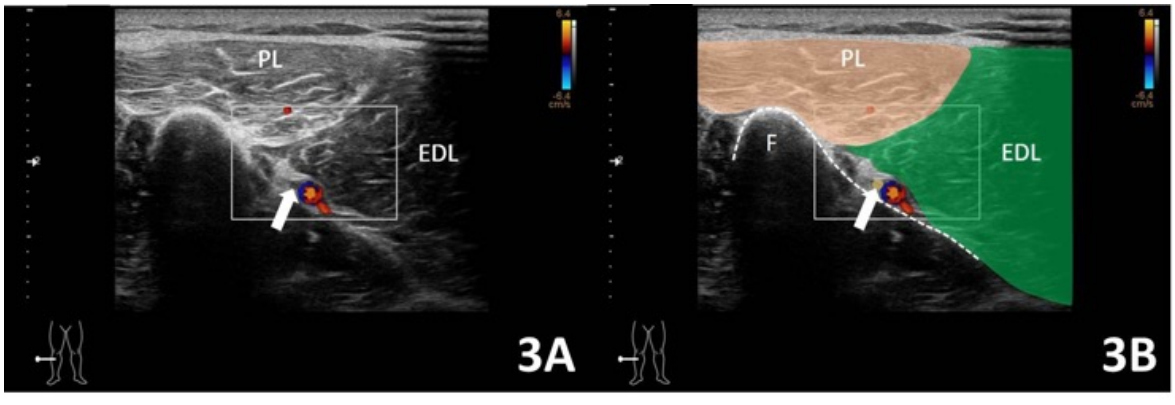

Fig 3. **3A:** Axial scan of US using a 12 MHz linear array transducer at the proximal aspect of the right leg (28-year-old man, below the fibular head) demonstrating the DPN coursing laterally to the ATA in the anterior fascial compartment with a honeycomb appearance (white arrow). **3B:** Area-representing schematic for US image demonstrating the DPN (yellow area pointed by the white arrow) in anterior fascial compartment of leg laterally accompanying the anterior tibial vessels (the structures with blue and red colors representing the blood flow directions in color-Doppler US). PL = peroneus longus muscle; EDL = extensor digitorum longus muscle; F = fibula with the curved dashed line as its boundary.

Fig 4. **4A:** Axial scan of US using a 12 MHz linear array transducer at the dorsum of the right foot (28-year-old man) demonstrating the MTB of the DPN, laterally accompanying the DPA, with a honeycomb appearance (white arrow). **4B**: Area-representing schematic for US image demonstrating the DPN (yellow area pointed by the white arrow) in the dorsum of foot located medial to the DPA (red area). EHL = extensor hallucis longus (tendon); EDL = extensor digitorum longus (tendon).

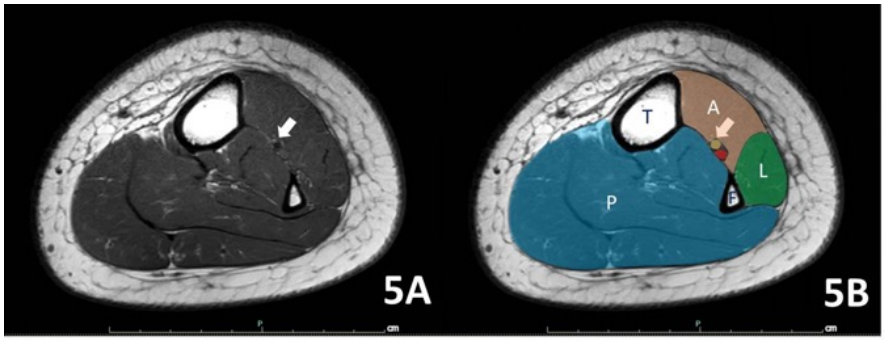

Fig 5. 5A: Axial T1-weighted MR image of the proximal aspect of the left leg (12-year-old girl, below the fibular head) demonstrating the DPN accompanying the ATA in the anterior fascial compartment (white arrow). **5B:** Area-representing schematic for MR image demonstrating the DPN (yellow area pointed by the white arrow) at the proximal aspect of the left leg. Red area = ATA; A = anterior fascial compartment; L = lateral fascial compartment; P = posterior fascial compartment; T = tibia; F = fibula.

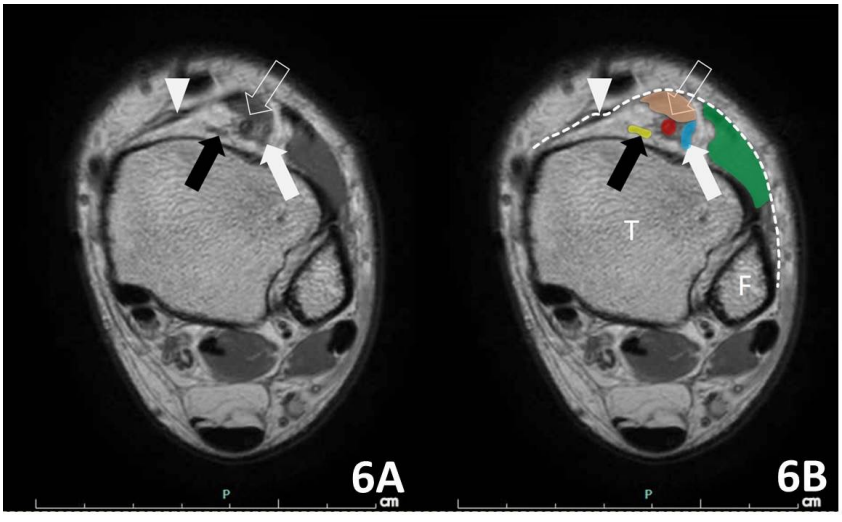

Fig 6. 6A: Axial proton density-weighted MR image of the left ankle (41-year-old man) demonstrating the MTB (black solid arrow) and the LTB (white solid arrow) of the DPN. The DPA (white open arrow) courses laterally to the MTB of the DPN. Extensor retinaculum is marked by the white arrow head. **6B:** Area-representing schematic for MR image demonstrating the MTB (yellow area pointed by the black solid arrow) and LTB (blue area pointed by the white solid arrow) of the DPN at the left ankle with the DPA (red area pointed by the white open arrow) located lateral to the MTB. Brown area = EHL (muscle and tendon); green area = EDL (muscle and tendon); curved dashed line pointed by the white arrow head = extensor retinaculum; T = tibia; F = fibula.

2. Direct imaging characteristics of DPN pathology

MRI and US can be used to evaluate the DPN pathology of both traumatic and non-traumatic causes as described below.

2.1 Traumatic pathology of the DPN

In traumatic causes, including direct contusion, traction injury, penetrating injury, and also post-surgical iatrogenic events, the DPN appears swollen and edematous, with hypoechoic thickening in US[33] with an increased T2W SI and decreased T1W SI in MRI. If partial or complete disruption of the nerve occurs, post-traumatic or stump neuroma may be seen in US as a hypoechoic mass-like lesion[28,33] and in MRI with an iso- to low T1W SI and iso- to high T2W SI with enhancement.[37,38] Other traumatic causes include compartment syndrome in the anterior or lateral fascial compartments[39,40] and compression from a fractured bone fragment or late sequelae of heterotopic ossification.[41]

2.2 Non-traumatic pathology of the DPN

Non-traumatic causes include intraneural and extraneural causes. Intraneural causes include a peripheral nerve sheath tumor either benign or malignant[42], and the less common intraneural ganglion cyst from metatarsophalangeal joint distension.[29,43] Extraneural causes include tumor (e.g., exostosis) and compression by adjacent structures, such as an extensor retinaculum, bony spur, ganglion cyst, or inadequate foot device.[43] The imaging findings depend on each pathologic nature. For example, a ganglion cyst may be found as a well-defined round-shaped high T2W SI lesion and iso- to hypo-T1W SI depending on its content[44] with either non- or rim enhancement in the post-gadolinium sequence of MRI.[45] Nerve thickening can be seen with an increased T2W SI in MRI.[43]

3. Indirect imaging characteristics of DPN pathology

Beside direct nerve abnormalities in peripheral neuropathy, indirect signs of nerve injury can also be observed in clinical imaging. One of the useful indirect signs is the corresponding denervation of the muscle. Varied imaging findings of muscle denervation depend on the timing, site, and degree of neural involvement[46,47], but they can still be used as a beneficial clue for the detection of neuropathy. Muscle denervation is edematous in the acute stage and then atrophic with fatty infiltration in the chronic stage. In the acute phase, US of denervated

muscle shows a, sometimes subtle, hypoechoic edematous appearance, while better evaluation can be achieved by utilizing fat suppression techniques with T2W MRI[43,48], seen as an increased SI in 24 to 48 hours after the event.[46,47,49] In the chronic phase, the denervated muscle shows increased echogenicity with a smaller size[33], whereas an increased fat SI of atrophic muscle can be observed in MRI.[46,47,49] Like other peripheral nerves, DPN neuropathy can be involved with muscles in the anterior fascial compartment (Fig 7) and, less frequently, the EHB muscle according to the degree and site of neuropathy.[46,49]

4. Key takeaway

Normal anatomy, including position, orientation, branching pattern and variation, is the key for understanding normal findings in radiology. Likewise, normal imaging appearance is also the key for abnormality detection. US and MRI have the capacity *per se* to evaluate the DPN pathology in different aspects. In certain aspects, efficacy of one modality can also be enhanced by the other. Not only the direct sign of nerve abnormality but also the indirect sign of muscle innervation is beneficial in detection of the DPN abnormality by clinical imaging.

Application in anesthesiology

1. Regional nerve block of the DPN

Regional nerve block of the DPN is an anesthetic approach that is preferably used in practice due to its low systemic risk.[50,51] Application in the ankle region is used in many situations, including ankle surgery and pain control.[52,53] However, certain conditions may contraindicate this method, such as a local infection at the injected site or in patients at risk of compartment syndrome.[53] Accurate knowledge of the DPN anatomy makes this nerve block perfect.

The landmark for DPN block in the ankle region is located lateral to the ATA[52], just lateral to the tendon of EHL[54], which can be easily found by active dorsiflexion of the big toe. US guidance for peripheral nerve block seems to be advantageous[50], such as using a directly observable nerve with adjacent vascular structures, for avoiding direct vessel injection and reducing the amount of drug used.[55–57] However, John *et al.* found that the ultrasound guidance technique showed no improvement in overall quality in DPN block at the ankle level.[58] Therefore, an anatomical landmark for DPN block is still important.

2. Key takeaway

Normal DPN anatomy is essential for successful regional DPN block in the ankle region, including adequacy of local anesthesia and complication avoidance, whether the ultrasound guidance technique is applied or not.

Application in rehabilitation medicine

1. Electrodiagnosis for DPN

Electrodiagnosis is a physiologic study that can help in localizing the DPN pathology, and for assessing the severity and signs of recovery. Moreover, it can be used in differential diagnosis and for ruling out other causes mimicking DPN mononeuropathy; for example, sciatic neuropathy, lumbosacral plexopathy, L5 radiculopathy, peripheral polyneuropathy, and upper motor neuron diseases. There are two types of electrodiagnostic study.

1.1 Nerve conduction study (NCS)

1.1.1 Motor NCS

Motor NCS evaluates the functioning motor axons by sending electrical impulses at the proximal site and recording the response over the muscle belly. The action potential recorded is a summation from the motor nerve,

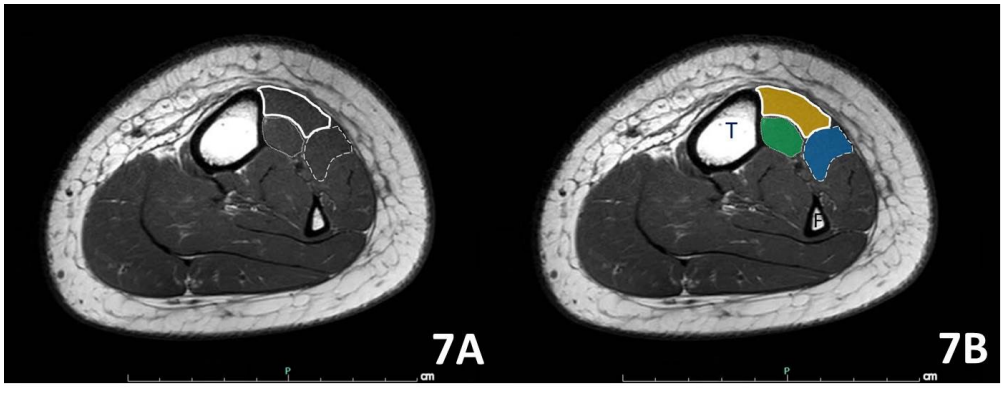

Fig 7. 7A: Axial T1-weighted MR image of the proximal aspect of the left leg (12-year-old girl, below the fibular head) demonstrating the muscles of the anterior fascial compartment, including the TA (white solid line), EDL (white dashed line) and EHL (white encircling dots) muscles. **7B:** Area-representing schematic for MR image demonstrating the muscles in the anterior fascial compartment of the proximal aspect of left leg, including the TA (yellow area), EDL (blue area) and EHL (green area) muscles. T = tibia; F = fibula.

neuromuscular junction, and all the muscle fiber action potentials (compound muscle action potential, CMAP) (Fig 8). The stimulation sites for the DPN are at the anterior ankle, fibular head, and lateral area of the popliteal fossa. Recording electrodes are usually placed on the EDB (Fig 9A) and TA muscles. The onset latency, amplitude, and nerve conduction velocity (NCV) are the common parameters recorded (Table 1).

Demographic factors can also affect some other parameters. A previous study found that a greater height of the subject was associated with increased onset latency and decreased NCV. In addition, it was also found that an older subject was correlated with a lower amplitude, area under the curve (AUC) and NCV. However, there was no statistically significant difference in NCS between the sides.[59,60] Moreover, the NCV across the fibular head when recorded at the TA was faster than that recorded from the EDB, with the mean difference in the NCV being 5 m/s.[60]

To use these parameters in testing, Buschbacher *et al.* reported a cutoff value as a 50% amplitude drop when compared to the contralateral side and recorded at the TA muscle for diagnosing an abnormality of the motor amplitude, if the affected limb showed normal values.[60] When recording at the EDB muscle, the upper limit of normal amplitude difference from side-to-side was 61%, which might not be sensitive enough to make a diagnosis of mononeuropathy.[59] To find a focal demyelinating lesion of the nerve, comparing the amplitude between stimulating at the proximal (popliteal fossa or fibular head) and distal (ankle) points, and recording at the EDB muscle is usually done. The upper limit of normal amplitude decrease was found as a 32% drop across the lower leg and 25% drop across the knee in one study.[59] While recording at the TA muscle, the upper limit of normal drop in amplitude from distal to proximal stimulation was 36%. This normal drop was high for a short nerve distance. However, it was possible in this condition because the phase cancellation from a volume-conducted tibial waveform could not be ruled out.[60] Additionally, when recorded at the EDB and comparing the NCV between below-knee and across-knee segments, the upper limit of normal drop was 10 m/s.[59]

1.1.2 Anatomical variation

The ADPN primarily emerges as both the motor nerve from the SPN to the EDB muscle and the sensory branches to the ankle joint. The presence of ADPN should be suspected if the EDB motor amplitude is smaller when stimulated at the ankle than at the fibular head. This can be confirmed by obtaining the CMAP from stimulating behind the lateral malleolus.[20,59] Another method is by comparing the CMAP area ratio between stimulating at the distal and proximal. The area ratio is higher in subjects without ADPN than those with ADPN (1.15 and 0.96, respectively). From a previous study, the distal CMAP amplitude of ADPN was around 1.27 mV with an average distal latency at 4.84 ms.[20]

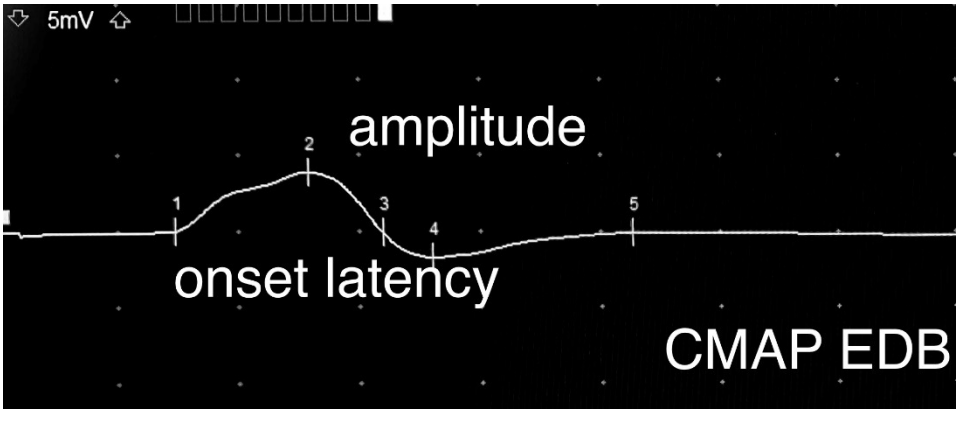

Fig 8. DPN motor waveform recorded at the EDB muscle. (marker 1 = onset latency; vertical distance from marker 1 to marker 2 = amplitude; area under peak from marker 1 to marker 3 = area under the curve)

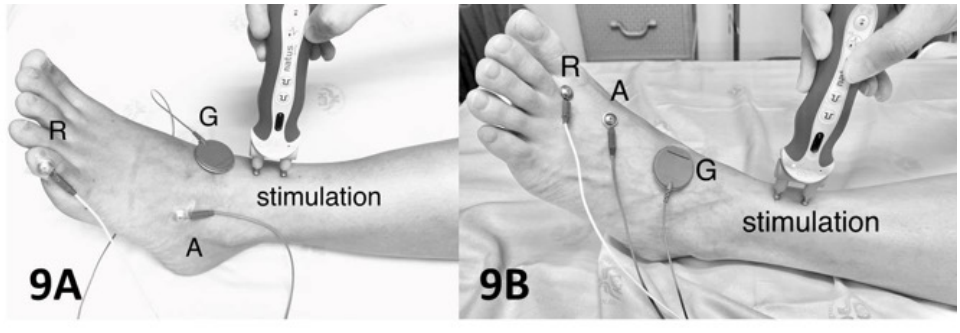

Fig 9. DPN stimulation for motor NCS recorded at the EDB muscle **(9A)** and for antidromic sensory NCS **(9B)**. (A = active electrode; R = reference electrode; G = ground electrode)

TABLE 1. Reference parameters for DPN in electrodiagnosis.

Electro-diagnosis study	Muscle/nerve, electrode placement	Stimulation	Age (year)	Sex	Onset latency (mean, ms)	Amplitude (mean, mV)	Velocity (mean, m/s)	Reference
CMAP	EDB - Active: midpoint of the muscle belly - Reference: slightly distal to the 5th metatarsophalangeal joint	(1) 8 cm proximal to the active electrode lateral to the TA tendon (2) posterior and inferior to the fibular head (3) 10 cm from (2) medial to the tendon of the biceps femoris	All 19–39 40–79		4.8 (6.5)^{U} 4.8 (6.5)^{U} 4.8 (6.5)^{U}	5.9 (1.3)^{L} 6.8 (2.6)^{L} 5.1 (1.1)^{L}	47 (38)^{L} 47 (38)^{L} 47 (38)^{L}	(59)
CMAP	TA - Active: one-third of the distance from tibial tubercle to lateral malleolus - Reference: on the bony surface of the tibia	(1) posterior and inferior to the fibular head (2) 10 cm from (1) medial to the tendon of the biceps femoris	All 19–29 30–79		3.6 (4.9)^{U} 3.6 (4.9)^{U} 3.6 (4.9)^{U}	3.8 (1.7)^{L} 4.3 (2.1)^{L} 3.6 (1.5)^{L}	62(43)^{L} 62(43)^{L} 62(43)^{L}	(60)
CMAP	EDB, ADPN	Posterior to lateral malleolus	All male female		4.84 4.95 4.69	1.27 0.97 1.67	55.7 56.85 58.11	(20)
SNAP	DPN - Active: the interspace between the 1st and 2nd metatarsal heads - Reference: 3 cm distal to the active electrode on the 2nd digit	12 cm proximal to the active electrode and just lateral to the EHL tendon	35 35–50 >50			9.73 μV 7.95 μV 6.65 μV	41.01 41.23 40.28	(61)

^{U} Upper limit of normality. ^{L} Lower limit of normality.

1.1.3 Sensory NCS

Sensory NCS assesses the density of the functioning nerve fibers. The action potential recorded is a summation of all the sensory fibers (sensory nerve action potential, SNAP). The study of the DPN is usually done in an antidromic manner and recorded at the first dorsal web space of the foot. The stimulation site is at the anterior ankle (Fig 9B). The estimated normal values are shown in Table 1. Lo *et al.* reported that the SNAP amplitude could be diminished in a normal population and even more in the elderly.[61] This should be considered in interpreting the results. Furthermore, anatomical variations could also affect the results. From a former study in healthy volunteers, the first dorsal web space of the toes was supplied by an isolated DPN for 34% of all studied limbs, SPN for 10%, both nerves for 44%, and

no response for 12%. The gross diameter of the nerve is very small and it is more difficult to stimulate in swollen limbs.[62]

One study reported that the NCV from the orthodromic method was more sensitive than that from the antidromic method in detecting lesions. The orthodromic method in the DPN involves stimulating at the ankle and recording the response at above and below the fibular head. The action potential recorded is a mix and not only from the DPN; hence it is called the mixed nerve action potential (MNAP). In healthy subjects, the mean sensory orthodromic NCV of the DPN was found to be 55.27 m/s. The mean MNAP amplitudes of the DPN under and above the fibular head were 1.13 μV and 0.52 μV, respectively. This method is easier to apply even in an elderly population. Therefore, an absent response may indicate a true abnormality.[63]

1.2 Needle electromyography (needle EMG)

This study can provide more information, such as whether the pathology is acute or chronic, and the signs of denervation and re-innervation from axonal loss, than NCS. In this method, a needle electrode is inserted into the muscle and electrical signals from muscle contractions are recorded. Spontaneous activity, and the number and morphology of the motor units are observed. However, a study by Dumitru *et al*. in an asymptomatic healthy population reported a prevalence of abnormal spontaneous activity of EDB in 60% of all subjects.[64] History taking and physical examination should be performed and the findings correlated since foot trauma can result in spontaneous activity in this muscle. Spontaneous activity in diffuse, decreased recruitment and an abnormal morphology may indicate the true pathology.[65]

2. Evaluation of DPN abnormality

Most pathologies of the DPN near the fibular head are axonal loss[66,67] because the fascicles at this level are located anteriorly, and thus are more sensitive to pressure or stretching. ATT is another common suspected area for DPN pathology, but is a rare condition. The mechanism is nerve compression by IER. The common presentations are a dull ache, numbness, or paresthesia radiating to the 1st interdigital space of the dorsum of the foot. An extremely serious condition is a weakness of the EDB muscle. The electrophysiologic study mostly finds chronic neuropathic patterns.[65] Two common electrodiagnostic findings are axonal loss and demyelination. For axonal loss, needle EMG can be used to show signs of denervation, whereas NCS can show an absent, low, or more than 50% decreased amplitude compared to the unaffected side. For focal demyelination, NCS may show a conduction block pattern (CMAP amplitude drop at the distal compared to in proximal stimulation) and a decreased NCV difference between segments of more than 10 m/s as described above. Significant demyelination is usually found co-existing with mild axonal loss.

3. Evaluation of DPN recovery

Derr *et al*. studied peroneal nerve recovery in both traumatic and non-traumatic cases by electrodiagnosis at 2 weeks to 24 months after onset. The stimulating site was at the fibular head. The recording sites were at the TA and EDB muscles. A good outcome was a TA motor power by manual muscle testing from grade 4 and higher. Presentation of a CMAP response in both EDB and TA muscles was a predictor for good outcome recovery (94% in all cases, 80% in trauma, and 100% in non-trauma). A good outcome was found in 81% and 94% of subjects who had CMAP presentation only in the TA and EDB, respectively. However, the absence of EDB CMAP and TA CMAP did not mean a poor outcome (46% had good outcome recovery). Most traumatic cases showed an absence of EDB CMAP. A response of EDB CMAP in the first three months can predict a good outcome (100% of all cases had good outcome recovery). From one needle EMG study, discrete or absence of motor unit recruitment in a trauma group predicted a worse outcome recovery, but without statistical significance. However, this was a small retrospective study and might not have had a large enough sample size.[68] Another study was performed in non-traumatic subjects and reported that if only a conduction block, which means demyelination, was found at 2–12 weeks after onset, a good recovery at 6 months could be anticipated.[69]

4. Evidence for the use of electrodiagnostic studies

Due to the nature of study, the supporting evidence was limited to class III for NCS and class IV for needle EMG for peroneal neuropathy diagnosis, according to an American Association of Neuromuscular and Electrodiagnostic Medicine review.[70]

5. Key takeaway

Being a nerve with both sensory and motor components, DPN can be electrophysiologically evaluated via the NCS for its sensory and motor function together with the needle EMG at its muscle targets. These studies can be summed up for identifying the abnormality and following the recovery of the DPN. Electrodiagnostic finding of the DPN should also be correlated with the

history and the physical examination of the patient to effectively evaluate the abnormality and to set the plan for treatment. However, evaluation techniques and anatomical variations can affect this finding. Therefore, anatomical knowledge is the important foundation to conduct the electrodiagnosis accurately and efficiently.

Application in surgery

1. Surgical application as a sensory nerve: Burned hand

The first web space contracture in a burned hand is one of the most common problems resulting in significantly decreased hand function. To achieve the goals following specific treatment principles[71,72], there are many options possible for the surgical reconstruction, including skin grafting[73,74], local flaps[75,76], regional flaps[77], and free flaps.[78,79,80] According to the principles, healthy tissue replacement or rearrangement is not sufficient. It requires sensory restoration together with glabrous skin restoration to achieve the ultimate goals, nearly-normal hand function.

With the aforementioned goals in mind, transferring tissue from another glabrous area with its sensory innervation is the choice. In the first web space, the connection between the MTB of the DPN and SPN provides sensory supply as the dorsal digital nerves to the 1st dorsal web space of the foot.[15] Either the DPN or the dorsal digital nerve can be transferred for harvesting an innervated free flap based on the shape and extension of the defect in the hand area. Understanding its anatomical variations, including level of bifurcation and absence of bifurcation will help surgeons prepare for additional steps in advance, such as intraneural dissection or nerve graft harvest. The former may require additional instrument for more meticulous dissection to minimize donor site morbidity such as motor nerve injury. On the other hand, the latter requires preparation of another donor site for nerve graft harvest. Either of the options, it is to perform tension-free microsurgical anastomosis of the donor nerve to a sensory nerve at the recipient site for ensuring the best condition for sensory recovery. In clinical scenarios, this innervated tissue transfer has been used with successful outcomes, such as a near-normal range of motion and sensation (2-point discrimination) of the reconstructed 1st web space.[80]

2. Surgical application as a motor nerve: Facial reanimation

The ultimate goal of reconstruction in patients with facial paralysis is to restore the lost function to normal, i.e., facial reanimation. Nevertheless, in cases of long-standing paralysis, the facial muscle is assumed to be atrophic after 24 months and muscle transfer is the option.[81] The transferred muscle can be connected with a source nerve for neural regeneration, resulting in a functional muscle. Principally, the donor muscle should be expendable and have a reliable neurovascular pedicle, sufficient length, and excursion muscle inset. In facial reanimation, especially smile reconstruction, gracilis muscle transfer is the gold standard.

Although not the gold standard option, another possible option is the DPN-innervated EDB muscle. The possibility of this flap in facial reanimation is not limited to smile reconstruction, but also to eyelid function.[82] This flap is mainly supplied by the LTA, and additional branches from the DPA and the peroneal artery[82], thereby considered as a Mathes–Nahai classification type 2.[83] The mean length and external diameter of the LTA were 2.3 cm and 2.4 mm, respectively, which were considered suitable as a choice for microsurgical anastomosis.[82] In addition to the vascular supply, the native function of EDB muscle is to assist the EDL muscle, harvesting this EDB muscle therefore results in a minimal deficit of the donor site.[84,85] Regarding this, understanding an anatomical course of the LTB of the DPN is important for safe dissection and flap harvest. It runs dorsolaterally along with the LTA and passes beneath the EDB muscle. Proximally, there is anatomical variation about its level of bifurcation. This may limit the length of the donor nerve possibly requiring nerve graft harvest. These issues share a similar principle of avoiding donor site morbidity (sensory nerve preservation in this application) and tension-free anastomosis of the nerve. In clinical scenarios, its application as a free flap in facial reanimation has been reported with successful results in variable cases.[86,87]

3. Key takeaway

Understanding the anatomy of the DPN, its variations, and its relation to adjacent structures is crucial for harvesting a flap for reconstruction such as the 1st web space reconstruction and free-functioning muscle transfer for facial reanimation. This is not only important for operative success, but also helps minimize both the donor site morbidities and the operative time due to the appropriate surgical planning.

CONCLUSION

As one of the nerves that is commonly manipulated in current clinical practice, anatomical knowledge and information on anatomical variations of the DPN are mandatorily essential for clinicians to understand the demographic nature of the DPN prior to its proper

application in patients. Nowadays, the clinical procedures implicated with this nerve can widely range from non-invasive ones, e.g., nerve imaging, to sophisticated surgical approaches, such as flap transfer for the reconstruction of a lower extremity, which have been regularly conducted in specialized clinical institutes.[88] This review therefore linked the fundamental anatomy of this nerve to its practical importance visualized in the examples of current clinical applications reviewed in this study by the main focus on its practicality and utilization. This review therefore presented the usefulness of translational research in this area for clinical implementation. Conclusively, the ultimate goal of this review is to help maximize the therapeutic effectiveness and to minimize the unanticipated complications of any clinical practices involving the DPN by inferring from its anatomical knowledge.

ACKNOWLEDGEMENTS

The authors are grateful to Dr. Supin Chompoopong for her guidance and suggestions. CT, SL, WD, TN, ArP, and AK also are thankful for their support from the Siriraj Chalermphrakiat Grant, Faculty of Medicine Siriraj Hospital, Mahidol University.

Conflict of interest: The authors declare no conflicts of interest.

REFERENCES

1. Standring S, editor. Gray's anatomy: the anatomical basis of clinical practice. 41st ed. Philadelphia: Elsevier; 2016.
2. Demiroglu M, Ozkan K, Kilic B, Akcal A, Akkaya M, Ozkan FU. Deep peroneal nerve palsy due to osteochondroma arising from fibular head and proximal lateral tibia. Int J Surg Case Rep. 2017;31:200-2.
3. Itou J, Itoh M, Maruki C, Tajimi T, So T, Kuwashima U, et al. Deep peroneal nerve has a potential risk of injury during open-wedge high tibial osteotomy. Knee Surg Sports Traumatol Arthrosc. 2020;28(5):1372-9.
4. Lu H, Chen L, Jiang S, Shen H. A rapidly progressive foot drop caused by the posttraumatic Intraneural ganglion cyst of the deep peroneal nerve. BMC Musculoskelet Disord. 2018;19(1):298.
5. Lui TH. Extensor tendons and deep peroneal nerve adhesion: treated by complete anterior ankle arthroscopic capsulotomy. Foot Ankle Surg. 2012;18(1):e1-3.
6. Takahashi S, Ogose A, Tajino T, Osanai T, Okada K. Osteosarcoma of the proximal fibula. An analysis of 13 cases in the northern Japan. Ups J Med Sci. 2007;112(3):366-72.
7. Stitgen SH, Cairns ER, Ebraheim NA, Niemann JM, Jackson WT. Anatomic considerations of pin placement in the proximal tibia and its relationship to the peroneal nerve. Clin Orthop Relat Res. 1992(278):134-7.
8. Soejima O, Ogata K, Ishinishi T, Fukahori Y, Miyauchi R. Anatomic considerations of the peroneal nerve for division of the fibula during high tibial osteotomy. Orthop Rev. 1994;23(3):244-7.
9. Chompoopong S, Apinhasmit W, Sangiampong A, Amornmettajit N, Charoenwat B, Rattanathamsakul N, et al. Anatomical considerations of the deep peroneal nerve for biopsy of the proximal fibula in Thais. Clin Anat. 2009;22(2):256-60.
10. Takeda A, Tsuchiya H, Mori Y, Tanaka S, Kikuchi S, Tomita K. Anatomical aspects of biopsy of the proximal fibula. Int Orthop. 2001;24(6):335-7.
11. Ryan W, Mahony N, Delaney M, O'Brien M, Murray P. Relationship of the common peroneal nerve and its branches to the head and neck of the fibula. Clin Anat. 2003;16(6):501-5.
12. Lawrence SJ, Botte MJ. The deep peroneal nerve in the foot and ankle: an anatomic study. Foot Ankle Int. 1995;16(11):724-8.
13. Ranade AV, Rajanigandha V, Rai R, Ebenezer DA. Relationship between the deep peroneal nerve and dorsalis pedis artery in the foot: a cadaveric study. Clin Anat. 2008;21(7):705-12.
14. Aktan Ikiz ZA, Ucerler H, Uygur M. Dimensions of the anterior tarsal tunnel and features of the deep peroneal nerve in relation to clinical application. Surg Radiol Anat. 2007;29(7):527-30.
15. Ikiz ZA, Ucerler H, Uygur M. The clinical importance of the relationship between the deep peroneal nerve and the dorsalis pedis artery on the dorsum of the foot. Plast Reconstr Surg. 2007;120(3):690-6.
16. Chitra R. The relationship between the deep fibular nerve and the dorsalis pedis artery and its surgical importance. Indian J Plast Surg. 2009;42(1):18-21.
17. Rab M, Ebmer J, Dellon AL. Innervation of the sinus tarsi and implications for treating anterolateral ankle pain. Ann Plast Surg. 2001;47(5):500-4.
18. Bryce TH. Long muscular branch of the musculocutaneous nerve of the leg. J Anat. 1896;31:5-12.
19. Prakash, Bhardwaj AK, Singh DK, Rajini T, Jayanthi V, Singh G. Anatomic variations of superficial peroneal nerve: clinical implications of a cadaver study. Ital J Anat Embryol. 2010;115(3):223-8.
20. Mathis S, Ciron J, du Boisgueheneuc F, Godeneche G, Hobeika L, Larrieu D, et al. Study of accessory deep peroneal nerve motor conduction in a population of healthy subjects. Neurophysiol Clin. 2011;41(1):29-33.
21. Kudoh H, Sakai T, Horiguchi M. The consistent presence of the human accessory deep peroneal nerve. J Anat. 1999;194(Pt 1):101-8.
22. Lambert EH. The accessory deep peroneal nerve. A common variation in innervation of extensor digitorum brevis. Neurology. 1969;19(12):1169-76.
23. Murad H, Neal P, Katirji B. Total innervation of the extensor digitorum brevis by the accessory deep peroneal nerve. Eur J Neurol. 1999;6(3):371-3.
24. Tomaszewski KA, Roy J, Vikse J, Pekala PA, Kopacz P, Henry BM. Prevalence of the accessory deep peroneal nerve: a cadaveric study and meta-analysis. Clin Neurol Neurosurg. 2016;144:105-11.
25. Saba EK. Electrophysiological study of accessory deep peroneal nerve in a sample of Egyptian subjects. Egypt Rhematol Rehabil. 2019;46:251-6.
26. Sinanovic O, Zukic S, Muftic M, Tinjic N. Prevalence of accessory deep peroneal nerve in sample of Bosnia and Herzegovina subjects: an electrophysiological study. Acta Inform Med. 2021;29(3):193-6.
27. Crutchfield CA, Gutmann L. Hereditary aspects of accessory

deep peroneal nerve. J Neurol Neurosurg Psychiatry. 1973;36(6):989-90.
28. Bianchi S, Martinoli C, editors. Ultrasound of the musculoskeletal system. Berlin: Springer; 2007.
29. Blitz NM, Amrami KK, Spinner RJ. Magnetic resonance imaging of a deep peroneal intraneural ganglion cyst originating from the second metatarsophalangeal joint: a pattern of propagation supporting the unified articular (synovial) theory for the formation of intraneural ganglia. J Foot Ankle Surg. 2009;48(1):80-4.
30. Nazarian LN. The top 10 reasons musculoskeletal sonography is an important complementary or alternative technique to MRI. AJR Am J Roentgenol. 2008;190(6):1621-6.
31. Yablon CM, Hammer MR, Morag Y, Brandon CJ, Fessell DP, Jacobson JA. US of the peripheral nerves of the lower extremity: a landmark approach. Radiographics. 2016;36(2):464-78.
32. Rumack CM, Levine D, editors. Diagnostic ultrasound. 5th ed. Philadelphia: Elsevier; 2018. 2 vol.
33. Becciolini M, Pivec C, Riegler G. Ultrasound imaging of the deep peroneal nerve. J Ultrasound Med. 2021;40(4):821-38.
34. Weig SG, Waite RJ, McAvoy K. MRI in unexplained mononeuropathy. Pediatr Neurol. 2000;22(4):314-7.
35. Panda S, Gourie-Devi M, Sharma A, Sud A. Isolated deep peroneal nerve palsy: role of magnetic resonance imaging in localization. Ann Indian Acad Neurol. 2015;18(4):451-3.
36. Vohra S, Arnold G, Doshi S, Marcantonio D. Normal MR imaging anatomy of the thigh and leg. Magn Reson Imaging Clin N Am. 2011;19(3):621-36.
37. Beggs I. Pictorial review: imaging of peripheral nerve tumours. Clin Radiol. 1997;52(1):8-17.
38. Ahlawat S, Belzberg AJ, Montgomery EA, Fayad LM. MRI features of peripheral traumatic neuromas. Eur Radiol. 2016;26(4):1204-12.
39. Hiramatsu K, Yonetani Y, Kinugasa K, Nakamura N, Yamamoto K, Yoshikawa H, et al. Deep peroneal nerve palsy with isolated lateral compartment syndrome secondary to peroneus longus tear: a report of two cases and a review of the literature. J Orthop Traumatol. 2016;17(2):181-5.
40. Rowdon GA, Richardson JK, Hoffmann P, Zaffer M, Barill E. Chronic anterior compartment syndrome and deep peroneal nerve function. Clin J Sport Med. 2001;11(4):229-33.
41. Henrot P, Stines J, Walter F, Martinet N, Paysant J, Blum A. Imaging of the painful lower limb stump. Radiographics. 2000;20 Spec No:S219-35.
42. Kransdorf MJ, Murphey MD. Imaging of soft tissue tumors. 2nd ed. Philadelphia: Lippincott, Williams & Wilkins; 2006.
43. Donovan A, Rosenberg ZS, Cavalcanti CF. MR imaging of entrapment neuropathies of the lower extremity. Part 2. The knee, leg, ankle, and foot. Radiographics. Radiographics. 2010;30(4):1001-19.
44. Neto N, Nunnes P. Spectrum of MRI features of ganglion and synovial cysts. Insights Imaging. 2016;7(2):179-86.
45. Bermejo A, De Bustamante TD, Martinez A, Carrera R, Zabia E, Manjon P. MR imaging in the evaluation of cystic-appearing soft-tissue masses of the extremities. Radiographics. 2013;33(3):833-55.
46. Sallomi D, Janzen DL, Munk PL, Connell DG, Tirman PF. Muscle denervation patterns in upper limb nerve injuries: MR imaging findings and anatomic basis. AJR Am J Roentgenol. 1998;171(3):779-84.
47. Galloway HR. Muscle denervation and nerve entrapment syndromes. Semin Musculoskelet Radiol. 2010;14(2):227-35.
48. Albayda J, van Alfen N. Diagnostic value of muscle ultrasound for myopathies and myositis. Curr Rheumatol Rep. 2020;22(11):82.
49. Bendszus M, Koltzenburg M, Wessig C, Solymosi L. Sequential MR imaging of denervated muscle: experimental study. AJNR Am J Neuroradiol. 2002;23(8):1427-31.
50. Kopka A, Serpell MG. Distal nerve blocks of the lower limb. Contin Educ Anaesth Crit Care Pain. 2005;5(5):166-70.
51. Pilny J, Kubes J. Operace prednozí ve svodné anestezii nohy [Forefoot surgery under regional anesthesia]. Acta Chir Orthop Traumatol Cech. 2005;72(2):122-4. Czech.
52. Gropper MA, Cohen NH, Eriksson LI, Fleisher LA, Leslie K, Wiener-Kronish JP, editors. Miller's anesthesia. 9th ed. Philadelphia: Elsevier; 2020. 2 vol.
53. Fung G, Liu SE. Regional anaesthesia for orthopaedic procedures. Anaesth Intensive Care Med. 2021;22(1):13–8.
54. Karmakar MK, editor. Musculoskeletal ultrasound for regional anaesthesia and pain medicine. 2nd ed. Hong Kong: The Chinese University of Hong Kong; 2016.
55. Marhofer P, Schrogendorfer K, Wallner T, Koinig H, Mayer N, Kapral S. Ultrasonographic guidance reduces the amount of local anesthetic for 3-in-1 blocks. Reg Anesth Pain Med. 1998;23(6):584-8.
56. Eichenberger U, Stockli S, Marhofer P, Huber G, Willimann P, Kettner SC, et al. Minimal local anesthetic volume for peripheral nerve block: a new ultrasound-guided, nerve dimension-based method. Reg Anesth Pain Med. 2009;34(3):242-6.
57. Latzke D, Marhofer P, Zeitlinger M, Machata A, Neumann F, Lackner E, et al. Minimal local anaesthetic volumes for sciatic nerve block: evaluation of ED 99 in volunteers. Br J Anaesth. 2010;104(2):239-44.
58. Antonakakis JG, Scalzo DC, Jorgenson AS, Figg KK, Ting P, Zuo Z, et al. Ultrasound does not improve the success rate of a deep peroneal nerve block at the ankle. Reg Anesth Pain Med. 2010;35(2):217-21.
59. Buschbacher RM. Peroneal nerve motor conduction to the extensor digitorum brevis. Am J Phys Med Rehabil. 1999;78(6 Suppl):S26-31.
60. Buschbacher RM. Reference values for peroneal nerve motor conduction to the tibialis anterior and for peroneal vs. tibial latencies. Am J Phys Med Rehabil. 2003;82(4):296-301.
61. Lo YL, Leoh TH, Dan YF, Tan YE, Nurjannah S, Fook-Chong S. An electrophysiological study of the deep peroneal sensory nerve. Eur Neurol. 2003;50(4):244-7.
62. Manning C, Cook S, Rand R, Mills J, Thomas A, Galloway K. Communications between the superficial and deep fibular nerves in the foot: an anatomical and electrophysiological study. Clin Anat. 2021;34(4):544-9.
63. Marchini C, Zambito Marsala S, Fabris F, Fornasier A, Ferracci F. Peroneal nerve orthodromic sensory conduction technique: normative data. Neurol Sci. 2009;30(3):201-5.
64. Dumitru D, Diaz CA, King JC. Prevalence of denervation in paraspinal and foot intrinsic musculature. Am J Phys Med Rehabil. 2001;80(7):482-90.
65. Logullo F, Ganino C, Lupidi F, Perozzi C, Di Bella P, Provinciali L. Anterior tarsal tunnel syndrome: a misunderstood and a misleading entrapment neuropathy. Neurol Sci. 2014;35(5):773-5.
66. Katirji MB, Wilbourn AJ. Common peroneal mononeuropathy: a clinical and electrophysiologic study of 116 lesions. Neurology.

1988;38(11):1723-8.
67. Karakis I, Khoshnoodi M, Liew W, Nguyen ES, Jones HR, Darras BT, et al. Electrophysiologic features of fibular neuropathy in childhood and adolescence. Muscle Nerve. 2017;55(5):693-7.
68. Derr JJ, Micklesen PJ, Robinson LR. Predicting recovery after fibular nerve injury: which electrodiagnostic features are most useful? Am J Phys Med Rehabil. 2009;88(7):547-53.
69. Bsteh G, Wanschitz JV, Gruber H, Seppi K, Loscher WN. Prognosis and prognostic factors in non-traumatic acute-onset compressive mononeuropathies - radial and peroneal mononeuropathies. Eur J Neurol. 2013;20(6):981-5.
70. Marciniak C, Armon C, Wilson J, Miller R. Practice parameter: utility of electrodiagnostic techniques in evaluating patients with suspected peroneal neuropathy: an evidence-based review. Muscle Nerve. 2005;31(4):520-7.
71. Greyson MA, Wilkens SC, Sood RF, Winograd JM, Eberlin KR, Donelan MB. Five essential principles for first web space reconstruction in the burned hand. Plast Reconstr Surg. 2020; 146(5):578e-587e.
72. Kalliainen LK, Schubert W. The management of web space contractures. Clin Plast Surg. 2005;32(4):503-14.
73. Moody L, Galvez MG, Chang J. Reconstruction of first web space contractures. J Hand Surg Am. 2015;40(9):1892-5.
74. Dantzer E, Queruel P, Salinier L, Palmier B, Quinot JF. Dermal regeneration template for deep hand burns: clinical utility for both early grafting and reconstructive surgery. Br J Plast Surg. 2003;56(8):764-74.
75. Hudson DA. Some thoughts on choosing a Z-plasty: the Z made simple. Plast Reconstr Surg. 2000;106:665-71.
76. Dautel G, Merle M. Direct and reverse dorsal metacarpal flaps. Br J Plast Surg. 1992;45(2):123-30.
77. Amouzou KS, Berny N, El Harti A, Diouri M, Chlihi A, Ezzoubi M. The pedicled groin flap in resurfacing hand burn scar release and other injuries: a five-case series report and review of the literature. Ann Burns Fire Disasters. 2017;30(1):57-61.
78. Woo SH, Seul JH. Optimizing the correction of severe postburn hand deformities by using aggressive contracture releases and fasciocutaneous free-tissue transfers. Plast Reconstr Surg. 2001; 107(1):1-8.
79. Muller-Seubert W, Horch RE, Schmidt VF, Ludolph I, Schmitz M, Arkudas A. Retrospective analysis of free temporoparietal fascial flap for defect reconstruction of the hand and the distal upper extremity. Arch Orthop Trauma Surg. 2021;141(1):165-71.
80. Woo SH, Choi BC, Oh SJ, Seul JH. Classification of the first web space free flap of the foot and its applications in reconstruction of the hand. Plast Reconstr Surg. 1999;103(2):508-17.
81. Zucker RM, Gur E, Hussain G, Manktelow RT. Facial paralysis. In: Rodriguez ED, Losee JE, Neligan PC, editors. Plastic surgery. 4th ed. Vol. 3, Craniofacial, head and neck surgery and pediatric plastic surgery. Philadelphia: Elsevier; 2018. p. 329-57.
82. Alagoz MS, Alagoz AN, Comert A. Neuroanatomy of extensor digitorum brevis muscle for reanimation of facial paralysis. J Craniofac Surg. 2011;22(6):2308-11.
83. Mathes SJ, Nahai F. Classification of the vascular anatomy of muscles: experimental and clinical correlation. Plast Reconstr Surg. 1981;67(2):177-87.
84. Pai CH, Lin GT, Lin SY, Lin SD, Lai CS. Extensor digitorum brevis rotational muscle flap for lower leg and ankle coverage. J Trauma. 2000;49(6):1012-6.
85. Sugg KB, Kim JC. Dynamic reconstruction of the paralyzed face, part II: Extensor digitorum brevis, serratus anterior, and anterolateral thigh. Oper Tech Otolaryngol Neck Surg. 2012; 23(4):275-81.
86. Rao VK, Butler JA. Microneurovascular free transfer of extensor digitorum brevis muscle for facial reanimation. In: Strauch B, Vasconez LO, Hall-Findlay EJ, editors. Grabb's encyclopedia of flaps. Vol. 3, Torso, pelvis, and lower extremities. Boston: Little, Brown; 1990. p. 613-7.
87. Mayou BJ, Watson JS, Harrison DH, Parry CB. Free microvascular and microneural transfer of the extensor digitorum brevis muscle for the treatment of unilateral facial palsy. Br J Plast Surg. 1981;34(3):362-7.
88. Akaranuchat N. Lower extremity reconstruction with vascularized free-tissue transfer: 20 years of experience in the faculty of medicine Siriraj hospital, Mahidol university, Bangkok, Thailand. Siriraj Med J. 2021;73(7):462–70.

Chronicle of Anatomical Education in Thailand: Experiences at Siriraj Medical School

Adisorn Ratanayotha, M.D., Ph.D.*,, Eve Mon Oo, MBBS, MMedSc, Ph.D.*,*****

**Department of Anatomy, Faculty of Medicine Siriraj Hospital, Mahidol University, Bangkoknoi, Bangkok, 10700, Thailand, **Laboratory of Integrative Physiology, Department of Physiology, Graduate School of Medicine, Osaka University, Suita, Osaka, 565-0871, Japan, ***Department of Anatomy, University of Medicine Taunggyi, Taunggyi, Shan State, 06017, Myanmar.*

ABSTRACT

Anatomical education in Thailand has advanced significantly since the first class at Siriraj Medical School in 1890. Gross anatomy was formerly taught by traditional lectures and demonstrations using human anatomical models until cadaveric dissection was officially integrated into the medical curriculum in 1906. Educational standard at the medical school was then raised to an international level during the reform of the medical curriculum with the cooperation of the Rockefeller Foundation in 1923-1935, with the main anatomical disciplines organized into correlated courses, and it has since been continuously improved to the present day. This review summarizes a brief history of anatomical education in Thailand based on experiences at Siriraj Medical School, together with detailing the most significant developments that have occurred over time. Advancements in cadaver preservation and modern educational materials for anatomy teaching are also covered. The primary goal of all advances in anatomical education is to provide students with positive learning experiences that will also improve their learning outcomes.

Keywords: Anatomical education; cadaveric dissection; cadaver preservation; anatomical specimens; educational multimedia; medical school (Siriraj Med J 2022; 74: 463-471)

Anatomical Education at Siriraj Medical School

1. First introduction of modern anatomical teaching in the medical school.

Modern anatomical teaching was introduced to Thailand after the establishment of Siriraj Hospital in 1888. Prince Damrong Rajanubhab was granted royal permission from King Chulalongkorn to establish the first medical school in Thailand at Siriraj Hospital, conducting a three-year diploma course in medicine beginning from 1890.[1] Gross anatomy was first taught by Dr. Thomas H. Hays from 1890, and then by Dr. George B. McFarland from 1892, mainly through traditional lectures and demonstrations with human anatomical models. Dissection was occasionally performed on non-preserved cadavers to provide students with the opportunity to become familiar with real human structures.[1-3]

In 1901, Siriraj Medical School was renamed the "Royal Medical College" by King Chulalongkorn, and the diploma course in medicine was expanded to five years. Cadaveric dissection remained optional until 1906 when it was formally incorporated into the medical curriculum. During that time, Dr. McFarland, Dr. Michel St. Ann Fernandes, and Dr. Walter B. Toy were in charge of teaching gross anatomy and cadaveric dissection.[2-4] To facilitate students' learning, Dr. McFarland also wrote *Human Anatomy with Plates and Diagrams Vols I, II, and III*, which included Thai translations of anatomical terms.[5,6] Students generally studied musculoskeletal

Corresponding author: Adisorn Ratanayotha
E-mail: adisorn.rat@mahidol.edu
Received 25 April 2022 Revised 18 May 2022 Accepted 19 May 2022
ORCID ID: https://orcid.org/0000-0003-3278-8587
http://dx.doi.org/10.33192/Smj.2022.55

anatomy without cadaveric dissection in the first year, and then dissected in the second and third years when studying blood vessels, the nervous system, and visceral organs. Non-preserved cadavers used for dissection were obtained from unclaimed human bodies and could only be dissected in a short period before the bodies decomposed.[2,3] Notably, cadaver preservation was most likely attempted before 1912, with a phenol-based solution infused into the femoral arteries of cadavers. However, the preservation efficiency was still inadequate.[7,8]

In 1917, King Vajiravudh founded Chulalongkorn University and merged the Royal Medical College to form the Faculty of Medicine. In 1919, the anatomical class was moved from Siriraj Hospital to the Faculty of Arts and Science in Pathum Wan District.[9,10] Dr. Toy, Luang Kayavibhag Banyai, and Lecturer Lim Chullabhandh were in charge of teaching gross anatomy and cadaveric dissection during that time. The course was revised to two years: students studied and dissected upper and lower extremities in the first year, followed by head and trunk in the second year, using cadavers preserved with a phenol-based solution and stored in large refrigerators.[8,9,11]

2. Anatomical education during the reform of the medical curriculum with the cooperation of the Rockefeller Foundation (1923-1935)

Anatomical education at the Faculty of Medicine was substantially improved when the Rockefeller Foundation, in cooperation with the Siamese Government, helped modernize medical education in Thailand. In 1923, a new six-year curriculum for a Bachelor of Medicine (M.B.) degree was implemented, and the anatomical class was returned to Siriraj Hospital.[10,11] In the same year, Prof. Claude W. Stump from the University of Edinburgh was appointed Professor of Anatomy at Siriraj Hospital. He introduced a new preservation method for cadavers using a formalin-based solution and conducted a one-year dissection class based on *Cunningham's Manual of Practical Anatomy*. He was also the first to teach embryology in the medical school. However, his embryology class appeared to have been limited to lectures and figure drawings due to a lack of microscopic slides.[2,8,12]

In 1925, Prof. Edgar D. Congdon from Peking Union Medical College (PUMC) was appointed Professor of Anatomy at Siriraj Hospital to replace Prof. Stump, who had completed his contact with the Rockefeller Foundation and relocated to the University of Sydney, Australia. In 1927-1928, Prof. Congdon broadened anatomical teaching to cover gross anatomy, microscopic anatomy, embryology, neuroanatomy, and topographic anatomy, in line with international standards.[2,3,13] He developed a new method of anatomical teaching known as the "correlated course," in which students learned the developmental, gross, and microscopic anatomy of individual organs together in the course schedule.[14] He organized a dissection class in which four students would dissect one cadaver (4:1) by following his laboratory directions for an entire academic year[2,12] – a practice that is still implemented at Siriraj Hospital today. He also began preparing microscopic slides of tissue sections, laying the groundwork for the development of microtechniques in the department.[8] Furthermore, Prof. Congdon initiated collections of anatomical specimens for class demonstration, some of which were displayed at the 8th Congress of the Far Eastern Association of Tropical Medicine at Chulalongkorn University in 1930. His collections later became the centerpieces at an anatomical museum at Siriraj Hospital.[15-17]

In 1930, Dr. Sood Sangvichien became an instructor at the Department of Anatomy and received a scholarship from the Rockefeller Foundation to study anatomy and microtechniques at the University of Michigan and Case Western Reserve University in the United States. After returning in 1933, Dr. Sood Sangvichien further developed microtechniques in the department, with the assistance of Lect. Lim Chullabhandh, and succeeded in preparing microscopic slides of the total mounted and serial sections of chick and pig embryos, tissues and organs sections, and brainstem sections.[18,19] Microtechnique development since then has enabled the in-house preparation of microscopic slides that could sufficiently be used for anatomical teaching at the Faculty of Medicine and other health science schools. In 1942-1943, during the Pacific War in World War II, Dr. Sood Sangvichien began writing laboratory directions and distributing them to students to conduct cadaveric dissection despite the wartime shortage of standard textbooks. Prof. Sood Sangvichien's directions were later revised by Prof. Sanjai Sangvichien and his colleagues in 2009.[17,20]

3. Anatomical education under the supervision of Prof. Sood Sangvichien

In 1943, the Faculty of Medicine was transferred to the University of Medical Sciences. Dr. Sood Sangvichien was appointed Head of the Department of Anatomy in 1944 and served in this position until 1969.[21] He passionately dedicated himself to advancing anatomical knowledge and related disciplines, such as medical genetics, medical illustrations, and physical anthropology. In terms of education, the correlated course designed by Prof. Congdon remained the core of anatomical teaching, and Dr. Sood Sangvichien modified it further

to fit the medical curriculum at the time. He improved Prof. Congdon's formalin-based solutions for better cadaver preservation. He also encouraged Thai people to donate their bodies for anatomical education so that students would have sufficient cadavers for standard dissection class (4 students:1 cadaver). His development of in-house microtechniques since before World War II enabled him and his colleagues at the Department of Anatomy to prepare sufficient amounts of microscopic slides for students.[20] In 1947, the Faculty of Medicine Chulalongkorn Hospital was established, with a similar anatomical curriculum as at Siriraj Hospital.[3,22]

In 1948, Dr. Sood Sangvichien expanded Prof. Congdon's collections of anatomical specimens and officially founded Congdon's Anatomical Museum at Siriraj Hospital to honor Prof. Congdon for his crucial contribution to early anatomical education in Thailand.[16] Nowadays, over 2,000 organ specimens from donors who donated their bodies for anatomical education are on display, including world masterpieces, such as the whole-body peripheral nervous system, the heart and whole-body arterial system, and the whole-body muscles and subcutaneous veins.[17] The museum continues to benefit medical personnel and the general public interested in learning human anatomy.

In 1952, Dr. Sood Sangvichien was appointed Professor of Anatomy and continued to make significant contributions to anatomical education in Thailand. In 1962, he founded the Prehistoric Museum at Siriraj Hospital: for which he continued to work even after his retirement in 1970.[23] Physical anthropology has long been one of the department's research interests and staff members are still working on this today.

In 1960, the Faculty of Medicine Nakorn Chiangmai Hospital was founded, with the assistance of staff from Siriraj Hospital in organizing the anatomical curriculum. In the same year, Prof. Sood Sangvichien invited anatomy staff from Siriraj Hospital, Chulalongkorn Hospital, and Nakorn Chiangmai Hospital to organize the first academic meeting for anatomists at Siriraj Hospital.[18,21] This initiative later became the Anatomy Club of Thailand in 1978, and officially the Anatomy Association of Thailand in 2002.

4. Anatomical education from the 1970s

The University of Medical Sciences became Mahidol University in 1969.[24] The Faculty of Medicine Siriraj Hospital and the Faculty of Medicine Ramathibodi Hospital (established in 1965) remain with Mahidol University, while the Faculty of Medicine Chulalongkorn Hospital and the Faculty of Medicine Nakorn Chiangmai Hospital were transferred to Chulalongkorn University and Chiangmai University, respectively. The anatomical curriculum at Siriraj Hospital was gradually changed over the years, with the correlated course remaining the core concept.[3]

The Faculty of Medicine Siriraj Hospital revised the medical curriculum in the early 1970s and later on a regular basis. Lecture and laboratory time were significantly reduced in all anatomical disciplines: from a total of 875 hours in 1956 to 726 hours in 1971, and 616 hours in 1982, and this trend has continued today. Topographic anatomy as a separate subject was discontinued in 1974, but it has since been incorporated into regional gross anatomy.[3,24,25] In 2014, gross anatomy, microscopic anatomy, and embryology were reorganized into functional systems (system-based curriculum) along with physiology, biochemistry, and related subjects. Furthermore, clinical applications have become increasingly integrated into anatomical teaching to ensure that students are well prepared for clinical practices.

5. Anatomical education in global trends and future perspective.

Thailand and many other countries appear to have comparable anatomical curriculums. In ASEAN countries, such as Myanmar, the curriculum prior to 2019 was quite similar to the previous one of Siriraj Hospital, as the main anatomical disciplines were organized into correlated courses based on regional anatomy. Case-based learning (CBL) was also used to help students gain more experience with clinical applications. However, since 2020, all medical universities in Myanmar have reorganized their anatomical curriculums into functional systems with a more holistic and integrated approach to medical education.

In other Asian countries, such as Japan, we learned that anatomical curriculums in certain universities are still based on regional anatomy but are condensed into half an academic year. Due to time constraints, student-centered and self-directed learning becomes increasingly important in laboratory practices. Meanwhile, many Japanese universities have implemented an integrated medical curriculum that combines basic and clinical medicine courses based on body organ systems.[26] This system-based approach is similar to the current preclinical curriculum at Siriraj Hospital, except that it also applies to clinical years. It should be noted that the preference for a system-based approach has increased in medical schools in various countries, including the United Kingdom and Ireland[27], the United States[28], and Australia and New Zealand.[29]

The coronavirus disease 2019 (COVID-19) pandemic

has disrupted current practices in anatomical education. Gross anatomy, in particular, has traditionally required cadaveric dissection, but the physical distancing regulation has limited such hands-on laboratory practice, posing enormous challenge to Siriraj Hospital and medical schools worldwide. Rapid adaptation has thus been made to overcome this challenge through the development of new online resources, digital technologies, and virtual reality workspaces.[30-34] This trend is likely to continue and will have a global impact on the future direction of anatomical education beyond the pandemic era.

Modern anatomical science at the Faculty of Medicine Siriraj Hospital

1. Gross anatomy

Gross anatomy is the study of visible structures in the human body, involving cadaveric dissection and medical imaging. It was the first anatomical discipline taught at Siriraj Medical School, dating back to 1890, before being integrated into the correlated course with microscopic anatomy and embryology by Prof. Congdon in the late 1920s.[14] The teaching of gross anatomy is organized into eight body regions: 1) body wall and axilla; 2) upper extremity; 3) head and neck; 4) thorax; 5) abdomen; 6) lower extremity; 7) perineum and pelvis; and 8) cranial nerves and organs of special senses.

Students attend lectures and conduct cadaveric dissection in parallel by following the laboratory directions. Generally, four students are assigned to dissect one cadaver (4:1) for an entire academic year. Studying gross anatomy by body regions allows students to appreciate human structures and their relations, thus conceptualizing anatomical knowledge more effectively. Regional anatomy at Siriraj Hospital has been reorganized to comply with the functional systems in the current medical curriculum while retaining the eight regions in the postgraduate curriculum. Clinical applications are integrated into the learning topics of all the regions to prepare students for advanced clinical knowledge.

2. Microscopic anatomy

Microscopic anatomy is the study of anatomical structures at the microscopic level, typically through a microscope to examine cells or tissues. Prof. Congdon first introduced and then incorporated microscopic anatomy into the correlated course in the late 1920s.[14]

Teaching microscopic anatomy at Siriraj Hospital begins with the fundamental concepts, such as the cellular components and basic cell types, and then proceeds to the detailed tissue structures correlated with organ systems learned in gross anatomy. Each student receives one optical microscope and one complete set of tissue-sectioned microscopic slides of all the essential organs (~250 slides) for individual use in laboratory classes during an academic year. Recently, high-resolution digital slides have also been implemented for teaching and demonstration. As with gross anatomy, teaching microscopic anatomy in the medical curriculum has been reorganized into functional systems while remaining a full-scale subject in our department's postgraduate curriculum.

3. Embryology

Embryology is the study of the prenatal development of embryos and fetuses, as well as congenital abnormalities. It was first taught at the medical school by Prof. Stump in 1923[2,3,13] and was integrated into the correlated course by Prof. Congdon in the late 1920s.[14]

Teaching embryology begins with the basic knowledge of gametogenesis, fertilization, and early embryonic development, and then progresses to the detailed morphogenesis and organogenesis correlated with gross anatomy. The course also covers congenital abnormalities and clinical applications. During an academic year, each student receives a complete set of total mount and serial section slides of chick and pig embryos at various stages of development. Currently, 3D models, digital slides, and interactive multimedia are also available to help students conceptualize embryonic development. Embryology has been integrated into the functional system of the current medical curriculum and redesigned into developmental biology in our department's postgraduate curriculum.

4. Neuroanatomy

Neuroanatomy is the study of the structures and organization of the nervous system, including the neuronal pathways and clinical correlation. Prof. Congdon first taught neuroanatomy at Siriraj Hospital in 1928.[2,3,13]

Teaching neuroanatomy begins with the fundamental knowledge, such as the general organization of the nervous system, and then proceeds to the detailed structures from the spinal cord to the cerebral hemispheres and internal neural connections. The rationale for teaching neuroanatomy in an "ascending manner" is that students begin with the simple structures in the spinal cord and progress to the more complex structures in the brainstem, and finally to the cerebral hemispheres and their associated circuitries. Functional and clinical correlations are integrated into all learning topics. In laboratory class, every two students are provided with a complete set of nervous tissue slides, including all the spinal cord levels, brainstem, and diencephalon,

all of which are prepared in our department. To better understand the brain's structures, students can also study whole brains and dissected brains impregnated with polyethylene glycol (PEG) as well as serial brain sections preserved in formalin-filled plastic boxes (brain boxes). Neuroanatomy has been integrated with neurophysiology in the current medical curriculum, and is currently being redesigned as clinical neuroanatomy and neuroscience in the postgraduate curriculum in our department.

5. Topographic anatomy

Topographic anatomy is the study of the human body focusing on the relationships between various structures in body parts. This can be accomplished by examining human serial sections in the same way that sectional radiographic images are examined. Prof. Congdon first taught topographic anatomy at Siriraj Hospital in 1927, using illustrations and 1-inch serial sections of embalmed cadavers as teaching materials.[3,25] Some samples of complete human serial sections are currently displayed in Congdon's Anatomical Museum.

In 1974, the teaching of topographic anatomy as a separate discipline was discontinued, but was later incorporated into gross anatomy.[3,25] However, our department recently resumed the subject as an elective course for medical students in 2020. The course begins with the fundamental concepts in topographic anatomy and then proceeds to serial sections of various parts of the human body based on regional anatomy. Clinical imaging is incorporated into all learning topics to help students correlate their knowledge with clinical practice. The course has yet to be resumed in the postgraduate curriculum at our department.

6. Applied anatomy

Applied anatomy at Siriraj Hospital initially focused on clinical applications based on topographic anatomy, and it involved teaching staff from various clinical departments, such as radiology, surgery, and internal medicine.[25,35] However, the teaching concept shifted with the discontinuation of topographic anatomy in 1974, and applied anatomy was subsequently integrated into all anatomical disciplines in the medical and postgraduate curriculums at Siriraj Hospital.

Beginning in 2019, our department has offered new elective courses in modern applied anatomy for medical students. The currently available courses are applied anatomy of the upper extremities, applied anatomy of the lower extremities, and evolutionary anatomy. We also offer refresher courses in clinical anatomy for residency training in collaboration with clinical departments, such as the Department of Otorhinolaryngology and the Department of Radiology. Additional courses in our plan include biomechanics and kinesiology, physical and forensic anthropology, modern media in anatomy, 3D anatomical reconstruction, and integrative clinical neuroscience.

Advancement in human cadaver preservation

Human cadavers have been used for anatomical education since the beginning of Siriraj Medical School. Medical students at the time typically used non-preserved cadavers in their dissection classes because the preservation methods were still underdeveloped. This situation created an inconvenient learning experience because non-preserved cadavers would decompose rapidly, especially under the tropical weather environment in Thailand. Notably, non-preserved cadavers were most likely used for dissection classes until around 1912 when a phenol-based solution was used to preserve human bodies at Siriraj Hospital. Nonetheless, the preservation efficiency was still inadequate and an intensely unpleasant odor remained the primary concern.[7,8]

Prof. Stump was the first to use formalin-based solution to preserve cadavers at Siriraj Hospital in 1923.[2,12,13] Several cadaver preservation methods have since been developed, including the conventional formalin/arsenic-based solution, the most commonly used in medical schools in Thailand. Currently, three types of preserved cadavers are available in the Department of Anatomy, the Faculty of Medicine Siriraj Hospital: 1) conventional embalmed human cadavers; 2) soft cadavers; and 3) fresh cadavers.[36] Each type has advantages and disadvantages, making them appropriate for different dissection purposes.

1. Conventional embalmed human cadavers

Human cadavers were preserved by infusing the femoral arteries with a mixture of formalin, potassium nitrate, arsenic, glycerin, ethanol, and phenol; the cadavers were then submerged in a phenol-glycerin immersion solution for at least three months before being used for cadaveric dissection. The method was first used by Prof. Congdon, likely around 1925, and then modified by Prof. Sood Sangvichien in 1927 to make the cadavers more suitable for use in Thailand. The detailed formula is available from our department upon request. Conventional embalming has since been used as the primary preservation method in our department because it is inexpensive, suitable for use in the long-term preservation of cadavers at room temperature, and ideal for general cadaveric dissection. However, it has significant drawbacks as it causes joint stiffness and tissue rigidity in cadavers.

2. Soft cadavers

Soft cadaver preservation was first implemented in our department in 2011, using a protocol adapted from Thiel's cadaver preservation.[36] The method was developed by Prof. Walter Thiel at Graz Institute of Anatomy.[37] Human cadavers were infused in the femoral arteries with Thiel's infusion solution – a mixture of various chemicals, including boric acid, ethylene glycol, ammonium nitrate, potassium nitrate, sodium sulfate, and formalin. The cadavers were then submerged in the immersion solution with similar components but different concentrations to the infusion solution for at least three months before being used for cadaveric dissection.[36-38] Unlike conventional embalming, Thiel's method preserves the tissue texture, plasticity, and joint flexibility similar to a fresh specimen; thus providing cadavers suitable for surgical skill practices. The disadvantages of this method, however, include its complicated formula, high cost, and lengthy preparation time.

3. Fresh cadavers

Our department began developing fresh cadaver preservation for surgical training in 2006.[36] Human cadavers were immediately preserved in a deep freezer at -20°C without a preservative solution; they were then defrosted just before being used. This method preserves the tissue consistency and joint motion as close to living humans as possible; thus, the cadavers are appropriate for surgical skill practices that require near-living cadavers, such as facial skin injection and laparoscopic surgery. However, because no preservative solution is used, the cadavers preserved with this method should be dissected in a low-temperature environment and are only available for a limited time.

4. Future direction of human cadaver preservation

The Department of Anatomy at Siriraj Hospital has long been dedicated to the advancement of cadaver preservation. Cadavers preserved in our department are widely used in anatomical teaching and research at Siriraj Hospital and are also distributed among medical and dental institutes throughout Thailand. We have collaborated with the Siriraj Training and Education Center for Clinical Skills (SiTEC) to host national and international surgical workshops using soft and fresh cadavers since 2014. Furthermore, we are currently developing "brain-preservative soft cadavers" – a method that combines traditional embalming with soft cadaver preservation[39] – for future anatomical education and research, particularly in the fields of neuroanatomy and neurosurgery.

Modern materials and multimedia in current anatomical education

Although cadaveric dissection has long been and will continue to be the primary method of anatomical education, a wide range of materials and multimedia are now available to help students better understand human anatomy. Summarized below are some examples of supplemental educational materials that have been successfully used in the Department of Anatomy at Siriraj Hospital.

1. Plastination

Dr. Gunther von Hagens of Heidelberg University first developed cadaveric plastination in 1979[40], and it has since been used for preparing specimens in medical schools and anatomical museums. In this technique, water and lipids in biological tissues are replaced with curable polymers, which are subsequently hardened, resulting in dry, odorless, and long-lasting specimens. Our department has used the Silicone S-10 standard plastination technique to preserve organ specimens for demonstrations in dissection classes and exhibitions in the anatomical museum.[41] The Plastination Unit of our department is dedicated to producing high-quality plastinated specimens, and we are currently developing thin-sheet plastination.

2. Cadaveric angiography

An angiographic approach has been used to infuse colorized polymers into the blood and lymphatic vessels of cadavers.[42,43] This technique can be used to colorize the vessels and preserve the vascular framework; therefore, it is useful for preparing vascular specimens for anatomical teaching, research, and exhibition. Masterpieces from our Cadaveric Angiography Unit include the colorized coronary arterial system, vasculatures of the adult liver and intestines, external facial vasculatures, arteries of the upper and lower extremities, and the entire arterial system of a newborn baby. This method is also utilized to investigate the vascular distribution and surgical anatomy of various organs.[44,45]

3. PEG-impregnated brains and serial brain sections (brain boxes)

Polyethylene glycol (PEG) has been used in our department to preserve brain specimens as an alternative to conventional formalin-embalming and plastination. PEG impregnation produces durable specimens with soft texture, high flexibility, and no skin irritation.[46,47] We have used PEG-impregnated brains for teaching neuroanatomy, enabling students to study and dissect

brain structures with greater appreciation. The specimens can be stored in closed plastic bags at room temperature and thus are suitable for long-term use as educational materials.

We have also prepared serial brain sections (brain boxes) for students. Conventional embalmed brains were serially cut in the horizontal, coronal, or sagittal planes with the appropriate thickness to display the internal structures. The specimens were then preserved in clear plastic boxes filled with formalin-based solution and arranged in series so that students could use them for reviewing the topographic anatomy of the brains in correlation with clinical imaging. Our serial brain sections have been used at Siriraj Hospital and distributed among medical schools throughout Thailand.

4. Three-dimensional printed models.

Three-dimensional (3D) printing technology has recently attracted considerable interest from those working in medicine and healthcare. 3D-printed anatomical models, the bio-printing of tissues and organs, and customized implants and prostheses are among the beneficial applications of this technology.[48-50] Our department at Siriraj Hospital has used 3D printing technology to create anatomical models of various organ structures, including those difficult to access in conventional cadaveric dissection, such as the ear ossicles and vestibular organs. These models help students conceptualize anatomical knowledge more effectively. We also plan to apply 3D printing technology in biomedical research in the near future.

5. Digital microscopic slides, interactive multimedia, and virtual dissection tables

Digital transformation is the leading future direction for anatomical education, particularly in the post-pandemic era. We have applied immersive technology[51] in teaching to help students understand basic anatomical concepts and clinical applications. Currently, histological and embryological slides produced in our department have been digitized to high-resolution images and stored in cloud libraries that are accessible by staff and students. Gross anatomical specimens and serial embryological sections have been reconstructed to create 3D interactive multimedia. Furthermore, virtual dissection tables, known as Anatomage tables, have recently been integrated into our anatomical courses, enabling students to simulate virtual cadaver-based dissections and surgical operations, complementing the conventional cadaveric dissection. These digital technologies, when combined, provide students with positive learning experiences and therefore improve their learning outcomes.

Conclusion and future perspective

Anatomical education in Thailand has advanced significantly since the first class at Siriraj Medical School in 1890. Teaching and research in anatomical disciplines have been expanded to all medical schools that have since been established. As Thailand's oldest anatomical department, the Department of Anatomy at the Faculty of Medicine Siriraj Hospital is constantly working to improve anatomical education by following our great professors' footsteps and incorporating new technologies to enhance students' understanding and learning experiences.

ACKNOWLEDGMENTS

We sincerely thank Prof. Sanjai Sangvichien (Faculty of Medicine Siriraj Hospital, Mahidol University, Thailand) for his valuable advice and inspiration in studying the history of Siriraj Hospital and Siriraj Medical School. We thank Prof. Sanya Sukpanichnant and Prof. Supin Chompoopong (Faculty of Medicine Siriraj Hospital, Mahidol University, Thailand) for their comments on the revision of the manuscript, as well as Dr. Rosarin Ratanalekha, Dr. Chairat Turbpaiboon, and all staff members at the department for their suggestions and encouragement. Our thanks also to Ms. Bongkoch Prakittikul (Siriraj Medical Library, Siriraj Hospital, Thailand) for her kind assistance in searching for publications on medical history, and Ms. Tanjira Ridtitid (Faculty of Medicine Siriraj Hospital, Mahidol University, Thailand) for her kind assistance during the submission process. This work was supported by Chalermprakiat Grant, Faculty of Medicine Siriraj Hospital, Mahidol University, Thailand (to A.R.).

Competing interests

The authors declares that no competing interests exist.

REFERENCES

1. Sangvichien S. Siriraj Hospital: the first hospital. In: Sirinavin C, Thongcharoen P, Ratanamaneechat S, editors. Siriraj Hospital's Centennial: history and development. Bangkok, Thailand: Victory Powerpoint Co. Ltd; 1988.p.1-26.
2. Sangvichien S. Anatomy in Thailand, Part I before 1928. Cremation volume for Luang Kayavibhag Banyai: Chuan Pim Press; 1964.p.84-100.
3. Diloksambandh V. The development of anatomy at Siriraj Medical School. Siriraj Hosp Gaz. 1982;34(10):823-7.
4. Sangvichien S. Royal Medical College. In: Sirinavin C, Thongcharoen P, Ratanamaneechat S, editors. Siriraj Hospital's Centennial:

history and development. Bangkok, Thailand: Victory Powerpoint Co., Ltd; 1988.p.35-84.
5. McFarland GB. Anatomy Vol. I and II. 2nd ed. Bangkok, Thailand; 1916.
6. McFarland GB. McFarland Family History. In: Borirakwetchakan, editor. Cremation volume for Prah Arj Vidyagom (George B McFarland). Bangkok, Thailand: Sereewanich Press; 1950. p. 1-23.
7. Khun Chamni Vejasarn. Siriraj Medical School 50 years ago (Part I). Siriraj Hosp Gaz. 1967;19(11):601-7.
8. Sangvichien S. Professor Crosby and the teaching of neuroanatomy in Thailand. Siriraj Hosp Gaz. 1984;36(5):327-40.
9. Sangvichien S. The development of the Faculty of Arts, Chulalongkorn University, as well as the Faculty of Medicine Siriraj Hospital, between 1923 and 1935. Siriraj Hosp Gaz. 1984; 36(1):35-53.
10. Sangvichien S. Faculty of Medicine and Siriraj Hospital, Chulalongkorn University. In: Sirinavin C, Thongcharoen P, Ratanamaneechat S, editors. Siriraj Hospital's Centennial: history and development. Bangkok, Thailand: Victory Powerpoint Co. Ltd; 1988.p.85-180.
11. Sangvichien S. Reform of the medical education in Thailand during the cooperation with the Rockefeller Foundation, between 1923-1935. Siriraj Hosp Gaz. 1983;35(7):661-70.
12. Sangvichien S. Anatomical knowledge in our country. In: Sangvichien S, editor. Professor Edgar Davidson Congdon and the History of Anatomy in Thailand until 1967. Bangkok, Thailand: Aksorn Sampan Press; 1967. p. 78-122.
13. Sangvichien S. Medical curriculum during the cooperation with the Rockefeller Foundation (1923-1935). Siriraj Hosp Gaz. 1983;35(6):569-83.
14. Congdon ED. An attempt to improve the methods of anatomical teaching, including the organization of the dissection to an unusual degree by systems and the bringing of the developmental, gross, and microscopic anatomy of individual organs together in the schedule. The Anatomical Record. 1930;45(4):323-37.
15. Sangvichien S. Professor E.D. Congdon. Siriraj Hosp Gaz. 1967;19(3):169-81.
16. Sangvichien S. History of Congdon's Anatomical Museum. In: Sangvichien S, editor. Memorial note: cerebration of Anatomy and Physiology Building with the official opening of Congdon's Anatomical Museum. Bangkok, Thailand: Thai Kosana; 1948.
17. Editorial Team of 120 Memorabilia of Siriraj. Medical education: how the medical school began and developed. In: Sangvichien S, Sukpanichnant S, Sangruji T, Mekanant P, Namatra C, Em-yam S, et al., editors. 120 Memorabilia of Siriraj. Bangkok, Thailand: Plan Printing Co., Ltd.; 2008.p.230-311.
18. Sangvichien S. Anatomy in Thailand, Part II. In: Sangvichien S, editor. Professor Edgar Davidson Congdon and the History of Anatomy in Thailand until 1967. Bangkok, Thailand: Aksorn Sampan Press; 1967.p.47-77.
19. Sangvichien S. In remembrance of Lim. In: Sangvichien S, editor. Cremation volume for Lim Chullabhandh. Bangkok, Thailand: Aksorn Sampan Press; 1970.p. 9-14.
20. Sangvichien S. Sood Sangvichien's Textbook of Anatomy: dissection directions. 2nd ed. Bangkok, Thailand; 2009.
21. Sangvichien S. Faculty of Medicine and Siriraj Hospital, the University of Medical Sciences. In: Sirinavin C, Thongcharoen P, Ratanamaneechat S, editors. Siriraj Hospital's Centennial: history and development. Bangkok, Thailand: Victory Powerpoint Co. Ltd; 1988. p. 181-264.
22. Diloksambandh V. The curriculum of anatomy at Siriraj. Siriraj Hosp Gaz. 1972;24(8):1319-32.
23. Subhavan V, Pramankij S, Solheim WG. Sood Sangvichien, 1907-1995. Asian Perspectives. 1997;36(2):260-4.
24. Sangvichien S. Faculty of Medicine Siriraj Hospital, Mahidol University. In: Sirinavin C, Thongcharoen P, Ratanamaneechat S, editors. Siriraj Hospital's Centennial: history and development. B angkok, Thailand: Victory Powerpoint Co. Ltd; 1988. p. 265-324.
25. Diloksambandh V. The teaching of topographic anatomy. Siriraj Hosp Gaz. 1984;36(4):251-4.
26. Shimura T, Aramaki T, Shimizu K, Miyashita T, Adachi K, Teramoto A. Implementation of integrated medical curriculum in Japanese medical schools. J Nippon Med Sch. 2004;71(1):11-6.
27. Smith CF, Freeman SK, Heylings D, Finn GM, Davies DC. Anatomy education for medical students in the United Kingdom and Republic of Ireland in 2019: A 20-year follow-up. Anat Sci Educ. 2021.
28. McBride JM, Drake RL. National survey on anatomical sciences in medical education. Anat Sci Educ. 2018;11(1):7-14.
29. Bouwer HE, Valter K, Webb AL. Current integration of dissection in medical education in Australia and New Zealand: Challenges and successes. Anat Sci Educ. 2016;9(2):161-70.
30. Pather N, Blyth P, Chapman JA, Dayal MR, Flack N, Fogg QA, et al. Forced Disruption of Anatomy Education in Australia and New Zealand: An Acute Response to the Covid-19 Pandemic. Anat Sci Educ. 2020;13(3):284-300.
31. Longhurst GJ, Stone DM, Dulohery K, Scully D, Campbell T, Smith CF. Strength, Weakness, Opportunity, Threat (SWOT) Analysis of the Adaptations to Anatomical Education in the United Kingdom and Republic of Ireland in Response to the Covid-19 Pandemic. Anat Sci Educ. 2020;13(3):301-11.
32. Harmon DJ, Attardi SM, Barremkala M, Bentley DC, Brown KM, Dennis JF, et al. An Analysis of Anatomy Education Before and During Covid-19: May-August 2020. Anat Sci Educ. 2021;14(2):132-47.
33. Shin M, Prasad A, Sabo G, Macnow ASR, Sheth NP, Cross MB, et al. Anatomy education in US Medical Schools: before, during, and beyond COVID-19. BMC Med Educ. 2022;22(1):103.
34. Nakai K, Terada S, Takahara A, Hage D, Tubbs RS, Iwanaga J. Anatomy education for medical students in a virtual reality workspace: A pilot study. Clin Anat. 2022;35(1):40-4.
35. Sangvichien S. Anatomical studies and research projects. In: Sangvichien S, editor. Professor Edgar Devidson Congdon and the History of Anatomy in Thailand until 1967. Bangkok, Thailand: Aksorn Sampan Press; 1967.p.123-42.
36. Sangchay N. The soft cadaver (Thiel's Method) : the new type of cadaver of Department of Anatomy, Siriraj Hospital. Siriraj Med J. 2014;66(6 Suppl):S228-S31.
37. Thiel W. Supplement to the conservation of an entire cadaver according to W. Thiel. Ann Anat. 2002;184(3):267-9.
38. Ottone NE, Vargas CA, Fuentes R, Del Sol M. Walter thiel's embalming method. Review of solutions and applications in different fields of biomedical research. International Journal of Morphology. 2016;34(4):1442-54.
39. Miyake S, Suenaga J, Miyazaki R, Sasame J, Akimoto T, Tanaka T, et al. Thiel's embalming method with additional intra-cerebral ventricular formalin injection (TEIF) for cadaver training of head and brain surgery. Anat Sci Int. 2020;95(4):564-70.

40. von Hagens G, Tiedemann K, Kriz W. The current potential of plastination. Anat Embryol. 1987;175(4):411-21.
41. Amonmettajit N, Waema M, Wiwatwongsakul A. Improvement S10 method for higher quality of plastinated gross specimens. Siriraj Med J. 2019;71(Suppl 1):S90-S2.
42. Ratanalekha R, Oonjitti T, Piyaman P, Ongsiriporn M, Ittawittayawat P. Colored contrast agent for three-dimensional CT angiography and anatomical dissection: a cadaveric study. Siriraj Med J. 2019;71(Suppl 1):S9-S13.
43. Ratanalekha R, Sangkamard K, Chongkolwatana W, Piyaman P, Predapramote P. Comparing orthodontic methylmethacrylate and polyurethane-based media in corrosion casting: for medical education. Siriraj Med J. 2019;71(Suppl 1):S14-S8.
44. Piyaman P, Patchanee K, Oonjitti T, Ratanalekha R, Yodrabum N. Surgical anatomy of vascularized submental lymph node flap: Sharing arterial supply of lymph nodes with the skin and topographic relationship with anterior belly of digastric muscle. J Surg Oncol. 2020;121(1):144-52.
45. Yodrabum N, Patchanee K, Oonjitti T, Piyaman P. Technical Challenges in "Micro" Lymph Node Identification during Vascularized Submental Lymph Node Flap Harvesting. Plast Reconstr Surg Glob Open. 2020;8(12):e3330-e.
46. Steinmann WF. Makroskopische Präparationsmethoden in der Medizin. Stuttgart, Germany: Thieme; 1982.
47. König HE, Probst A, Sora C, Dier H. Production of anatomical specimens for teaching practice in veterinary anatomy by means of polyethylene glycol (PEG) impregnation. a comparison with the method of plastination. Chilean J Agric Anim Sci. 2013;29: 59-64.
48. Ventola CL. Medical applications for 3D printing: current and projected uses. P T. 2014;39(10):704-11.
49. AbouHashem Y, Dayal M, Savanah S, Štrkalj G. The application of 3D printing in anatomy education. Med Educ Online. 2015; 20:29847.
50. Ye Z, Dun A, Jiang H, Nie C, Zhao S, Wang T, et al. The role of 3D printed models in the teaching of human anatomy: a systematic review and meta-analysis. BMC Med Educ. 2020; 20(1):335.
51. Srikong M, Wannapiroon P. Immersive technology for medical education: Technology enhance immersive learning experiences. Siriraj Med J. 2020;72(3):265-71.

Human Maxillary Sinus Development, Pneumatization, Anatomy, Blood Supply, Innervation and Functional Theories: An Update Review

Mohammad Ahmad Abdalla, M.D., Ph.D.

Department of Human Anatomy, Trikrit University College of Medicine, Iraq.

ABSTRACT

The maxillary sinus is one of four pair's air-filled spaces that surround the nasal cavity. The majority of previously published researches considering the maxillary sinus commonly concentrated on its pathological conditions and the recent surgical or medical management procedures. However, to understand the diseases of this sinus in a better manner, it is essential to have some basic medical details. Therefore, the present review is an attempt to focus light on this sinus by doing a cosmopolitan update on its development and anatomy, besides the functional theories by searching through many well-known scientific databases including Medline, Scopus, EMBASE, PubMed Central (PMC), PubMed, Cochrane Library, and Web of Science.

In the current review, the author tried to approach, recognize and explain the fundamental data that may provide better ideas to imagine the pathological problems related to the maxillary sinus. In addition, the author did not conduct a new study on human nor animal subjects because the previously implemented articles were the chief and the only source for this review.

In conclusion, the functions and physiology of the maxillary sinus are the subjects that reflect the anatomical complexity mentioned in the most recent articles may probably show that all its functions could be a part of a large and more complicated image than that apparent nowadays.

Keywords: Human maxillary sinus development; maxillary sinus anatomy; maxillary sinus morphology; theories of paranasal sinus functions; mucous membrane (Siriraj Med J 2022; 74: 472-479)

INTRODUCTION

In the fifteenth century, drawings of Leonardo da Vinci demonstrated the human paranasal sinuses, despite some sources that regarded an Italian physician known as Berengar del Carpi as the first scientist who mentioned these sinuses in the sixteenth century. In the same century, another Italian anatomist, Vesalius reported that these sinuses containing only air and nothing more.[1]

In the seventeenth century, the details of maxillary sinus anatomy were recorded by Nathaniel Highmore; while in the eighteenth century, Morgagni noticed that this sinus might be absent in occasional cases.[2]

In the nineteenth century, the work of two anatomists, Adolf Onodi and Zuckerkandl was the cornerstone for the modern anatomy of the human paranasal sinuses. In addition, anatomical reports done by Van Alyea and Mosher were published in the earlier years of the twentieth century, while the radiologist Zinreich was the first scientist who described paranasal sinus anatomy based on computerized tomography.[3]

Corresponding author: Mohammad Ahmad Abdalla
E-mail: dr.mohammad68@tu.edu.iq
Received 3 February 2022 Revised 31 March 2022 Accepted 2 April 2022
ORCID ID: https://orcid.org/0000-0001-8122-3692
http://dx.doi.org/10.33192/Smj.2022.56

MATERIALS AND METHODS

Many scientific databases include; Medline, Scopus, EMBASE, PubMed Central (PMC), PubMed, Cochrane Library, and Web of Science searched. The following words and statements were searched in the title, keyword, abstract, introduction, and article heading: human maxillary sinus, maxillary sinus development, maxillary sinus pneumatization, maxillary sinus anatomy, maxillary sinus blood supply, maxillary sinus innervation, and maxillary sinus functions or functional theories. The Boolean searching strategy was used (or, and or not). All scientific articles include; original articles, case reports, systemic reviews, meta-analyses, and the references of these articles were further searched and evaluated until October 2021. No obvious limitations of this study need to be mentioned.

RESULTS AND DISCUSSION

Development of the human maxillary sinus

Human paranasal sinus develops as an invagination of the nasal fossa into its corresponding bone (frontal, maxillary, ethmoid, and sphenoid). The first sinus that undergoes development is the maxillary sinus which can be apparent on day 17th of embryonic life. The paranasal sinuses development start in the 3rd week of pregnancy and lasts into early adulthood. Ectodermal cells multiply and move medially to produce the notochord at the 4th week. The notochord forms in the embryonic disc's caudal area and rotates to become behind the primitive foregut.[4]

The dorsal part of the first pharyngeal arch forms a maxillary process that extends anteriorly below the developing eye to form the maxilla. At the ending of the second month of development, the maxillary sinus demonstrated as an invagination start just superior to the inferior concha and grows to the lateral side. At the twelfth week of development, the mucous membrane evaginates in the lateral surface of the middle meatus until the nasal epithelium invades the entire maxillary mesenchyme.[5]

Birth, this sinus appears as a small, slit-like structure that is mostly filled with fluid and found at the medial wall of maxillary bone with its greatest dimension recorded at the anteroposterior plane with less than eight millimeters. In newly born children, through routine radiographic procedures, these sinuses are usually not visualized. Also, the rudimentary aerated sinus is about 6-8 cm^3 at birth, with its maximum dimension at the anteroposterior plane.[6]

At the ending of the first year of life, the lateral border of this sinus projects below the medial wall of the orbit; but it extends laterally to the infraorbital fossa by the age of four years old and reaches the maxilla by the age of nine years old.[7] The inferior growth usually reaches the hard palate plane by age of nine years old too. Despite the timing for the above different stages of maxillary sinus development is extremely variable but in general, they are closely related in time.[8]

This sinus remains to grow in a downward direction in association with the alveolar maxillary bone pneumatization to reach the nasal floor level at the age of twelve years old.[9]

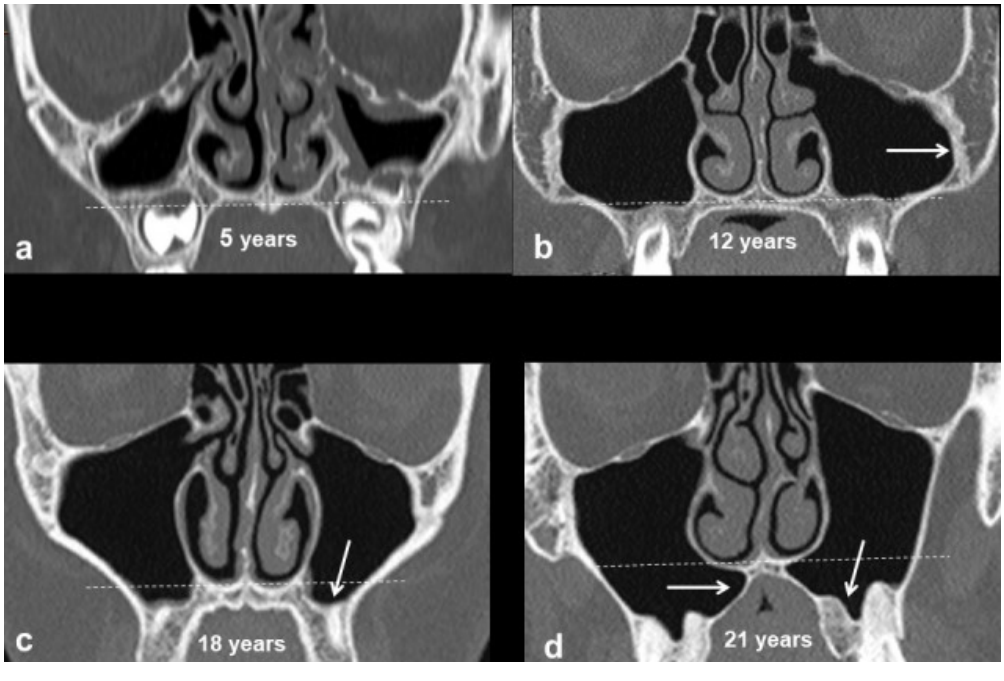

Fig 1. Development of the maxillary sinuses. Up to the age of 12 years, growth of the maxillary sinus is predominantly in a lateral direction towards the zygoma creating the zygomatic recess (white arrow in b) and inferiorly to the level of the hard palate. Thereafter, the sinus expands inferiorly below the level of the nasal floor (white arrows in c, d).[10]

Ultimately, the maxillary sinus floor extends about 4-5 mm below the floor of the nose. Asymmetry in the size and shape of the sinus is common; hypoplasia may be unilateral in 7% or bilateral in 2% of adult individuals. In earlier years of human life, the complete or partial opacity recorded in the maxillary sinus may be regarded as normal.[10]

The mature size of the human maxillary sinus is demonstrated at about the age of twenty years old when all permanent teeth are fully developed; therefore during adulthood, its size and shape alter particularly as a result of teeth loss. After the period of maximum growth, the sinus volume decreases in both sexes which may be due to the loss of the minerals in the matrix of the entire bony structure that surrounding the sinus in each direction to contract that sinus and decreases its volume.[11]

Anatomy of human maxillary sinus

The human maxillary air sinus or antrum of Highmore ("Antron" is a Greek word meaning "a cave") was firstly mentioned in 1651 by Nathaniel Highmore who treated a maxillary sinus empyema by extracting a canine tooth.[1] It is the largest human paranasal sinus recognized as a pyramidal-shaped cavity within the maxilla body and characterized by its apex, base, and four borders.[12]

A thin lateral border from the nasal cavity comprised by the maxillary sinus base to form the hiatus semilunaris in the disarticulated maxilla. However, in articulated bone this orifice is usually decreased in its size by the process of maxilla from inferior nasal concha inferiorly. While the uncinate process of the ethmoidal bone and the descended portion of lacrimal bone superiorly, and the perpendicular plate of palatine bone posteriorly.[12]

The maxillary sinuses are two air-filled spaces situated within the maxillary bones and may be of different shapes and sizes. The walls of these sinuses are thin, and their apex may reach the zygomatic process of the maxilla and may occupy the entire zygomatic bone.[13]

Therefore, the two sinuses may occupy a great part of the maxillae bone bodies and the lateral border from the nasal cavity forms the sinus base. Whereas the orbital floor formed by the sinus roof that is ridged via overlying the infraorbital canal.[14]

The internal surface of the sinus may be ridged or smooth with a specific prominent bony septum and the lateral border includes grooves or canals for particular blood vessels and nerves that supply the superior posterior teeth.[15]

The maxillary sinus communicates with the posterior portion of the hiatus semilunaris at the middle meatus through an orifice, the maxillary ostium on average diameter is 3-6 mm.[16] In a prepared skull this opening is double, but in a recent state the posterior orifice is usually closed by mucoperiosteum and another accessory ostium sometimes is found posterior to principle one and it may be even but larger than the normal one.[12] In rare cases, two or even three accessory openings may be present. The apex of the sinus is created by the zygomatic process of the maxillary bone and in some instances when the sinus is large it extends into the zygomatic bone itself. The roof of the antrum is the floor of orbit while the alveolar process is the floor of the antrum.[17]

In adults, the floor of the sinus is about 1.2 - 1.5 cm under the level for the nasal cavity floor, and in most cases, the radiating bony septum is found on the sinus floor located at spaces between the particular roots of

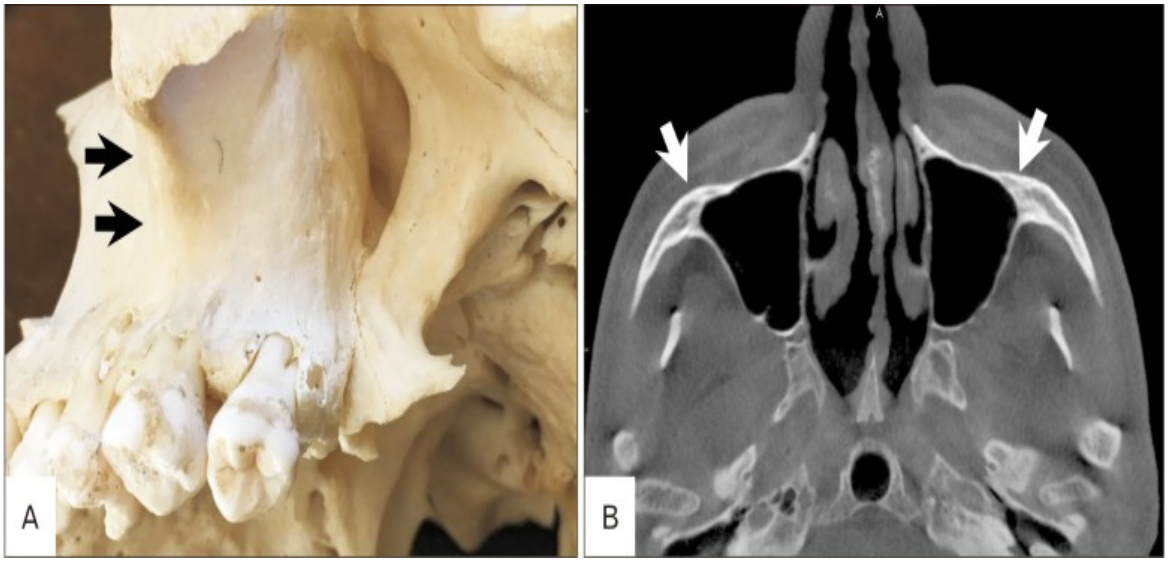

Fig 2. The maxillary sinus extending into the zygomatic process (arrows). (A) Dry skull (inferolateral view). (B) Computed tomography (axial image).[13]

neighboring teeth and occasionally the floor is perforated by apices of corresponded teeth.[17]

Due to individual variations in the air space size, the exact number of the upper teeth which roots reveal direct association with the maxillary sinus is inconstant, but the upper molar is most consistently nearby.[10]

Generally, the lateral and central incisor teeth roots are not found closely nearby to this sinus, besides the maxillary molars and premolars roots; however, are consistently situated under the floor of the sinus. The second molars roots are in closest proximity to this sinus floor, pursued in frequency by the first molar, second premolar, third molar, first premolar, and finally canine roots.[15] The maxillary sinus floor is formed by an alveolar process; the first, the second, and the third molars with the canine roots can elevate the sinuses or can perforate their floor.[12]

The sinus pneumatization was identified when a maxillary posterior tooth was extracted which explains the large expansion of that sinus after the tooth extraction enveloped with the upper curving floor of the same sinus and by extraction of the second molar and some neighboring posterior teeth.[9]

In adults, the level of the floor is about 1.0-1.2 cm below that of the nasal cavity but in the edentulous skull, the level of the floor rises above that belongs to a nasal cavity. The two sinuses are usually equal in size but are not necessarily so, rarely one sinus is absent completely.[4]

The nasal surface of the maxillary body and portions of lacrimal, palatine, inferior turbinate, and ethmoidal bones are the structure that bound the medial border of the antrum.[17] The existence of those bones markedly decreases the size of the orifice between the nasal cavity and antrum during life.[14]

The maxillary sinus is lined by a pseudostratified ciliated columnar epithelium, its cilia constantly move and sweep the mucous into a particular sinusal opening and this flow process is definitive to each paranasal sinus and found even where there is an alternative orifice maybe exist. Fluids of this sinus drain by specific osteomeatal complex into the nasal cavity; if this outflow is obstructed, it leads to mucosal thickening, sinusitis, retention cyst, or polyp formation. Maxillary sinuses remain relatively larger in males than females throughout life.[18] All the mentioned developmental changes may be summarized in Table 1.

TABLE 1. Morphological changes occur in the human maxillary sinus according to age.

Age	Morphological changes
At birth	It filled by the deciduous tooth germ.
20th month	The posterior part develops more than the anterior part.
3 years old	It will be about one half of the adult size sinus.
4-6 years old	It increases in width that associated with fast facial growth, and it locates at the second deciduous molar and the crypts of the first permanent molar teeth.
7-9 years old	Its growth corresponds to the eruption of the permanent teeth.
10-12 years old	The floor of the antrum locates at the same level of the floor of the nasal cavity.
13-15 years old	Its floor locates below the nasal floor, and the sinus floor is at the first molar, second molar and first premolar teeth.
≥16 years old	A thin layer of cortical bone left to separate between the oral mucosa and the sinus mucosa due to the continuous pneumatization process of the sinus and the reposition of the ridge. With age, the enlarging maxillary sinus may even begin to surround the roots of the maxillary posterior teeth and extend its margins into the body of the zygomatic bone. If the maxillary posterior teeth are lost, the maxillary sinus may expand even more, thinning the bony floor of the alveolar process so that only a thin shell of bone is present.

Thus the anatomical description of the maxillary sinus includes the following features; the antral roof is formed by the orbital floor and it is flat structure slopes gradually forward and laterally. On contrary, its floor is a curve structure rather than flat and formed by the alveolar process of the maxillary bone.[6] The floor situates about 1 cm beneath the nasal floor level and closely relates to the root apices of the molar and premolar maxillary teeth. The facial surface of the maxillary bone forms the anterior wall of the maxillary sinus where the canine fossa regards as a remarkable structure at this wall. The sphenomaxillary wall forms the posterior wall of the sinus and a thin cortical bony plate separates the infratemporal fossa from the antral cavity. The lateral wall relates to the zygoma and cheeks, while its medial wall bounds by the nasal cavity. The maxillary sinus opening is closely related to its floor and situated at a higher level compared to the floor.[16]

This sinus is supplied by branches from the maxillary artery; these include the sphenopalatine, infraorbital, posterior superior alveolar, and greater palatine arteries. While it's venous drainage mainly into the facial vein anteriorly and the maxillary vein posteriorly and then into the internal jugular vein.[13]

The maxillary sinus is innervated by the superior alveolar (anterior, middle, and posterior) and infraorbital nerves from the maxillary branch V2 which is the second division of the fifth cranial nerve (the trigeminal nerve); and those alveolar nerves pass downward into the teeth that situated in the maxillary sinus walls, and they penetrate the bony structure of this sinus through delicate nervous branches to give supplement into its mucous membrane. It drains the lymph into the submandibular, deep cervical, and retropharyngeal lymph nodes.[8]

Mucous membrane of paranasal sinuses

Each paranasal sinus is lined by a pseudostratified ciliated columnar epithelium that continuities with the nasal cavity mucosa. This epithelial layer is thinner compared with the nasal epithelium. The four specific cell kinds in this epithelium are the non-ciliated columnar, ciliated columnar, goblet, and basal cells. The experiments reveal that the ciliated cells move approximately 700-850 times/minute, which moves the mucus about nine mm/minute.[19] The non-ciliated cells have microvilli that are found on their apices aspect to increase the surface area of those cells which may facilitate the warming and humidification of the inspired air. The number of non-ciliated cells increases at the sinus orifice or ostium to about 50% compared to other sites. The basal cells are varying in shape, size, and number; their function is unknown. However, there is a theory assumed that these cells are regarded as stem cells that may be differentiated to other required cells. The glycoproteins produced by the goblet cells can be essential for the elasticity and viscosity of the mucus. These cells are innervated by the sympathetic and parasympathetic nervous stimulations.[20] Therefore, the sympathetic innervation increases the water concentration in the mucus secretion, while the parasympathetic innervation causes thicker mucus. The goblet cells are apocrine glands, i.e they pour their secretion through rupture of their apical cell membrane that gets regenerated. So these goblet cells have all the criteria of synthesizing and secreting cells.[21]

The epithelial layer supports by a delicate basement membrane, particularly lamina propria that directly adheres to the periosteum. Both, mucinous and serous glands trace downward toward its lamina propria. Previous reports reveal a general rarity of submucosal glands and goblet cells within the paranasal sinus compared to mucosa of the nose. Among the four sinuses, the human maxillary sinus contains an increased number of the goblet cells. In addition, the ostia of the anterior ethmoid, sphenoid, and maxillary sinuses show a high density of submucosal mucinous and serous glands.[22]

The cilia of each sinus are composed of typical '9+2' architecture that includes 9 outer doublet microtubules with central microtubule pair and moves in a particular direction leading the mucus flow in a specific pattern. As these sinuses may develop in an inferior and outward fashion; therefore, the mucosal cilia usually move the materials such as the debris, mucous film, and even some micro-organisms against the gravity towards the exit of that sinus. In other words, the mucus formed close to the sinus ostium, when it is at the afferent border, it will move around the whole sinus cavity that is usually against the gravity before it reaches that ostium.[23] The previous description explains the presence of an accessory ostium in situations outside the normal physiological ostium will not markedly improve the sinus drainage. In general, this feature sometimes leads to draining mucus from the natural ostium then reenters the sinus through the newly formed orifice and cycles throughout the same sinus cavity again. Therefore, the mucus of each sinus flows in a specific pattern. The stagnation phenomenon demonstrates when two ciliated borders become in contact with each other, especially occurs in osteomeatal complex region. This leads to disruption in the clearance of the mucociliary mucus and causes sinusitis so that recovery from that disease is associated with this clearance process.[24]

Functions of the paranasal sinuses

The functions and physiology of the paranasal sinuses had been a subject for many previous articles.[25] Unfortunately, nowadays researchers are still uncertain about all recorded functions of those sinuses. Many theories regarding the functions are present.[26] These functions include assistance to regulate the intranasal pressure and also gas-serum pressures that subsequently delicate the ventilation, warm/humidify of the inspired air, participate in the immune response, increase the surface area of the mucosa, lighten the skull, give resonance to the voice power, absorb the head shock, and contribute to the growth of human face.[27]

The nose is a powerful warmer and humidifier of the inspired air. It does not reach its maximum capacity to achieve this function even at 7 liters/minute of the airflow. The humidification of the nasal cavity shows a contribution of as much as 6.95 mmHg on the serum pO_2. In spite of the mucosa of the nose considers as the best part that adapts to carry out this task, also these sinuses participate in the warming ability and increase the surface area of that mucosa. Several reports showed that mouth breathing has a low end-tidal CO_2 that can elevate the serum CO_2 and cause sleep apnea.[20,23,27]

However, the most famous theory regards the existence of these paranasal sinuses decreases the skull weight and fixes the splanchnocranium bones mechanically. Absorption of the head shock, protection, and insulation for the neural structures and especially the brain is also assumed. Another conception suggests decreasing the nasal pressure during the mastication process; pressure control and warming of the inspired air, amplification of the voice resonance, and smell sense properties. The multiple physiological functions contribute by these air-filled spaces are thus controversial. These sinuses play an important role in heat insulation, pressure damping, voice resonance, and conditioning for the inspired air.[28]

The sinuses contribute markedly to air filtration/immune defense achieve by the nose due to the production of copious mucous by those sinuses. The sinus and nasal mucosa are covered by cilia that move the mucus into the nasal choanae and eventually into the stomach. The thick mucus on the superficial layer of the nasal cavity mucosa acts to trap various types of bacteria and tiny particles within the substance that contains a high amount of antibacterial proteins, antibodies, and immune cells. On contrary, the underlying layer regards thinner and acts to supply a thin substrate that helps the cilia to beat. In addition, their tips principally grab the superficial layer and push it into the same direction of that beat. If there is no obstruction caused by anatomical variance or disease, this sinus moves the mucous throughout its cavity and out of its ostium into the choane.[29]

The formation of intranasal nitrous oxide (NO) occurs in these sinuses primarily. This substance is toxic to fungi, viruses, and bacteria at low levels (100 ppb). Its concentration at the nasal cavity may reach up to 30,000 ppb that may regard it as the principal of the theory of the sinus sterilization mechanism. In addition, this substance reveals to speed up the ciliary motility. According to previous research, the epithelial cells of the human paranasal sinuses create NO, which is prevalent within the sinus air in extremely high levels, near to the maximum allowable levels of atmospheric pollution. These observations, combined with NO's well-known bacteriostatic properties, imply that NO plays a role in maintaining sterility inside the individual paranasal sinuses.[30]

Theories concerning the functions of the paranasal sinuses:-

Several functional theories that tried to explain the existence of paranasal sinuses have met with varying levels of acceptance among researchers:[31-33]

1. Increasing resonance of the voice.
2. Humidify, warm, and filters the inspired air due to the slow air turnover process in the area.
3. Increase the mucosal surface area.
4. Absorption of the shock that applies to the head.
5. Mucus secretion to keep the nasal cavity moist.
6. Help in the growth of the face and its architecture.
7. Lightening the bones of the skull (especially the facial bones) for maintenance of proper balance.
8. Insulation of sensitive structures such as eyes and dental roots from the fast fluctuations in the temperature of the nasal cavity.
9. Serve as an accessory olfactory organ.

Various hypotheses are developed regarding the human paranasal sinuses but the most popular are three principal hypotheses. The first is the structural theory which depends on the following facts; lightening of skull weight to decrease the muscular efforts at the neck region. Also, optimization of the required balance between the head, as a mass, over the neck, as axis, to promote its movement in the stable upright position. In addition, plastic skull remodeling is essential for the inordinate growth between the neurocranium and splanchnocranium.[34]

The second hypothesis is the functional or potentiation theory that includes the following facts; significant absorption of the effect forces to avoid concussions. Also, vocal resonance; however, the sinus variability and dimensions are imperfectly related with the vocal force.

Furthermore, the attenuation of the characteristic bone transmission of the sound vibrations features.[31] Thermal insulations of the vital organs and structures. Specific enlargement of the olfactory region in human that no more exist as a hunter; these sinuses symbolize some remnants of special structures that aimed to enhance this sense; therefore, absence of this olfactory mucosa represent no significant function is exist at it. Ultimately, a supplementary activity in the defending mechanism by the mucosa of the nasal cavity throughout humidification, enrichment of preventive factors (lysozyme and IgA), and sterile secretion of diluted mucus.[35]

The third hypothesis is the evolutionary theory which can be explained through the following historical facts. The paranasal sinuses are the outcome of water adaptation of human beings species throughout its recorded evolutionary history. During the evolution, the existence of air within the splanchnocranium supplies a hydrodynamic thrust that is necessary to retain the airways structures above the notable aquatic medium.[29] The other ideal human characteristics that might solidify this theory include bipedalism, significant loss of the body hair, subcutaneous fat existence, various productions of tears and sweat, and Shrapnell's membrane presence that dampens the sound waves within the above described liquid medium. Despite the fact that its actual function is ambiguous until nowadays, the evolutionary theory possibly best demonstrates the existence of large-sized and more numbered sinuses in humans compared to primates and other mammals.[31] Another principal feature that keeps in consideration is that despite the exact function of those paranasal sinuses is vague until now, they can be the biological regard of the recurrent pathological processes. Therefore, the physiological elements that are regarded may include the following functions; mucociliary transport, ventilation, local immune response, and drainage of specific secretions.[36]

CONCLUSION

In general, the functions and physiology of the maxillary sinus are the subjects that reflect the anatomical complexity and the most recent reports can probably show that all the mentioned functions could be a part of a big and more complicated image than that apparent nowadays.

Conflict of interest: The author notified that there are no conflicts of interest about the publication of this article.

REFERENCES

1. Harle F. The history of maxillary sinus surgery from Leonardo da Vinci until today. Bull Hist Dent. 1992;40(2):79-84.
2. Kaluskar SK. Evolution of Rhinology. Indian J Otolaryngol Head Neck Surg. 2008; 60: 101-5.
3. Tange RA. Some historical aspects of the surgical treatment of the infected maxillary sinus. Rhinology. 1991;29(2):155-62.
4. Lawson W, Patel ZM, Lin FY. The development and pathologic processes that influence maxillary sinus pneumatization. Anat Record. 2008;291(11):1554-63.
5. Bhushan B, Rychlik K, Schroeder JW. Development of the maxillary sinus in infants and children. Int J Pediatr Otorhinolaryngol 2019;91:146-51.
6. Przystańska A, Kulczyk T, Rewekant A, Sroka A, Jończyk-Potoczna K, Gawriołek K, et al. The Association between Maxillary Sinus Dimensions and Midface Parameters during Human Postnatal Growth. Biomed Res Int. 2018;18:6391465.
7. Mohammad SA, Abdalla MA, Mahdi AJJ. Orbitometry of orbital opening and orbital cavity in neonate compared adult. Tikrit Med J. 2011;17:210-6.
8. Standring S. Gray's anatomy: the anatomical basis of clinical practice. 42nd ed. London: Elsevier Health Sciences; 2020.
9. Abdalla MA. Pneumatization patterns of human sphenoid sinus associated with the internal carotid artery and optic nerve by CT scan. Ro J Neurol. 2020;19(4):244-51.
10. Whyte A, Boeddinghaus R. The maxillary sinus: physiology, development and imaging anatomy. Dentomaxillofac Radiol. 2019;48(8):20190205.
11. Alqahtani S, Alsheraimi A, Alshareef A, Alsaban R, Alqahtani A, Almgran M, et al. Maxillary Sinus Pneumatization Following Extractions in Riyadh, Saudi Arabia: A Cross-sectional Study. Cureus. 2020;12(1):e6611.
12. Levi I, Halperin-Sternfeld M, Horwitz J, Zigdon-Giladi H, Machtei EE. Dimensional changes of the maxillary sinus following tooth extraction in the posterior maxilla with and without socket preservation. Clin Implant Dent Relat Res. 2017;19:952-8.
13. Abdalla MA. Age differences of human sphenoid sinus dimensions: A comparative study by gross anatomical dissection and CT scan imaging. Medicina Moderna. 2021;28(3):321-328.
14. Neychev D, Kanazirska P, Simitchiev K, Yordanov G. CBCT images: an important tool in the analysis of anatomical variations of maxillary sinus related to Underwood septa features. Biotechnol Biotechnol Equip. 2017;31(6):1210-5.
15. Fernandes CL. Forensic ethnic identification of crania: the role of the maxillary sinus- a new approach. Am J Forensic Med Pathol. 2004;25(4):302-13.
16. Abdalla MA, Mahdi AJJ. Maxillary Sinus Measurements in Different Age Groups of Human Cadavers. Tikrit J Dent Sci. 2013;1:107-12.
17. Maspero C, Farronato M, Bellincioni F, Annibale A, Machetti J, Abate A, et al. Three-Dimensional Evaluation of Maxillary Sinus Changes in Growing Subjects: A Retrospective Cross-Sectional Study. Materials. 2020;13:1007.
18. Aksoy U, Orhan K. Association between odontogenic conditions and maxillary sinus mucosal thickening: a retrospective CBCT study. Clin Oral Investig. 2019; 23(1):123-31.
19. Reid L, Meyrick B, Antony VB, Chang LY, Crapo JD, Reynolds HY. The mysterious pulmonary brush cell: a cell in search of a function. Am J Respir Crit Care Med. 2005;172(1):136-9.
20. Hadar T, Yaniv E, Shvili Y, Koren R, Shvero J. Histopathological changes of the nasal mucosa induced by smoking. Inhal Toxicol.

2009;21(13):1119-22.
21. Sato K, Chitose SI, Sato K, Sato F, Ono T, Umeno H. Histopathology of maxillary sinus mucosa with odontogenic maxillary sinusitis. Laryngoscope Investig Otolaryngol. 2020;5(2):205-9.
22. Scherzad A, Hagen R, Hackenberg S. Current Understanding of Nasal Epithelial Cell Mis-Differentiation. J Inflamm Res. 2019;12:309-17.
23. Harkema JR, Carey SA, Wagner JG, Dintzis SM, Liggitt D. Nose, Sinus, Pharynx, and Larynx. Comp Anat Histol. 2018;1:89-114.
24. Hung K, Montalvao C, Yeung AW, Li G, Bornstein MM. Frequency, location, and morphology of accessory maxillary sinus ostia: a retrospective study using cone beam computed tomography (CBCT). Surg Radiol Anat. 2020;42(2):219-28.
25. Abdalla MA. Maxillary Sinus Dimensions of Different Human Age Groups by CT Scan Imaging. Medicina Moderna. 2021;28(2):235-41.
26. Papadopoulou AM, Chrysikos D, Samolis A, Tsakotos G, Troupis T. Anatomical Variations of the Nasal Cavities and Paranasal Sinuses: A Systematic Review. Cureus. 2021;13(1):e12727.
27. Pohunek P. Development, structure and function of the upper airways. Paediatr Respir Rev. 2004;5(1):2-8.
28. Cappello ZJ, Minutello K, Dublin AB. Anatomy, Head and Neck, Nose Paranasal Sinuses. [Updated 2021 Oct 7]. In: StatPearls [Internet]. Treasure Island (FL): StatPearls Publishing; 2022 Jan. Available from: https://www.ncbi.nlm.nih.gov/books/NBK499826/
29. Dahl R, Mygind N. Anatomy, physiology and function of the nasal cavities in health and disease. Adv Drug Deliv Rev. 1998;29:3-12.
30. Lundberg J, Farkas-Szallasi T, Weitzberg E, Rinder J, Lidholm J, Anggaard A, et al. High nitric oxide production in human paranasal sinuses. Nat Med. 1995;1(4):370-3.
31. Rhŷs Evans PH. The paranasal sinuses and other enigmas: an aquatic evolutionary theory. J Laryngol Otol. 1992;106(3):214-25.
32. Abdalla M A. Age Differences of Human Frontal Sinus Measurements using CT Scan. J Adv Med Biomed Res. 2021;29(136):293-301.
33. Dawood S. Normal Anatomic Variants of Paranasal Sinus Region Studied by Computed Tomography. Zanco J Med Sci. 2020;24:187-96.
34. Möhlhenrich SC, Heussen N, Peters F, Steiner T, Hölzle F, Modabber A. Is the Maxillary Sinus Really Suitable in Sex Determination? A Three-Dimensional Analysis of Maxillary Sinus Volume and Surface Depending on Sex and Dentition. J Craniofac Surg. 2015;26(8):e723-6.
35. Sieron HL, Sommer F, Hoffmann TK, Grossi AS, Scheithauer MO, Stupp F, et al. Funktion und Physiologie der Kieferhöhle [Function and physiology of the maxillary sinus]. HNO. 2020;68(8):566-72.
36. Pérez SM, Suárez QJ, Chamorro PC, Suárez JM, López JP, García FG, et al. Volumetric study of the maxillary sinus in patients with sinus pathology. PLos One. 2020;15(6):e0234915.